

Photoinduced Isomerization of Allyl Alcohols to Carbonyl Compounds Using Dendrimer Disulfide as Catalyst

Takaaki Tsuboi, Yutaka Takaguchi, and Sadao Tsuboi

Graduate School of Environmental Science, Okayama University, Tsushima-Naka 3-1-1, Okayama 700-8530, Japan

Received 5 March 2008; revised 14 July 2008

ABSTRACT: *Allyl alcohols were isomerized to carbonyl compounds using diphenyl disulfide derivatives upon photoirradiation. Especially, dendrimer disulfide catalyzed the isomerization of allyl alcohols. Photoinduced isomerization in water was also succeeded by the use of water-soluble dendrimer disulfide.* © 2009 Wiley Periodicals, Inc. *Heteroatom Chem* 20:1–11, 2009; Published online in Wiley InterScience (www.interscience.wiley.com). DOI 10.1002/hc.20504

INTRODUCTION

Photoreactivity of diphenyl disulfide derivatives has attracted scientific attention in the past few decades [1,2]. Sulfanyl radical generated by homolytic cleavage of the S–S bond plays important roles in photoinitiated reactions such as sulfonylation of aryl halides [3] and hindered phenols [4], vinyl polymerization [5], and vicinal dichalcogenation of unsaturated compounds [6–10]. A few examples of transformation of the functional groups using photoreaction of disulfide were also reported [11]. Recently, we have reported the photoinduced oxidation of allyl alcohols to acrylaldehydes using diphenyl disulfide derivatives [12]. However, much less is known about the transformation of func-

tional groups using disulfide as a photocatalyst. Meanwhile, with a growing demand for environmentally benign reactions, catalytic reactions that are atom efficient receive increasing attention [13]. Isomerization of allyl alcohols forms an elegant shortcut to carbonyl compounds in a completely atom-economical process that offers several useful applications in natural-product syntheses and in bulk chemical processes [14]. Although many reports described isomerization of allyl alcohols using metal catalysts [15–18] such as Ru complexes [16,17] and Fe-carbonyl complexes [15,18], isomerization without metal catalyst was quite rare [19]. In this paper, we describe photoinduced isomerization of allyl alcohols to carbonyl compounds using diphenyl disulfide. Especially, dendrimer disulfide catalyzed the isomerization of allyl alcohols. Photoinduced isomerization in water by the use of water-soluble dendrimer disulfide is also examined.

RESULTS AND DISCUSSION

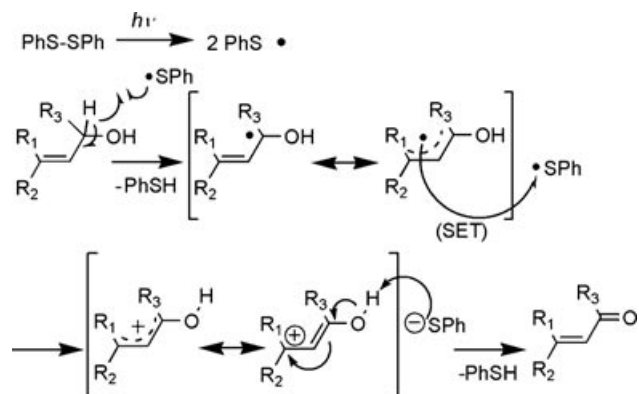
In previous work, we reported that diphenyl disulfide derivatives mediate oxidation of various allyl alcohols to give acrylaldehydes upon photoirradiation [12]. A plausible mechanism of photoinduced oxidation of allyl alcohol is shown in Scheme 1. The reaction was triggered by the sulfanyl radical generated by photolysis of the diphenyl disulfide. Then, the abstraction of an α -hydrogen, which occurred from the allyl alcohol to the sulfanyl radical, produced the allylic radical and thiophenol. Next, a single electron transfer (SET) occurred from the allylic radical to another sulfanyl radical, and an allylic cation was

Correspondence to: Yutaka Takaguchi; e-mail: yutaka@cc.okayama-u.ac.jp.

Contract grant sponsor: The Ministry of Education, Culture, Sports, Science and Technology (MEXT), Japan.

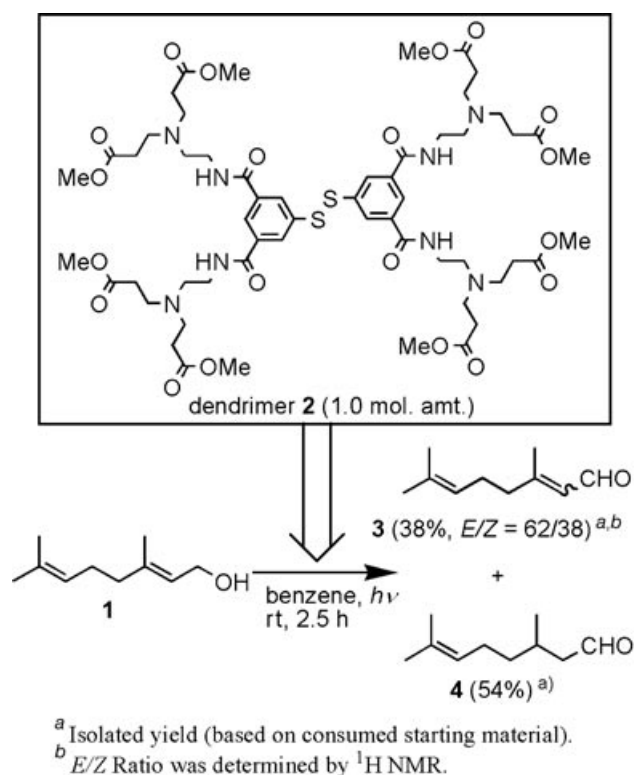
Contract grant number: 19010105.

© 2009 Wiley Periodicals, Inc.



SCHEME 1 Plausible mechanism of oxidation of allyl alcohol using photolysis of diphenyl disulfide.

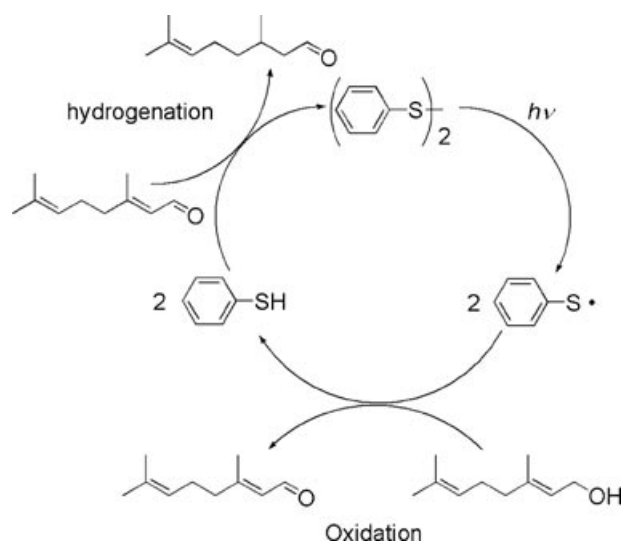
formed. The thiolate anion, which was generated by SET, abstracted the proton of $-OH$ group to give the oxidized product and thiophenol. Interestingly, photoirradiation of geraniol (**1**) in the presence of dendrimer disulfide (**2**) gave isomerization product, 3,7-dimethyl-6-octenal (citronelal, **4**), in 54% yield (Scheme 2).



SCHEME 2 Photoinduced oxidation of geraniol (**1**) using dendrimer disulfide **2**.

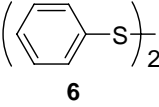
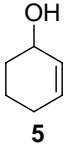
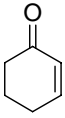
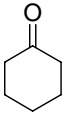
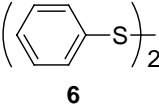
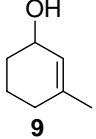
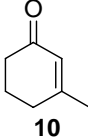
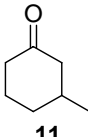
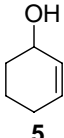
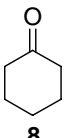
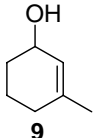
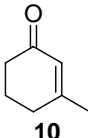
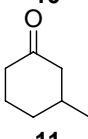
We followed the time course of this reaction by an NMR and observed that citronellal (**4**), isomerized product, was not formed until 20 min after the start of the reaction, although oxidized product, citral (**3**), was observed immediately after the start of the reaction [12]. A catalytic cycle was proposed to explain this isomerization result as Scheme 3. The first step was photolysis of disulfide. Subsequent oxidation of allyl alcohols yields acrylaldehydes and thiols. Final hydrogenation of acrylaldehydes produces isomerized products and disulfides.

Komiya reported that isomerization of 2-cyclohexene-1-ol using Ru catalyst gave higher yield of isomerized product than yields of products of the isomerization of 3-buten-2-ol or 1-phenylallyl alcohol [16]. This result prompted us to investigate isomerization of 2-cyclohexene-1-ol using diphenyl disulfide derivatives. A benzene solution of 2-cyclohexene-1-ol (**5**) in the presence of diphenyl disulfide (**6**) was irradiated with a high-pressure mercury lamp ($\lambda > 300$ nm) through a Pyrex filter at room temperature under an argon atmosphere for 5.5 h to give 2-cyclohexenone (**7**) and cyclohexanone (**8**) in 14% and 56% yields, respectively (Table 1, entry 1). Reactions in the dark or in the absence of diphenyl disulfide (**6**) did not proceed. Hence, the isomerization is a photoreaction mediated by diphenyl disulfide (**6**). Isomerization of 3-methyl-2-cyclohexene-1-ol (**9**) was also examined, since photoinduced oxidation of trisubstituted allyl alcohol gave higher yield of oxidized product than



SCHEME 3 Catalytic cycle of photoinduced isomerization of allyl alcohol.

TABLE 1 Photoinduced Isomerization of Allyl Alcohols Using Diphenyl Disulfide Derivatives^a

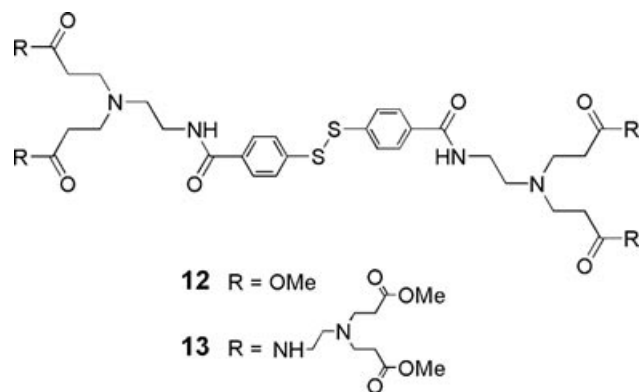
Entry	Disulfide	Allyl Alcohol	Time	Conversion	Product	Yield ^b
1	 6	 5	5.5 h	>99%	 7	14%
					 8	56%
2	 6	 9	5.5 h	>99%	 10	trace
					 11	60%
3	Dendrimer 12	 5	2.5 h	>99%	 8	81%
4	Dendrimer 12	 9	2.5 h	>95%	 10	16%
					 11	79%

^aReactions initiated with UV-light (high-pressure mercury lamp, $\lambda > 300$ nm) in benzene at rt.^bGC yield (based on consumed starting material).

the result of oxidation of nonsubstituted allyl alcohol [12]. Photoinduced isomerization of allyl alcohol **9** using diphenyl disulfide (**6**) gave trace amount of 3-methyl-2-cyclohexenone (**10**) and 60% yield of 3-methylcyclohexanone (**11**) (entry 2). Trace amount of by-products, which might be formed by the addition reaction of disulfide or thiol to the olefins, was observed in each photoreactions by GC analysis.

Although UV-vis spectra (λ_{\max} and ϵ) of dendrimer disulfide is almost the same as diphenyl disulfide, dendrimer disulfide is a good mediator of photoinduced oxidation reaction of allyl alcohols

because dendritic substituents are quite effective to inhibit side reactions initiated by the addition of sulfanyl radical to unsaturated bonds [12]. Hence, we carried out the isomerization using dendrimer disulfide **12**. Surprisingly, photoinduced isomerization of allyl alcohol **5** using dendrimer disulfide **12** gave ketone **8** as a sole product in 81% yield (entry 3). The reaction of allyl alcohol **9** afforded product **11** in 79% yield (entry 4). In this case, enone **10**, a product of oxidation of allyl alcohol **9**, was also obtained in 16% yield. These results indicated dendrimer disulfide **12** was effective for photoinduced isomerization.



Because of the high reactivity, dendrimer disulfide **12** was expected to catalyze the isomerization of allyl alcohols. We carried out the isomerization using 10 mol % of dendrimer disulfide **12**. Results were shown in Table 2. Isomerization of 2-cyclohexene-1-ol (**5**) using 10 mol % of dendrimer disulfide **12** afforded cyclohexanone (**8**) in 90% yield (entry 1). This result proved that the photoinduced isomerization was a catalytic reaction. Unfortunately, photoreaction in the presence of 1 mol % of dendrimer disulfide was not completed (entry 2). Even though longer reaction time was required, isomerization of 3-methyl-2-cyclohexene-1-ol (**9**) using 10 mol % of dendrimer disulfide **12** gave 3-methylcyclohexanone (**11**) in 91% yield (entry 3). Furthermore, isomeriza-

tion of 2-cyclopentene-1-ol (**14**) using 10 mol % of dendrimer **12** gave corresponding cyclopentanone (**15**) in 90% yield (entry 4).

Although the exact reaction mechanism is not completely clear, a plausible mechanism of the catalytic isomerization was shown in Scheme 4. The oxidation step of isomerization was triggered by the sulfanyl radical generated by the photolysis of the diphenyl disulfide. Then, the abstraction of an α -hydrogen, which occurred from the allyl alcohol to the sulfanyl radical, produced the allylic radical and thiophenol. Next, a single electron transfer (SET) occurred from the allylic radical to another sulfanyl radical, and an allylic cation was formed. The thiolate anion, which was generated by SET, abstracted the proton of alcohol to give the oxidized product and thiophenol. The hydrogenation step of isomerization was initiated by the addition of sulfanyl radical to the C=C bond of enone, a product of oxidation. Next, the abstraction of hydrogen occurred from the thiol to the carbon radical, and a sulfide was formed (path A). This sulfide could also be formed by the ionic addition reaction in the dark (path B). After the tautomerization from keto-form to enol-form, another sulfanyl radical (path C) or thiolate anion (path D) attacked C-S bond to form disulfide. Finally, the abstraction of hydrogen (path C) or proton (path D) occurred from the thiol and hydrogenated product was formed. Recently, Ogawa

TABLE 2 Photoinduced Isomerization of Allyl Alcohols Using Dendrimer Disulfide **12** As Catalysts^a

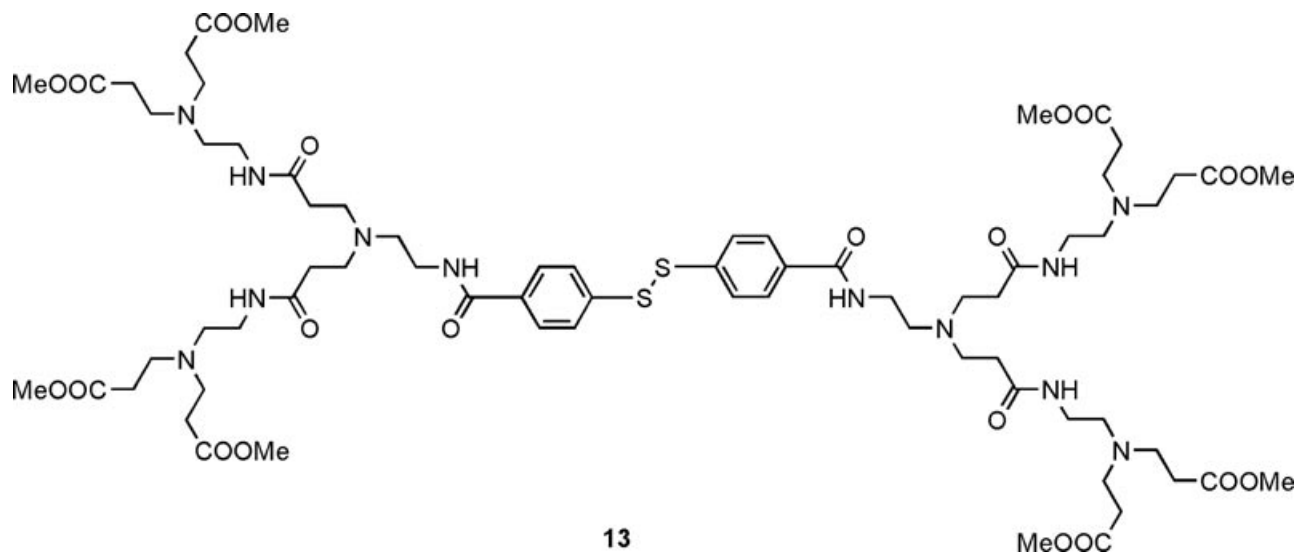
Entry	Disulfide (mol %)	Allyl Alcohol	Time	Conversion	Product	Yield ^b
1	Dendrimer 12 (10 mol %)		2.5 h	>99%		90%
2	Dendrimer 12 (1 mol %)		12 h	54%		34%
3	Dendrimer 12 (10 mol %)		12 h	>99%		91%
4	Dendrimer 12 (10 mol %)		2.5 h	>99%		90%

^aReactions initiated with UV-light (high-pressure mercury lamp, $\lambda > 300$ nm) in benzene at rt.

^bGC yield (based on consumed starting material).

and coworkers have been reported photoinduced reduction of conjugate dienes using a $\text{PhSH}-(\text{PhSe})_2$ binary system [20]. The reaction mechanism of the reduction of diene was similar to the plausible mechanism of hydrogenation step of our isomerization. There could be alternative pathways, that is, direct isomerizations via the formation of cation radical of allyl alcohol by photoinduced SET process or the hydrogen atom donation from a thiol to an allyl radical instead of SET process [21,22]. However, since we observed the enone as an intermediate, the alternative pathway might be excluded.

On the contrary to dendrimer **12**, higher generation dendrimer disulfide **13** was not so effective to mediate photoinduced isomerization (Table 3, entries 3 and 4). This result might indicate that dendrimer having too bulky dendritic wedge inhibited not only side reactions but also isomerization reaction.



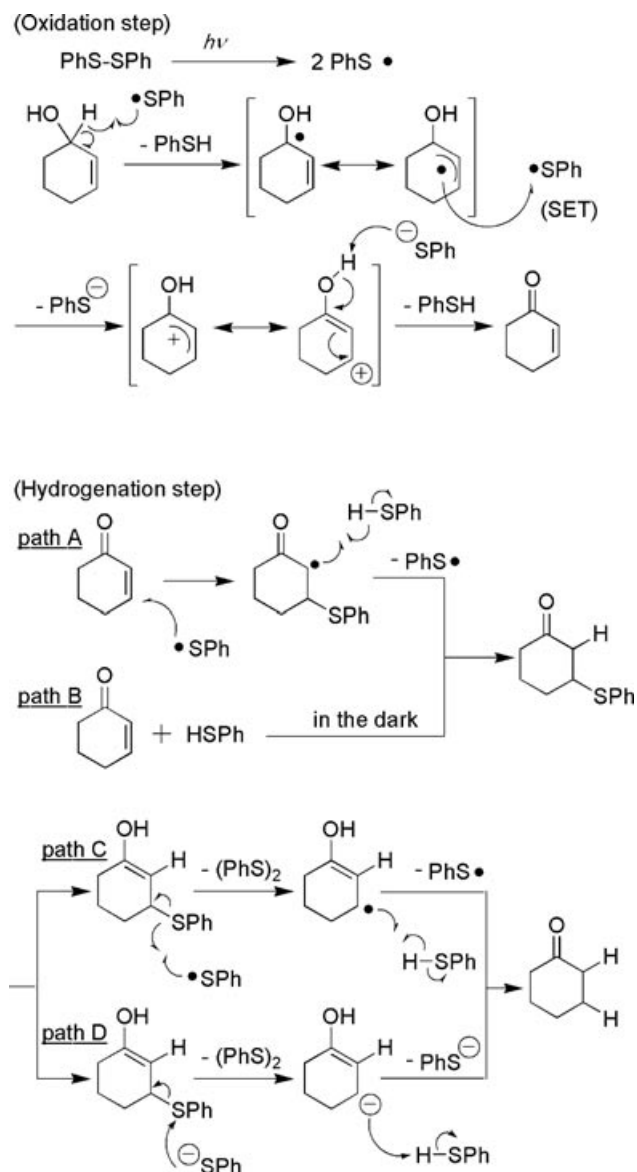
It is notable that the products of the photoreaction, oxidized product or isomerized product, do not depend on the reaction conditions but depend on ΔG° of the reaction, that is, the difference of thermodynamic stability between allyl alcohols (starting materials), carbonyl compounds (oxidized products), and saturated carbonyl compounds (isomerized products). The heats of formation (ΔH_f) of allyl alcohols, allyl carbonyl compounds, and carbonyl compounds derived from PM3 calculations were shown in Fig. 1. The change in the ΔH_f before and after photoinduced isomerization proved stabilization by the photoinduced isomerization. The stabilization by isomerization from 2-cyclohexene-

1-ol (**5**) to cyclohexanone (**8**) is $-59.86 \text{ kJ mol}^{-1}$, and that from 3-methyl-2-cyclohexene-1-ol (**9**) to 3-methylcyclohexanone (**11**) is $-43.92 \text{ kJ mol}^{-1}$. The stabilization by isomerization from geraniol (**1**) to citrinal (**4**) is $-27.96 \text{ kJ mol}^{-1}$, which is the smallest value among these three examples. These calculated results are in good accordance with the difference of reactivity among 2-cyclohexene-1-ol (**5**), 3-methyl-2-cyclohexene-1-ol (**9**), and geraniol (**1**).

To extend the scope of the reaction, we carried out the photoinduced isomerization using water-soluble dendrimer disulfide as a catalyst in water. Water-soluble dendrimer disulfide **16**, which has sugar moiety at the terminals, was synthesized as Scheme 5. The treatment of dendrimer disulfide **12** with ethylenediamine produced dendrimer disulfide **17**. Subsequently, **17** was allowed to react with glucono- δ -lactone to give dendrimer disulfide **16** (66%, two steps). The structure of dendrimer

disulfide **16** was confirmed by ^1H NMR spectroscopy and MALDI-TOF-MS. The MALDI-TOF-MS spectrum of dendrimer disulfide **16** showed the parent peak at m/z 1559.34, which was consistent with the calculated data (1559.64 [MH^+]), as shown in Fig. 2.

We then carried out photoinduced isomerization of allyl alcohols using dendrimer disulfide **16** in water (Scheme 6). Photoirradiation of 2-cyclohexene-1-ol (**5**) in the presence of 10 mol % of dendrimer disulfide **16** gave cyclohexanone (**8**) in 60% yield. 3-Methyl-2-cyclohexene-1-ol (**9**) was also employed for this reaction to achieve stereoselective isomerization. However, racemic 3-methylcyclohexanone (**11**) was obtained in 56% yield.



SCHEME 4 Plausible mechanism of photoinduced isomerization.

CONCLUSION

In summary, we disclosed a novel photoinduced isomerization of allyl alcohols mediated by diphenyl disulfide. In particular, an effective isomerization of allyl alcohol was accomplished by the use of dendrimer disulfides as catalysts. The reaction using water-soluble dendrimer disulfide in water was also succeeded. Further work is in progress to explore the applications and advantages of photoinduced isomerization using dendrimer disulfide.

EXPERIMENTAL SECTION

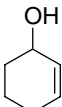
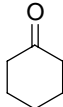
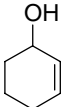
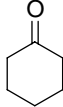
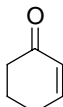
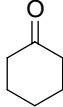
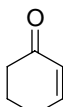
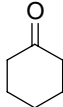
General Method

The NMR spectra was measured using a spectrometer (AL300; JEOL, Tokyo, Japan). Matrix-assisted laser desorption ionization time-of-flight mass spectroscopy (MALDI-TOF-MS) was performed on a mass spectrometer (Autoflex; Bruker Daltonics Inc., Tokyo, Japan). Gas chromatography (GC) analyses were carried out on a gas chromatograph (GC18A; Shimadzu Corp., Tokyo, Japan) equipped with an FID detector and a fused silica capillary column (30 m \times 0.53 mm i.d., coating DB-1; J&W Scientific Inc., Tokyo, Japan). The oven was maintained at 40°C for 5 min, programmed at 2°C min⁻¹ between 40 and 100°C, and programmed at 20°C min⁻¹ between 100 and 270°C. The GC-MS analyses were performed on a GC-MS workstation (QP5000; Shimadzu Corp., Tokyo, Japan) with a fused silica capillary column (30 m \times 0.25 mm i.d., coating TC-5; GL Science Co. Ltd., Tokyo, Japan). Optical rotations were recorded on a polarimeter (SEPA-300; HORIBA Corp., Tokyo, Japan, λ = 589 nm). Photoirradiation was carried out using a Pyrex reactor. Prior to irradiation, solvents were degassed with nitrogen for 30 min. A 500 W high-pressure mercury lamp (EHB-500; Eikosha Corp., Osaka, Japan) was used as the light source. Unless otherwise noted, the reagents were obtained from Wako Pure Chemical Industries Ltd. (Tokyo, Japan), Tokyo Kasei Kogyo Co. Ltd. (Tokyo, Japan), Kanto Kagaku (Tokyo, Japan), or Aldrich Chemical Co. Inc. (Tokyo, Japan). The Et₂O used in reactions was further purified using a general method. Other solvents and reagents were used as received without further purification. Dendrimer disulfide **12** and **13** were synthesized according to the previously reported method [10,12].

3-Methyl-2-cyclohexen-1-ol (**10**)

3-Methylcyclohexen-1-one (**11**) (5.00 g, 45.4 mmol) in dry Et₂O (5 mL) was added simultaneously over 20 min to lithium aluminum hydride (0.86 g, 22.7 mmol) in dry Et₂O (10 mL) at -50°C. After stirring at -50°C for 1 h, ice-cold water (1.5 mL), 4 N aqueous solution of NaOH (1.5 mL), and water (7 mL) were added in order. The aqueous slurry was extracted with Et₂O. Et₂O layer was washed with brine, dried over MgSO₄, and evaporated under ice cooling. The residue was purified using distillation (bp 52°C) and silica gel column chromatography (eluent, chloroform:methanol = 40:1) to afford 3-methyl-2-cyclohexen-1-ol (**10**) (1.34 g, 11.9 mmol) as a colorless liquid in 26% yield, identically to that of an authentic sample [23]: ¹H NMR (300 MHz, CDCl₃)

TABLE 3 Photoinduced Isomerization of Allyl Alcohols Using Dendrimer **12** and Higher Generation Dendrimer **13**^a

Entry	Disulfide (mol %)	Allyl Alcohol	Time	Conversion	Product	Yield ^b
1	Dendrimer 12 (100 mol %)	 5	2.5 h	>99%	 8	90%
2	Dendrimer 12 (10 mol %)	 5	2.5 h	>99%	 8	90%
3	Dendrimer 13 (100 mol %)		2.5 h	55%	 7	trace
					 8	66%
4	Dendrimer 13 (10 mol %)		2.5 h	27%	 7	trace
					 8	72%

^aReactions initiated with UV-light (high-pressure mercury lamp, $\lambda > 300$ nm) in benzene at rt.^bGC yield (based on consumed starting material).

δ 1.33 (dd, $J = 2.7$ and 9.0 Hz, 1H), 1.50–1.61 (m, 2H), 1.69 (s, 3H), 1.74–1.80 (m, 2H), 1.87–1.96 (m, 2H), 4.17 (s, 1H), 5.50 (s, 1H).

Preparation of the Dendrimer Disulfide **16**

A solution of dendrimer disulfide **12** (511 mg, 0.70 mmol) in methanol (38 mL) was added dropwise to ethylenediamine (38 mL, 556 mmol) under ice cooling. The mixture was stirred at room temperature for 13 h. After removal of the solvent under reduced pressure at 45°C , the residue was reprecipitated from a methanol–ether solution to obtain dendrimer disulfide **17**, which was used for the following reaction without further purification.

A solution of **17** in methanol (5 mL) was added to a vigorously stirred solution of Glucono- δ -lactone (2.48 g, 13.9 mmol) in methanol (139 mL) at 50°C . After stirring at 50°C for 2 h, the reaction mixture

was cooled at $<0^\circ\text{C}$ for 18 h. A white precipitate was filtered, washed with Et_2O , and dried to afford the dendrimer disulfide **16** (725 mg, 0.46 mmol) as a white solid in 66% yield: ^1H NMR (300 MHz, D_2O) δ 2.29 (m, 4H), 2.50–2.80 (m, 7H), 3.00–3.20 (m 8H), 3.23 (s, 2H), 3.30–3.75 (m, 12H), 3.96 (s, 2H), 4.17 (s, 2H), 7.51 (d, $J = 8.4$ Hz, 2H), 7.59 (d, $J = 7.8$ Hz, 2H); MALDI-TOF-MASS (matrix, sinapic acid): m/z 1559.34 ($[\text{MH}]^+$). Calcd. for $\text{C}_{142}\text{H}_{238}\text{N}_{28}\text{O}_{46}\text{S}_2$: m/z 1559.64; $[\alpha]_{\text{D}}^{25} = +19.1$ ($c = 1.06$, water).

Photoinduced Isomerization of the 2-Cyclohexene-1-ol (**5**) Using 100 mol % of Diphenyl Disulfide (**6**)

A mixture of 2-cyclohexene-1-ol (**5**) (18.4 mg, 0.19 mmol) and diphenyl disulfide (**6**) (41.5 mg, 0.19 mmol) in benzene (3.2 mL) was irradiated with a high-pressure mercury lamp for 5.5 h at

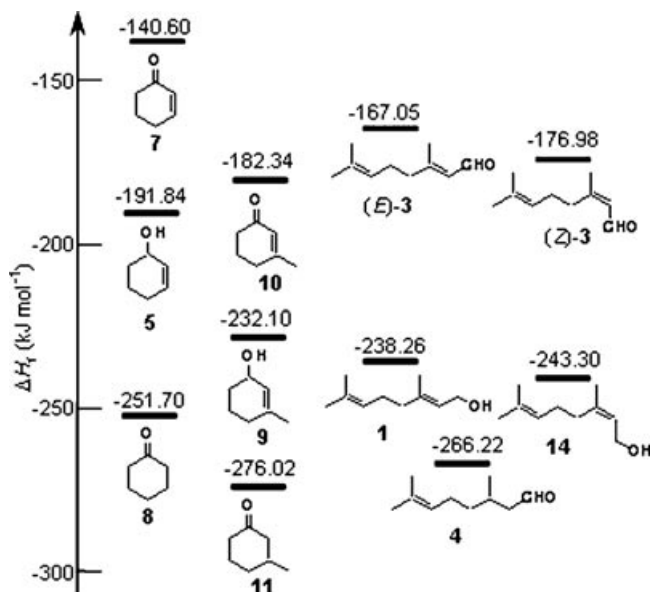


FIGURE 1 Heats of formation (ΔH_f) of allyl alcohols, α,β -unsaturated carbonyl compounds, and saturated carbonyl compounds derived from PM3 calculations.

room temperature. The resulting mixture was analyzed by GC. Decane was used as the internal standard. Three compounds were identified with the following retention times: (a) retention time 9.0 min, cyclohexanone (**8**) (56%); (b) retention time 9.4 min, 2-cyclohexene-1-ol (**5**) (trace); (c) retention time 11.0 min, 2-cyclohexenone (**7**) (14%).

Photoinduced Isomerization of the 3-Methyl-2-cyclohexene-1-ol (9) Using 100 mol % of Diphenyl Disulfide (6)

A mixture of 3-methyl-2-cyclohexene-1-ol (**9**) (21.3 mg, 0.19 mmol) and diphenyl disulfide (**6**) (41.5 mg, 0.19 mmol) in benzene (3.2 mL) was irradiated with a high-pressure mercury lamp for 6 h at room temperature. The resulting mixture was analyzed by GC. Decane was used as the internal standard. Two compounds were identified with the following retention times: (a) retention time 12.7 min, 3-methylcyclohexanone (**11**) (60%); (b) retention time 19.7 min, 3-methyl-2-cyclohexenone (**10**) (trace).

Photoinduced Isomerization of the 2-Cyclohexene-1-ol (5) Using 100 mol % of Dendrimer Disulfide 12

A mixture of 2-cyclohexene-1-ol (**5**) (15.0 mg, 0.15 mmol) and dendrimer disulfide **12** (110 mg, 0.15 mmol) in benzene (2.5 mL) was irradiated with a high-pressure mercury lamp for 2.5 h at room

temperature. The resulting mixture was analyzed by GC. Decane was used as the internal standard. Cyclohexanone (**8**) was identified with the retention time 9.0 min (81%).

Photoinduced Isomerization of the 2-Cyclohexene-1-ol (5) Using 10 mol % of Dendrimer Disulfide 12

A mixture of 2-cyclohexene-1-ol (**5**) (34.8 mg, 0.36 mmol) and dendrimer disulfide **12** (26.1 mg, 0.036 mmol) in benzene (6 mL) was irradiated with a high-pressure mercury lamp for 2.5 h at room temperature. The resulting mixture was analyzed by GC. Decane was used as the internal standard. Cyclohexanone (**8**) was identified with the retention time 9.0 min (90%).

Photoinduced Isomerization of the 2-Cyclohexene-1-ol (5) Using 1 mol % of Dendrimer Disulfide 12

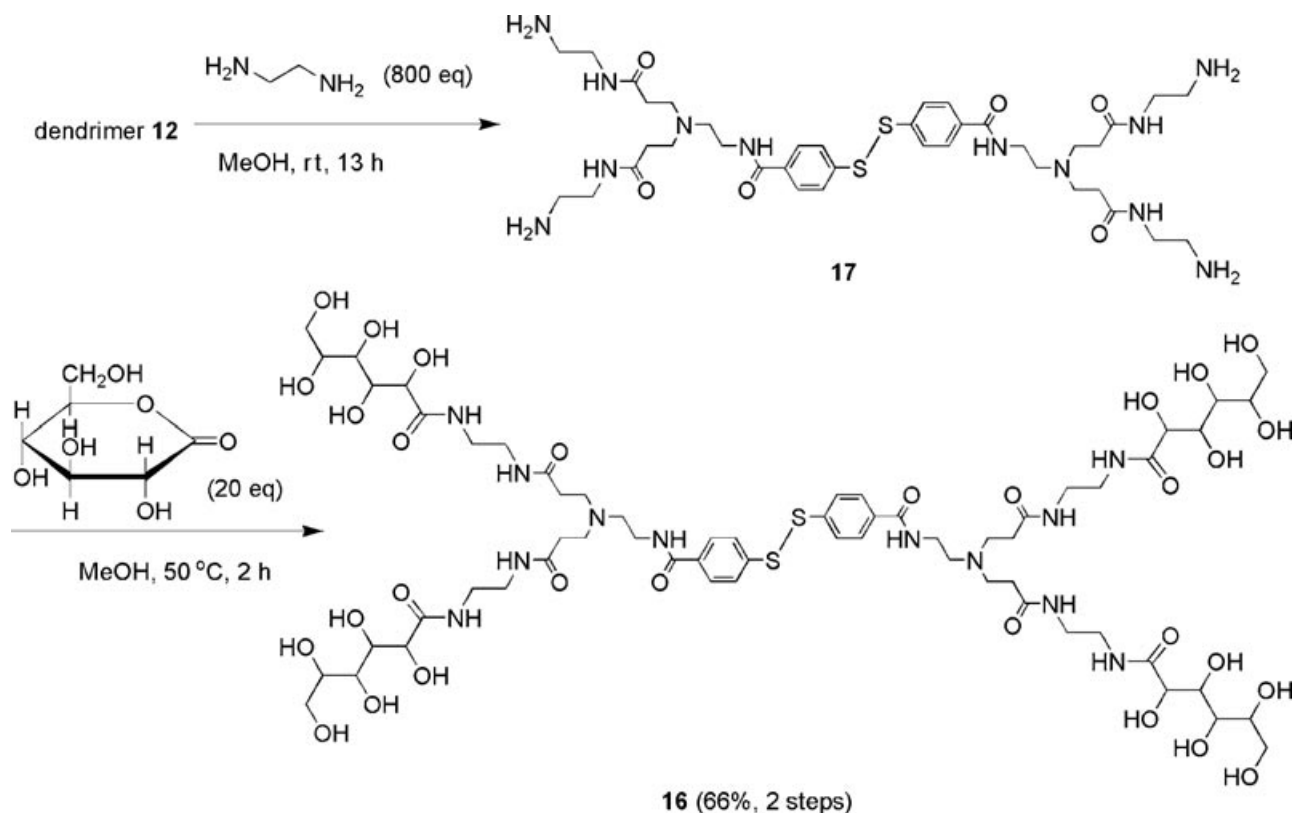
A mixture of 2-cyclohexene-1-ol (**5**) (33.4 mg, 0.34 mmol) and dendrimer disulfide **12** (2.5 mg, 3.4×10^{-3} mmol) in benzene (5.7 mL) was irradiated with a high-pressure mercury lamp for 12 h at room temperature. The resulting mixture was analyzed by GC. Decane was used as the internal standard. Two compounds were identified with the following retention times: (a) retention time 9.0 min, cyclohexanone (**8**) (18%); (b) retention time 9.4 min, 2-cyclohexene-1-ol (**5**) (46%).

Photoinduced Isomerization of the 3-Methyl-2-Cyclohexene-1-ol (9) Using 100 mol % of Dendrimer Disulfide 12

A mixture of 3-methyl-2-cyclohexene-1-ol (**9**) (38 mg, 0.34 mmol) and dendrimer disulfide **12** (249 mg, 0.34 mmol) in benzene (5.7 mL) was irradiated with a high-pressure mercury lamp for 2.5 h at room temperature. The resulting mixture was analyzed by GC. Decane was used as the internal standard. Three compounds were identified with the following retention times: (a) retention time 12.7 min, 3-methylcyclohexanone (**11**) (75%); (b) retention time 15.5 min, 3-methyl-2-cyclohexene-1-ol (**9**) (5%); (c) retention time 19.7 min, 3-methyl-2-cyclohexenone (**10**) (15%).

Photoinduced Isomerization of the 3-Methyl-2-Cyclohexene-1-ol (9) Using 10 mol % of Dendrimer Disulfide 12

A mixture of 3-methyl-2-cyclohexene-1-ol (**9**) (35.1 mg, 0.31 mmol) and dendrimer disulfide **12**



SCHEME 5 Synthesis of water-soluble dendrimer disulfide **16**.

(23.0 mg, 0.031 mmol) in benzene (5.3 mL) was irradiated with a high-pressure mercury lamp for 12 h at room temperature. The resulting mixture was analyzed by GC. Decane was used as the internal standard. 3-Methylcyclohexanone (**11**) was identified with the retention time 12.7 min (91%).

*Photoinduced Isomerization of the 2-Cyclopentene-1-ol (**14**) Using 10 mol % of Dendrimer Disulfide **12***

A mixture of 2-cyclopentene-1-ol (**14**) (33.7 mg, 0.40 mmol) and dendrimer disulfide **12** (29.7 mg, 0.040 mmol) in benzene (5.0 mL) was irradiated with a high-pressure mercury lamp for 2.5 h at room temperature. The resulting mixture was analyzed by GC. Decane was used as the internal standard. Cyclopentanone (**15**) was identified with the retention time 7.2 min (90%).

*Photoinduced Isomerization of the 2-Cyclohexene-1-ol (**5**) Using 100 mol % of Dendrimer Disulfide **13***

A mixture of 2-cyclohexene-1-ol (**5**) (17.1 mg, 0.17 mmol) and dendrimer disulfide **13** (268 mg,

0.17 mmol) in benzene (2.9 mL) was irradiated with a high-pressure mercury lamp for 2.5 h at room temperature. The resulting mixture was analyzed by GC. Decane was used as the internal standard. Three compounds were identified with the following retention times: (a) retention time 9.0 min, cyclohexanone (**8**) (18%); (b) retention time 9.4 min, 2-cyclohexene-1-ol (**5**) (73%); (c) retention time 11.0 min, 2-cyclohexenone (**7**) (trace).

*Photoinduced Isomerization of the 2-Cyclohexene-1-ol (**5**) Using 10 mol % of Dendrimer Disulfide **13***

A mixture of 2-cyclohexene-1-ol (**5**) (34.8 mg, 0.36 mmol) and dendrimer disulfide **13** (26.1 mg, 0.036 mmol) in benzene (6 mL) was irradiated with a high-pressure mercury lamp for 2.5 h at room temperature. The resulting mixture was analyzed by GC. Decane was used as the internal standard. Three compounds were identified with the following retention times: (a) retention time 9.0 min, cyclohexanone (**8**) (36%); (b) retention time 9.4 min, 2-cyclohexene-1-ol (**5**) (45%); (c) retention time 11.0 min, 2-cyclohexenone (**7**) (trace).

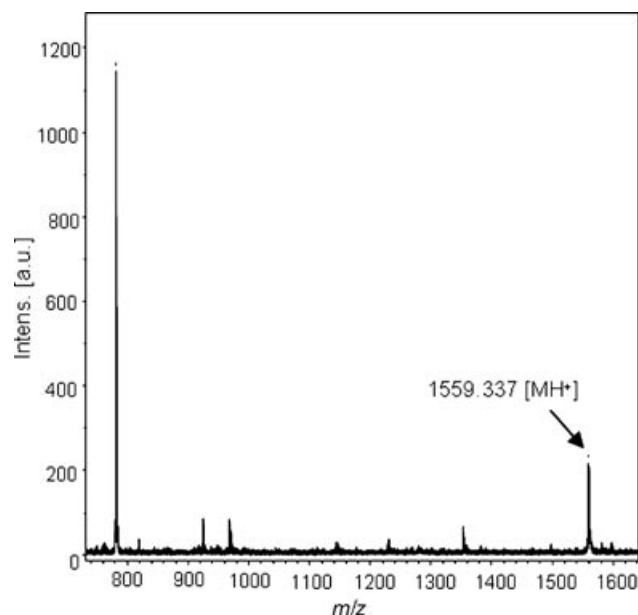
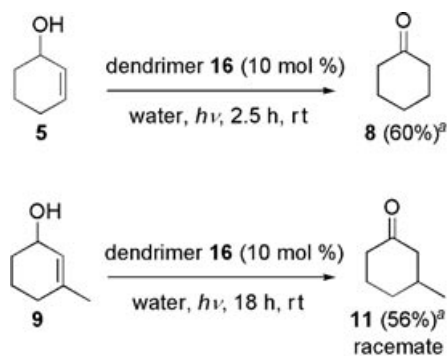


FIGURE 2 MALDI-TOF-MS spectrum of dendrimer sulfide 16.

Photoinduced Isomerization of the 2-Cyclohexene-1-ol (5) Using 10 mol % of Dendrimer Disulfide Having Sugar Moiety 15

A mixture of 2-cyclohexene-1-ol (**5**) (18.6 mg, 0.19 mmol) and dendrimer disulfide **15** (29.6 mg, 0.019 mmol) in deionized water (3.2 mL) was irradiated with a high-pressure mercury lamp for 2.5 h at room temperature. The resulting mixture was analyzed by GC. 4-Methyl-3-pentene-2-one was used as the internal standard. Two compounds were identified with the following retention times: (a) retention time 9.0 min, cyclohexanone (**8**) (47%); (b) retention time 9.4 min, 2-cyclohexene-1-ol (**5**) (22%).



^aGC yield (based on consumed starting material).

SCHEME 6 Photoinduced isomerization using dendrimer 16 in water.

Photoinduced Isomerization of the 3-Methyl-2-cyclohexene-1-ol (9) Using 10 mol % of Dendrimer Disulfide Having Sugar Moiety 15

A mixture of 3-methyl-2-cyclohexene-1-ol (**9**) (21.3 mg, 0.19 mmol) and dendrimer disulfide **15** (30.0 mg, 0.019 mmol) in deionized water (3.2 mL) was irradiated with a high-pressure mercury lamp for 18 h at room temperature. The resulting mixture was analyzed by GC. Cyclohexanone was used as the internal standard. 3-Methylcyclohexanone (**11**) was identified with the retention time 12.7 min (56%).

Calculations

The semiempirical calculations by the PM3 method were performed using MOPAC version 6.02 [24] with parameters in Ref. [25]. In the calculation, totally optimized molecular geometries in the ground state were used.

REFERENCES

- [1] Lyons, W. E. *Nature* 1948, 162, 1004.
- [2] Moussebois, C.; Dale, J. *J Chem Soc* 1966, 260.
- [3] Fujisawa, T.; Ohta, H. *Bull Chem Soc Jpn* 1976, 49, 2341.
- [4] Fujisawa, T.; Kojima, T. *Bull Chem Soc Jpn* 1977, 50, 3061.
- [5] Tsuda, K.; Kobayashi, S.; Otsu, T. *Bull Chem Soc Jpn* 1965, 38, 1517.
- [6] Ogawa, A.; Sonoda, N.; Synth, J. *Org Chem Jpn* 1996, 54, 894.
- [7] Ogawa, A.; Tanaka, H.; Yokoyama, H.; Obayashi, R.; Yokoyama, K.; Sonoda, N. *J Org Chem* 1992, 57, 111.
- [8] Ogawa, A.; Sonoda, N. *Phosphorus, Sulfur Silicon Relat Elem* 1994, 95, 331.
- [9] Tsuchii, K.; Tsuboi, Y.; Kawaguchi, S.; Takahashi, J.; Sonoda, N.; Nomoto, A.; Ogawa, A. *J Org Chem* 2007, 72, 415.
- [10] Takaguchi, Y.; Katayose, Y.; Yanagimoto, Y.; Motoyoshiya, J.; Aoyama, H.; Wakahara, T.; Maeda, Y.; Akasaka, T. *Chem Lett* 2003, 32, 1124.
- [11] Tada, M.; Katayama, E.; Sakurai, N.; Murofushi, K. *Tetrahedron Lett* 2004, 45, 17.
- [12] Tsuboi, T.; Takaguchi, Y.; Tsuboi, S. *Bull Chem Soc Jpn* 2008, 81, 361.
- [13] Trost, B. M. *Acc Chem Res* 2002, 35, 695.
- [14] van der Drift, R. C.; Bouwman, E.; Drent, E. *J Organomet Chem* 2002, 650, 1.
- [15] Iranpoor, N.; Mottaghinejad, E. *J Organomet Chem* 1992, 423, 399.
- [16] Kanaya, S.; Imai, Y.; Komine, N.; Hirano, M.; Komiya, S. *Organometallics* 2005, 24, 1059.
- [17] Takai, Y.; Kitaura, R.; Nakatani, E.; Onishi, T.; Kurosawa, H. *Organometallics* 2005, 24, 4729.
- [18] Chong, T. S.; Tan, S. T.; Fan, W. Y. *Chem Eur J* 2006, 12, 5128.
- [19] May, S. W.; Steltenkamp, M. S.; Borah, K. R.; Katopodis, A. G.; Thowsen, J. R. *J Chem Soc Chem Commun* 1979, 845.

- [20] Mitamura, T.; Imanishi, Y.; Nomoto, A.; Sonoda, M.; Ogawa, A. *Bull Chem Soc Jpn* 2007, 80, 2443.
- [21] Escoubet, S.; Gastaldi, S.; Timokhin, V. I.; Bertrand, M. P.; Siri, D. *J Am Chem Soc* 2004, 126, 12343.
- [22] Bartrand, M. P.; Escoubet, S.; Gastaldi, S.; Timokhin, V. I. *Chem Commun* 2002, 216.
- [23] Fristad, W. E.; Bailey, T. R.; Paquette, L. A. *J Org Chem* 1980, 45, 3028.
- [24] MOPAC ver. 6, J. J. P. Stewart, *QCPE Bull* 1989, 9, 10.; Revised as Ver. 6.01 by T. Hirano, University of Tokyo, for HITAC and UNIX machines, *JCPE Newsletter*, 1989, 1, 10; Revised as Ver. 6.02 by N. Senda, Idemitsu Kousan Co., Ltd., for Windows machines (Winmoster), *Idemitsu Gihou*, 2006, 49, 106.
- [25] Stewart, J. J. P. *J Comput Chem* 1989, 10, 209.

Thiirane of 2'-Adamantylidene-9-Benzonorbornenylidene Using 4,4'-Oligothiodimorpholine and Brønsted Acid

Yoshiaki Sugihara, Hiroko Nozumi, and Juzo Nakayama

Department of Chemistry, Graduate School of Science and Engineering,
Saitama University, Sakura-ku, Saitama 338-8570, Japan

Received 12 September 2008; revised 16 October 2008

ABSTRACT: On leaving 4,4'-dithiodimorpholine **6** powder undisturbed at room temperature over 10 years, it led to the formation of 4,4'-tetrathiodimorpholine **7**. Reactions of 2'-adamantylidene-9-benzonorbornenylidene **1** with **6**, **7**, and 4,4'-thiodimorpholine **8** and a Brønsted acid in CH_2Cl_2 at room temperature proceeded to afford the corresponding thiiranes, **2** and **3**. The order of reactivity of 4,4'-oligothiodimorpholines combined with a Brønsted acid is $7 > 6 > 8$. The thiirane **3** was transformed to **1** and **2** under the reaction conditions. © 2009 Wiley Periodicals, Inc. *Heteroatom Chem* 20:12–18, 2009; Published online in Wiley InterScience (www.interscience.wiley.com). DOI 10.1002/hc.20505

INTRODUCTION

The chemistry of three-membered heterocyclic compounds has been attracting considerable interest from the viewpoints of synthesis, structure, reactions, and synthetic applications [1–5]. Oxiranes and aziridines can easily be synthesized from alkenes by

oxirane (epoxidation) with an oxidant such as peracid and peroxide and by aziridination with a nitrene equivalent, respectively, and have been used as precursors for syntheses of functional materials and biologically active compounds [1–3]. Thiiranes are considered to be superior precursors to oxiranes and aziridines because their sulfur atom makes their conversion to other compounds more facile than that of oxiranes and aziridines having oxygen and nitrogen atoms, respectively [6–9]. Although syntheses of thiiranes have been investigated so far [4,5], fewer reports have dealt with thiirane of alkenes in comparison with the oxirane and aziridination [10]. There are problems with the thiirane, such as being limited to alkenes used, difficulty of synthesizing a sulfuration reagent, and further reactions of the resulting thiirane. One of the most widely used laboratory methods for thiirane synthesis has been a two-step transformation of alkenes to thiiranes through oxiranes.

We have studied the chemistry of sterically hindered alkenes such as 9,9'-bibenzonorbornenylidenes, 2'-adamantylidene-9-benzonorbornenylidene **1**, and related compounds [11–17]. In the course of that study, we found that **1** reacted with sulfuration reagents to afford the corresponding thiiranes **2** and **3** [17]. Thus, heating **1** with elemental sulfur in *o*- $\text{Cl}_2\text{C}_6\text{H}_4$ or *N,N*-dimethylformamide (DMF) gave an approximately 16:1 or 9:1 mixture of **2** and **3** together with **1**. The alkene **1** reacted with S_xCl_2 ($x = 1, 2$) at -78°C to

Correspondence to: Yoshiaki Sugihara and Juzo Nakayama; e-mail: ysugi@chem.saitama-u.ac.jp and nakayama@mail.saitama-u.ac.jp.

Contract grant sponsor: Japan Society for the Promotion of Science.

© 2009 Wiley Periodicals, Inc.

give **2** and *vic*-dichloride **4**. No other products were observed in the reactions. The thiirane **3** isomerized easily to **2**, which is thermally more stable than **3** by 3.2 kcal mol⁻¹, and both **2** and **3** decomposed to **1** and **4** under the reaction conditions. Thus, when **3** was heated with or without elemental sulfur under the same conditions, a mixture of **2** and **3** of in a ratio of about 20:1 was obtained together with **1**. Each thiirane also reacted with S_xCl₂ to form **2** and **4**. The isomerization and decomposition must be regarded as a side reaction of thiiranes to form other compounds that accompanies thiirane-ring opening, such as polymerization. In addition, using **1** in the study would facilitate the analysis of the reaction mixture by ¹H NMR. Thus, both the bridge-head hydrogens of 2-adamantylidene group in **1–4** and the axial hydrogens at 4-position of the group in **1**, **2**, and **4** were affected by an anisotropic effect of the benzene ring in the 9-benzonorbornenylidene group, causing these hydrogen signals to appear at separated positions. Therefore, we concluded that **1** would be a model compound for research on suitable reaction conditions of the thiirane of alkenes.

4,4'-Oligothiodimorpholine **5** is a reagent known to react with rubber on heating [18]. In particular, 4,4'-dithiodimorpholine **6** is a widely used and commercially available, inexpensive vulcanizing agent. If a Brønsted acid is present in a reaction medium, **5** would be activated without heating because of the presence of the basic nitrogen atoms adjacent to the sulfur atoms [19,20]. Therefore, a combination of **5** and the Brønsted acid would act as a sulfuration reagent for the thiirane. Furthermore,

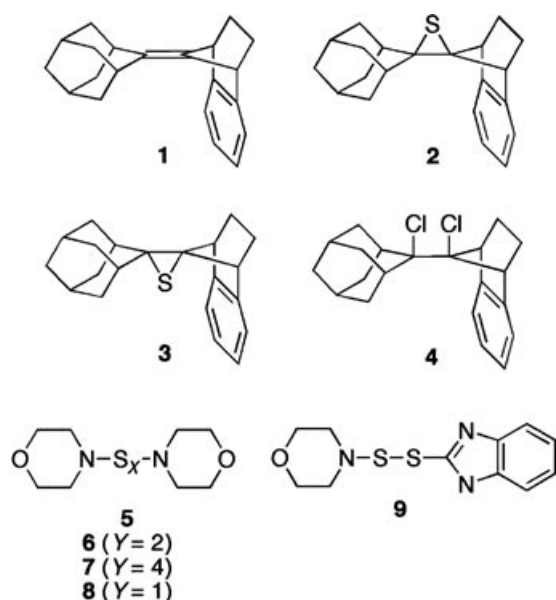


FIGURE 1

replacement of the chlorine atom in S_xCl₂ with a 4-morpholino group would prevent formation of by-products, such as **4**. In this study, we observed that **6** transformed over a long period of time into a mixture containing 4,4'-tetrathiodimorpholine **7** in the solid state. As the proportion of sulfur atoms in a vulcanizing agent becomes higher, its vulcanization-accelerating activity should increase. Here, we report thiirane of **1** using **7** and a Brønsted acid. Decomposition of the resulting thiirane and the thiirane using **6**, 4,4'-thiodimorpholine **8**, and 2-(4'-morpholinodisulfanyl) benzothiazole **9** are also reported.

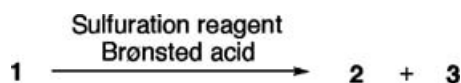
RESULTS AND DISCUSSION

Transformation of 4,4'-Dithiodimorpholine **6** to 4,4'-Tetrathiodimorpholine **7**

The 4,4'-dithiodimorpholine **6** mentioned in the Introduction section was gifted to our laboratory more than 10 years ago by Ouchi Shinko Chemical Industrial Co. Ltd. (Tokyo, Japan). During that time, the colorless powder **6** had changed slowly into a faint gray powdery mixture containing **7** [21], which was probably formed through disproportionation of **6** with the evolution of morpholine and the related volatile molecules, at room temperature for a long time. In fact, both this mixture and a purchased sample of **6** had a subtle odor, similar to morpholine, at room temperature. When the aforementioned mixture was carefully crystallized several times from EtOH, **7** was obtained as faint yellow needles in a pure form. Pure **6** was obtained by recrystallization of the purchased **6** from EtOH as colorless needles [22]. Both **6** and **7** can be stored in a freezer at -18°C for several months without decomposition. Attempted syntheses of **7** from **6** in the solid state failed. Thus, two processes were tested: heating **6** at 120°C/24 mmHg in a Kugelrohr distillation apparatus to remove the volatile materials and heating around its melting point under oxygen atmosphere. Both resulted in the quantitative recovery of **6**.

Thiirane of 2'-Adamantylidene-9-Benzonorbornenylidene **1** with 4,4'-Tetrathiodimorpholine **7** and Brønsted Acid

A combination of **7** and carboxylic acid or sulfonic acid was used for the thiirane of **1** (Scheme 1);



SCHEME 1

TABLE 1 Reactions of **1** with **7** and Brønsted Acids^a

Entry	Brønsted Acid	Conditions	Yield (%) ^b		
			2	3	1
1	CF ₃ CO ₂ H	CH ₂ Cl ₂ , r. t., 26 h	53	29	17
2	CH ₃ CO ₂ H	CH ₂ Cl ₂ , r. t., 26 h	—	—	Quant.
3	CHF ₂ CO ₂ H	CH ₂ Cl ₂ , r. t., 240 h	9	3	88
4	NCCH ₂ CO ₂ H	CH ₂ Cl ₂ , r. t., 720 h	15	Trace	85
5	NCCH ₂ CO ₂ H	CH ₂ Cl ₂ , reflux, 24 h	21	29	50
6	NCCH ₂ CO ₂ H	CH ₂ Cl ₂ , reflux, 16 h	15	12	73
7	<i>p</i> -TsOH·H ₂ O	CH ₂ Cl ₂ , r. t., 50 h	42	43	14

^a**7** (0.4 molar equivalent), Brønsted acid (0.5 molar equivalent).^bBy ¹H NMR.

the results are summarized in Table 1. The thiirane formation with CF₃CO₂H ($pK_a=0.23$) [23] in CH₂Cl₂ for 26 h gave **2** and **3** in 53% and 29% yields, respectively, together with **1** in 17% yield (entry 1). When CH₃CO₂H ($pK_a=4.76$) [23] was used under the same conditions, **1** was recovered quantitatively (entry 2). Using CHF₂CO₂H ($pK_a=1.24$) [23] or NCCH₂CO₂H ($pK_a=2.43$) [23] brought about slow progress of the thiirane formation (entries 3 and 4). These results suggest that increasing a pK_a value of carboxylic acids tends to decrease the yields of the thiiranes. The thiirane formation with NCCH₂CO₂H in refluxing CH₂Cl₂ gave **2** and **3** in a moderate total yield (entry 5), but raising the reaction temperature above 84°C (the boiling point of (CH₂Cl₂) inhibited the thiirane formation (entry 6). Overheating of the reaction mixture would lead to decomposition of the products. On the other hand, *p*-TsOH·H₂O ($pK_a=-1.7$) [24] acted as a good activating agent in a similar way to CF₃CO₂H (entry 7).

Effect of Molar Ratios of **7** and Brønsted Acids

We studied effect of the molar ratios of the **7** and the Brønsted acids on the thiirane formation (Table 2). The reactions of **1** with 1.0 molar equivalent of **7** and the Brønsted acid each gave **2** and **3** in a good total yield (entries 1–4). The yields of the thiiranes decreased when 0.5 molar equivalent of the Brønsted acid was used (entries 5–8). An exception was CF₃CO₂H, which led to the quantitative formation of **2**. Diminishing the quantities of **7** and the carboxylic acid to 0.5 molar equivalents each did not affect the yields of the products (entries 9–11). In contrast, using 0.5 molar equivalents of **7** and *p*-TsOH·H₂O each caused a slight improvement in the yield of **3** compared with using 1.0 molar equivalent of **7** and 0.5 molar equivalent of *p*-TsOH·H₂O (entry 12). When 0.33 molar equivalent of **7** was used, the total yield of **2** and **3** decreased but was between 39% and 71% (entries

TABLE 2 Effect of a Molar Ratio of **7** and Brønsted Acid on the Formations of **2** and **3**^a

Entry	Molar Equivalent of 7	Brønsted Acid (Molar Equivalent)	Time (days)	Yield (%) ^b		
				2	3	1
1	1.0	CF ₃ CO ₂ H (1.0)	5	Quant.	—	—
2	1.0	CHF ₂ CO ₂ H (1.0)	11	23	65	12
3	1.0	NCCH ₂ CO ₂ H (1.0)	11	23	48	19
4	1.0	<i>p</i> -TsOH·H ₂ O (1.0)	5	61	28	11
5	1.0	CF ₃ CO ₂ H (0.5)	2	Quant.	—	—
6	1.0	CHF ₂ CO ₂ H (0.5)	6	27	44	29
7	1.0	NCCH ₂ CO ₂ H (0.5)	6	20	27	54
8	1.0	<i>p</i> -TsOH·H ₂ O (0.5)	6	31	22	48
9	0.5	CF ₃ CO ₂ H (0.5)	5	94	2	5
10	0.5	CHF ₂ CO ₂ H (0.5)	7	26	43	31
11	0.5	NCCH ₂ CO ₂ H (0.5)	7	13	39	48
12	0.5	<i>p</i> -TsOH·H ₂ O (0.5)	7	37	38	26
13	0.33	CF ₃ CO ₂ H (0.5)	7	27	38	36
14	0.33	CHF ₂ CO ₂ H (0.5)	7	26	41	33
15	0.33	NCCH ₂ CO ₂ H (0.5)	7	20	27	53
16	0.33	<i>p</i> -TsOH·H ₂ O (0.5)	7	44	27	29
17	0.33	CF ₃ CO ₂ H (0.33)	7	65	5	30
18	0.33	CHF ₂ CO ₂ H (0.33)	7	17	35	48
19	0.33	NCCH ₂ CO ₂ H (0.33)	7	11	28	61
20	0.33	<i>p</i> -TsOH·H ₂ O (0.33)	7	26	17	57

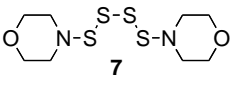
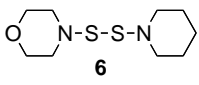
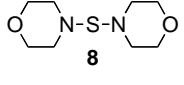
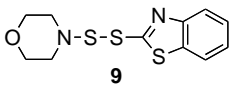
^aIn CH₂Cl₂ at r. t.^bBy ¹H NMR.

13–20). These results reveal that although decreasing the quantity of **7** tended to decrease the yields of the thiiranes, more than one sulfur atom in **7** was introduced into the products. In the reactions with any Brønsted acid, using an equimolar amount of **7** and the Brønsted acid against **1** produced the best result for the thiirane formations.

Thiirane formation of **1** with Other Sulfuration Reagent and Brønsted Acid

The reactions with **6**, 4,4'-thiodimorpholine **8** [21], and 2-(4'-morpholinodisulfanyl) benzothiazole **9** were investigated (Table 3). In case of using any Brønsted acid, decreasing the sulfur atoms in the oligothiodimorpholines tended to decrease the production of **2** and **3** (entries 1–11). Under these reaction conditions, 4,4'-thiodimorpholine **8** was much less reactive than **7** and **6**. The compound **9** also reacted with **1** in the presence of the Brønsted acids to give the thiiranes (entries 12–15). The ratio of the thiiranes and the recovered **1** in these reactions was similar to that in the reactions using **6**. Therefore, the order of reactivity of the sulfuration reagents combined with a Brønsted acid is **7**>**6** ~ **9**>**8**.

TABLE 3 The Reactions with 6–9 and Brønsted Acids^a

Entry	Sulfuration Reagent	Brønsted Acid	Time (days)	Yield (%) ^b		
				2	3	1
1	 7	CF ₃ CO ₂ H	5	Quant.	–	–
2		CHF ₂ CO ₂ H	11	23	65	12
3		NCCH ₂ CO ₂ H	11	33	48	19
4		<i>p</i> -TsOH·H ₂ O	5	61	28	11
5	 6	CF ₃ CO ₂ H	5	36	10	54
6		CHF ₂ CO ₂ H	11	12	26	63
7		NCCH ₂ CO ₂ H	11	8	11	81
8		<i>p</i> -TsOH·H ₂ O	5	9	13	78
9	 8	CF ₃ CO ₂ H	7	13	5	82
10		CHF ₂ CO ₂ H	7	3	5	92
11		<i>p</i> -TsOH·H ₂ O	7	2	3	95
12	 9	CF ₃ CO ₂ H	7	41	17	42
13		CHF ₂ CO ₂ H	7	6	12	82
14		NCCH ₂ CO ₂ H	7	7	4	89
15		<i>p</i> -TsOH·H ₂ O	7	26	15	62

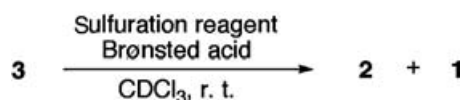
^aSulfuration reagent (1.0 molar equivalent), Brønsted acid (1.0 molar equivalent), in CH₂Cl₂ at r. t.^bBy ¹H NMR.

Decomposition of the Thiirane 3 Under the Thiirane Conditions

When the reactions of **1** with **7** and CF₃CO₂H that resulted in the quantitative formation of **2** were monitored by thin-layer chromatography (TLC), in some cases, two spots due to the thiiranes were observed in the initial stage of the reaction and then the spot due to **2** enlarged and the other due to **3** disappeared. This probably means that **3** easily isomerizes to **2** and decomposes to **1** under these conditions. Therefore, we monitored the reactions of **3** with the sulfuration reagents (1.0 molar equivalent) and Brønsted acids (1.0 molar equivalent) in CDCl₃ with ¹H NMR (Scheme 2). When **3** reacted with 4,4'-tetrathiodimorpholine **7** and CF₃CO₂H for 15 h, **3** transformed to **2** quantitatively. As the pK_a value of the carboxylic acid used was increased, the consumption of **3** slowed. Thus, the reactions with CHF₂CO₂H and NCCH₂CO₂H were still in progress after 15-h reaction time (Figs. 2a and 2b). The decomposition of **3** proceeded rapidly in the initial stage, and then, both **1** and **3** were gradually consumed and the formation of **2** increased as time went by (CHF₂CO₂H after 15 min: **2**, 33%;

1, 20%; **3**, 46%; after 1 h: **2**, 61%; **1**, 13%; **3**, 26%; after 3 h: **2**, 66%; **1**, 10%; **3**, 24%; after 1 day: **2**, 81%; **1**, 7%; **3**, 12%; NCCH₂CO₂H after 20 min: **2**, 5%; **1**, 22%; **3**, 73%; after 2 h: **2**, 23%; **1**, 22%; **3**, 73%; after 8 h: **2**, 28%; **1**, 21%; **3**, 51%; after 1 day: **2**, 34%; **1**, 18%; **3**, 48%), suggesting that the resulting alkene **1** is sulfurated to form **2** and **3** under these reaction conditions. The reaction with *p*-TsOH·H₂O for 16 h gave **2**, **1**, and **3** in 15%, 10%, and 45% yields, respectively. Allowing more time for the reaction resulted in no change of the product ratio (after 32 h: **2**, 45%; **1**, 10%; **3**, 45%).

Using **6** instead of **7** brought about a slower consumption of **3**. Thus, when CF₃CO₂H was used, 56% of **3** still existed even after a reaction time of 1 day, and **2** and **1** were produced in 16% and 28% yields, respectively (Fig. 2c). In the case of CHF₂CO₂H, 79% of **3** remained after 3 days (Fig. 2d). In both the reactions, the consumption of **3** seemed to proceed only in the initial stage (CF₃CO₂H after 15 min: **2**, 8%; **1**, 25%; **3**, 67%; after 3 h: **2**, 11%; **1**, 29%; **3**, 60%; after 1 day: **2**, 16%; **1**, 28%; **3**, 56%; CHF₂CO₂H after 1 h: **2**, 5%; **1**, 13%; **3**, 82%; after 4 h: **2**, 3%; **1**, 15%; **3**, 82%; after 8 h: **2**, 3%; **1**, 15%; **3**, 82%; after 3 days: **2**, 6%; **1**, 15%; **3**, 79%). The reaction with NCCH₂CO₂H for 5 days led to the quantitative recovery of **3**. When *p*-TsOH·H₂O was used, only a slight decomposition of **3** to **1** was observed in the initial stage (after 1 h: **2**, none; **1**, 7%; **3**, 93%; after 3 days: **2**, none; **1**, 3%; **3**, 97%). Consequently, a combination of **6** and NCCH₂CO₂H or *p*-TsOH·H₂O is considered to be better for preventing both the isomerization



SCHEME 2

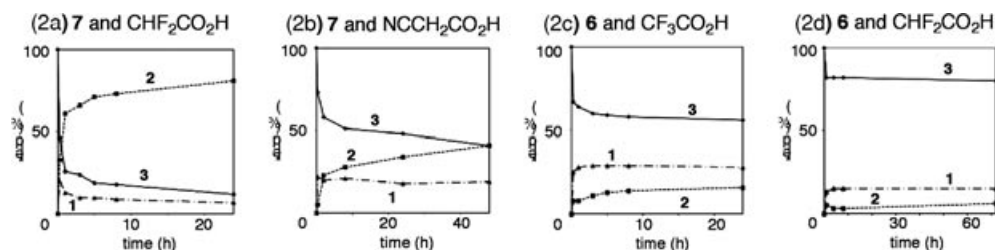
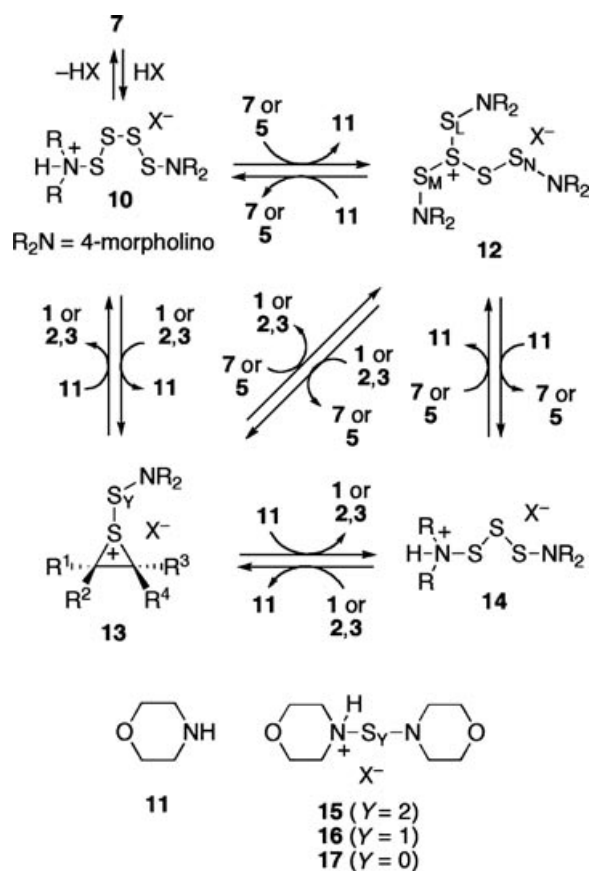


FIGURE 2 Diachronic change of product yields in the reaction of **3** with the sulfuration reagent and carboxylic acids. Sulfuration reagent (1.0 molar equivalent), Brønsted acid (1.0 molar equivalent) in CDCl_3 at r. t. By ^1H NMR.

and decomposition of **3** than other combinations. However, the combinations unfortunately did not produce satisfactory results for the thiirane.

Possible Mechanism of the Thiirane

The possible mechanism of the thiirane of **1** and the decomposition of **3** is as follows (Scheme 3). One of the basic nitrogen atoms of **7** is protonated by a



SCHEME 3

Brønsted acid (HX) to give the ammonium salt **10**, which then reacts with **7** to form morpholine **11** and the sulfonium salt **12**. The reactions of **1** with **10** and **12** gives the thiiranium salt **13**, which is also produced by the reactions of **2** and **3**, together with **11** in the case of **10**, and 4,4'-oligothiodimorpholine **5** in the case of **12**. The sulfonium salt **12** may be less reactive to **3** than **10**, so that the drastic decomposition of **3** proceeds in the initial stage of the reaction. A substitution reaction at the sulfur atom next to the positively charged sulfur atom in **13** with **11** takes place to give **2**, **3**, and the ammonium salt **14**, which also reacts with **7** to form **12** and **11**. These sequential processes are reversible and, therefore, the decomposition of **3** to **1** proceeds. Thus, the substitution reaction at the positively charged sulfur atom in **13** with **7** or **11** affords **1**. The similar processes for the reaction of **1** with **14**, **15**, or **16** lead to the formation of **2** and **3**, together with **15**, **16**, or **17**. The ammonium salt **15** or **16** is also produced by the reaction of **6** or **8** with a Brønsted acid. The reason why the thiirane becomes slower as the number of sulfur atoms in **5** decreases must be that steric congestion around the reactive sulfur atom in the ammonium salts and **12** increases and electronic repulsions among their lone pairs of the nitrogen and sulfur atoms decrease.

Two mechanisms of the isomerization of **3** to **2** are possible. One includes the reverse pathway of the thiirane formation mentioned above, which results in the formation of **1**, followed by the resulfuration of **1**. The other contains five sequential reversible processes: (1) formation of **18**, (2) cleavage of the C–S bond close to the 9-benzonorbornenyldiene group to give intermediates **19**, which is stabilized by neighboring-group participation of the benzene ring, (3) rotation about the central C–C bond, (4) recombination of the C–S bond in **20** to form **21**, and (5) removal of the ammonium salt like **10** and the sulfonium salt **12** to form the thermally more stable **2** rather than **3** [13,14].

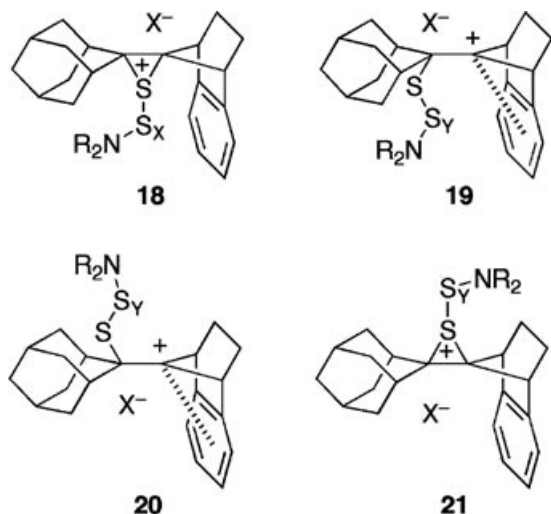


FIGURE 3

EXPERIMENTAL

Solvents were dried and purified in the usual manner. 4,4'-tetrathiodimorpholine **7** was recrystallized several times from EtOH. 4,4'-dithiodimorpholine **6** was purchased from Tokyo Chemical Industry (Tokyo, Japan) and purified by recrystallization from EtOH. 4,4'-thiodimorpholine **8** was prepared and purified by the literature method [21]. 2-(4'-morpholinodisulfanyl) benzothiazole **9** was gifted from Ouchi Shinko Chemical Industrial and purified by recrystallization from EtOH. All the reactions were carried out under argon. Silica gel column chromatography was performed on silica gel 60N (Kanto, 63–210 μm , spherical, neutral). Melting points were determined on a Mel-Temp capillary tube apparatus and are uncorrected. ^1H and ^{13}C -NMR spectra were recorded on a Bruker AC300P (300.1 MHz for ^1H) or a Bruker AC200 (200.1 MHz for ^1H and 50.3 MHz for ^{13}C) spectrometer using CDCl_3 as the solvent with TMS for ^1H and with CDCl_3 for ^{13}C as the internal standard. Elemental analyses were performed by the Molecular Analysis and Life Science Center of Saitama University.

4,4'-Tetrathiodimorpholine **7**

Faint yellow needles (from EtOH), mp 121.2–121.8°C (mp 118.5–119.5°C) [21]; ^1H NMR (300.1 MHz) δ 3.03 (t-like, 8H), 3.74 (t-like, 8H); ^{13}C NMR (50.3 MHz) δ 55.7, 67.0; Anal. Calcd for $\text{C}_8\text{H}_{16}\text{N}_2\text{O}_2\text{S}_4$: C, 31.89; H, 5.37; N, 9.32. Found: C, 32.17; H, 5.28; N, 9.19.

4,4'-Dithiodimorpholine **6**

Colorless needles (from EtOH), mp 126.5–127.0°C (mp 124–125°C) [22]; ^1H NMR (300.1 MHz) δ 2.83 (t-like, 8H), 3.74 (t-like, 8H); ^{13}C NMR (50.3 MHz) δ 55.7, 67.2; Anal. Calcd for $\text{C}_8\text{H}_{16}\text{N}_2\text{O}_2\text{S}_2$: C, 40.65; H, 6.28; N, 11.85. Found: C, 40.89; H, 6.48; N, 11.74.

General Procedures for Sulfuration of **1** with the Sulfuration Reagent and Brønsted Acid

A solution of **1** (73–100 μmol), the sulfuration reagent, and Brønsted acid in solvent (2.0 mL) was allowed to stand at room temperature or was heated at reflux. The reaction was quenched by addition of aqueous NaHCO_3 solution. After CH_2Cl_2 was added to the mixture, the organic layer was separated, washed with H_2O , dried over K_2CO_3 , and evaporated under reduced pressure. A ratio of the products was estimated by ^1H NMR.

General Procedures for Reaction of **3** with the Sulfuration Reagent and Brønsted Acid

A solution of **3** (7.7 mg, 25 μmol), the sulfuration reagent (25 μmol), Brønsted acid (25 μmol), and triptycene as an internal standard in CDCl_3 (0.50 mL) was allowed to stand at room temperature. Progress of the reaction was monitored by ^1H NMR.

ACKNOWLEDGMENTS

This work was supported by Grants-in-Aid for Scientific Research from Japan Society for the Promotion of Science. The authors thank Ouchi Shinko Chemical Industrial Co. Ltd. for the gift of vulcanizing agents, **6** and **9**.

REFERENCES

- [1] Pearson, W. H.; Lian, B. W.; Bergmeier, S. C. In *Comprehensive Heterocyclic Chemistry II*; Padwa, A. (Ed.); Pergamon: Oxford, 1996; Vol. 1A, Ch. 1.01, pp. 1–60.
- [2] Rai, K. M. L.; Hassner, A. In *Comprehensive Heterocyclic Chemistry II*; Padwa, A. (Ed.); Pergamon: Oxford, 1996; Vol. 1A, Ch. 1.02, pp. 61–96.
- [3] Erden, I. In *Comprehensive Heterocyclic Chemistry II*; Padwa, A. (Ed.); Pergamon: Oxford, 1996; Vol. 1A, Chs. 1.03, pp. 98–144 and 1.04, pp. 145–171.
- [4] Ando, W.; Choi, N.; Tokitoh, N. In *Comprehensive Heterocyclic Chemistry II*; Padwa, A. (Ed.); Pergamon: Oxford, 1996; Vol. 1A, Ch. 1.05, pp. 173–240.
- [5] Harring, S. R.; Livinghouse, T. In *Comprehensive Heterocyclic Chemistry II*; Padwa, A. (Ed.); Pergamon: Oxford, 1996; Vol. 1A, Ch. 1.06, pp. 241–258.

- [6] Block, E. Reactions of Organosulfur Compounds; Academic Press: New York, 1973.
- [7] Oae, S. Organic Sulfur Chemistry: Structure and Mechanism; CRC: Florida, 1991.
- [8] Metzner P.; Thuillier, A. Sulfur Reagents in Organic Synthesis; Academic Press: London, 1993.
- [9] Cremlyn, R. J. An Introduction to Organosulfur Chemistry; John Wiley and Sons: Chichester, 1996.
- [10] Adam, W.; Bargon, R. M. Chem Rev 2004, 104, 251–262, and references cited therein.
- [11] Sugihara, Y.; Noda, K.; Nakayama, J. Bull Chem Soc Jpn 2000, 73, 2351–2356.
- [12] Sugihara, Y.; Noda, K.; Nakayama, J. Tetrahedron Lett 2000, 41, 8907–8911.
- [13] Sugihara, Y.; Noda, K.; Nakayama, J. Tetrahedron Lett 2000, 41, 8913–8916.
- [14] Sugihara, Y.; Aoyama, Y.; Nakayama, J. Chem Lett 2001, 980–981.
- [15] Sugihara, Y.; Aoyama, Y.; Okada, H.; Nakayama, J. Chem Lett 2008, 668–669.
- [16] Sugihara, Y.; Ohtsu, R.; Nakayama, J. Heterocycles 2008, 75, 2415–2420.
- [17] Sugihara, Y.; Kobiki, A.; Nakayama, J. Heterocycles 2009, 78, 103–115.
- [18] Saville, R. W. J Chem Soc 1958, 2880–2882.
- [19] Furukawa, M.; Sato, K.; Okawara, T. Chem Lett 1982, 2007–2010.
- [20] Okawara, T.; Yamasaki, T.; Sato, K.; Miyazaki, H.; Furukawa, M. Chem Pharm Bull 1985, 33, 5225–5230.
- [21] Diaz, V. C.; Arancibia, A. Phosphorus Sulfur Silicon Relat Elem 1989, 44, 1–8.
- [22] Blake, E. S. J Am Chem Soc 1943, 65, 1267–1269.
- [23] Dippy, J. F. J.; Hughes, S. R. C.; Rozanski, A. J Chem Soc 1959, 2492–2498.
- [24] Bordwell, F. G. Acc Chem Res 1988, 21, 456–463.

Syntheses and Crystal Structures of Triorganotin (IV) Derivatives with 2,2'-Bipyridine-4,4'-Dicarboxylic Acid

Ru-Fen Zhang,¹ Qian-Li Li,¹ and Chun-Lin Ma^{1,2,*}

¹Department of Chemistry, Liaocheng University, Liaocheng, People's Republic of China

²Department of Chemistry, Taishan University, Taian, People's Republic of China

Received 28 October 2008; revised 5 November 2008

ABSTRACT: Four organotin complexes with 2,2'-bipyridine-4,4'-dicarboxylic acid, H_2dcbp : $(Ph_3Sn)_2(dcbp)$ **1**, $[(PhCH_2)_3Sn]_2(dcbp) \cdot 2CH_3OH$ **2**, $[(Me_3Sn)_2(dcbp)]_n$ **3**, $[(Bu_3Sn)_2(dcbp)]_n$ **4** have been synthesized. The complexes **1–4** were characterized by elemental, IR, 1H , ^{13}C , ^{119}Sn NMR, and X-ray crystallographic analyses. Crystal structures show that complex **1** is a monomer with one ligand coordinated to two triorganotin moieties, and a 1D infinite polymeric chain generates via intermolecular C–H...N hydrogen bond; complex **2** is also a monomer and forms a 2D network by intermolecular O–H...O weak interaction; both of complexes **3** and **4** form 2D network structures where 2,2'-bipyridine-4,4'-dicarboxylate acts as a tetradentate ligand coordinated to trimethyltin and tri-*n*-butyltin ions, respectively.

© 2009 Wiley Periodicals, Inc. *Heteroatom Chem* 20:19–28, 2009; Published online in Wiley InterScience (www.interscience.wiley.com). DOI 10.1002/hc.20506

INTRODUCTION

Organotin carboxylates have received considerable attention because of their various structural types that may be adopted in the solid state. Several

products such as monomers, dimers, tetramers, oligomeric ladders, and hexameric drums have been isolated [1–4]. It has also been demonstrated that other structural types are formed because of the presence of additional coordinating sites (e.g., N, O, S) along with a carboxylate moiety [5–6]. Chandrasekhar and coworkers have reported the self-assembly of macrocycle networks in the reaction of pyrazole-3,5-dicarboxylic acid and Bz_2SnCl_2 [7]. García-Zarracino and Höpfl obtained the supramolecular architectures by the reaction of 2,5-pyridinedicarboxylic acid and R_2SnO ($R = Me, n-Bu, Ph$) [8]. Wang reported a monomer with 2,2'-biquinoline-4,4'-dicarboxylate and triphenyltin chloride [9]. In our previous work, we have also reported several novel molecular structures on it, such as two 15-membered trinuclear macrocyclic complexes with 2-pyrazinecarboxylic acid [10], and a series of triorganotin pyridinedicarboxylates with 2,5-, 3,5-, and 2,6-pyridinedicarboxylic acid [11]. To continue our research, we selected another interesting ligand, 2,2'-bipyridine-4,4'-dicarboxylic acid, on the basis of the following considerations: (a) the 2,2'-bipyridine and carboxylate functional groups of H_2dcbp all have coordinate abilities, either singly or in unison, so several potential multiple molecular models in organotin complexes may be possess; (b) it can act not only as a hydrogen bond acceptor but also as a hydrogen bond donor, so the preparation of hybrid networks combining the strength of coordination bonding with the flexibility of hydrogen bonding is also feasible; and (c) it possesses high symmetry that

*Correspondence to: Chun-Lin Ma; e-mail: macl@lcu.edu.cn.
Contract grant sponsor: National Natural Foundation, People's Republic of China.

Contract grant number: 20741008.
© 2009 Wiley Periodicals, Inc.

may be helpful for the crystal growth of the product formed.

The synthesis and characterization of some transition metal complexes of 2,2'-bipyridine-4,4'-dicarboxylic acid have been carried out previously [12–19]. Besides, the preparation and the crystal of structures of trimethyltin derivative of 2,2'-bipyridine-4,4'-dicarboxylic acid have been reported by Stocco et al. [20]. They obtained the complex by the condensation of H₂dcbp and Me₃SnOH in 1:2 molar ratio, but we employ Me₃SnCl instead of Me₃SnOH to prepare the complex. Herein, we report four triorganotin (IV) complexes constructed from H₂dcbp, with a 1:2:2 molar ratio of H₂dcbp: EtONa: R₃SnCl.

EXPERIMENTAL DETAILS

Materials and Measurements

Trimethyltin chloride, triphenyltin chloride, tri-*n*-butyltin chloride and 2,2'-bipyridine-4,4'-dicarboxylic acid and were commercially available, and they were used without purification. Tribenzyltin (IV) chloride was prepared by a standard method reported in the literature [21]. The melting points were obtained with Kofler micro melting point apparatus and uncorrected. Infrared spectra were recorded on a Nicolet-5700 (Thermo Electron Corporation) spectrophotometer using KBr disks and sodium chloride optics. ¹H, ¹³C, and ¹¹⁹Sn NMR spectra were recorded on Varian Mercury Plus400 (Varian Medical Systems) spectrometer operating at 400, 100.6 and 149.2 MHz, respectively. The spectra were acquired at room temperature (298 K) unless otherwise specified; ¹³C spectra are broadband proton decoupled. The chemical shifts are reported in parts per million (ppm) with respect to the references and are stated relative to external tetramethylsilane for ¹H and ¹³C NMR and Me₄Sn for ¹¹⁹Sn NMR. Elemental analyses were performed with a PE-2400II apparatus.

Syntheses of the Complexes 1–4

(Ph₃Sn)₂(dcbp) 1. The reaction is carried out under nitrogen atmosphere. The 2,2'-bipyridine-4,4'-dicarboxylic acid (0.244 g, 1 mmol) and the sodium ethoxide (0.136 g, 2 mmol) were added to the solution of methanol (30 mL) in a Schlenk flask and stirred for 30 min. Then the triphenyltin chloride (0.771 g, 2 mmol) was added to the reactor, the reaction mixture was stirred for 12 h at 40°C. After cooling down to room temperature, it was filtered. The solvent of the filtrate was gradually removed by evaporation under vacuum un-

til solid product was obtained. The solid was recrystallized from ether, and a transparent colorless crystal was formed. Yield: 85%; mp > 220°C. Anal. Calcd for C₄₈H₃₆N₂O₄Sn₂: C, 61.19; H, 3.85; N, 2.97%. Found: C, 60.93; H, 4.01; N, 2.71%. IR (KBr, cm⁻¹): ν_{as}(COO), 1635; ν_s(COO), 1331; ν(Sn–C), 558; ν(Sn–O), 447. ¹H NMR [(CD₃)₂SO, ppm]: δ = 7.59–8.68 (m, 6H, bipyridine); 7.28–7.49 (m, 30H, Ph). ¹³C NMR [(CD₃)₂SO, ppm]: δ = 170.16 (COO); 121.85, 124.06, 142.25, 150.77, 157.11 [bipyridine(=CH)]; 130.43–137.43 (Ar–C). ¹¹⁹Sn NMR [(CD₃)₂SO, ppm]: –44.8.

[(PhCH₂)₃Sn]₂(dcbp)·2CH₃OH 2. The procedure is similar to that of complex 1: 2,2'-bipyridine-4,4'-dicarboxylic acid (0.244 g, 1 mmol), sodium ethoxide (0.136 g, 2 mmol), and tribenzyltin chloride (0.854 g, 2 mmol) were reacted for 12 h at 40°C. Recrystallized from methanol, a transparent colorless crystal was formed. Yield: 78%; mp > 220°C. Anal. Calcd for C₅₆H₅₆N₂O₆Sn₂: C, 61.18; H, 5.18; N, 2.57%. Found: C, 60.98; H, 5.37; N, 2.31%. IR (KBr, cm⁻¹): ν(OH), 3207; ν_{as}(COO), 1636; ν_s(COO), 1337; ν(Sn–C), 560; ν(Sn–O), 452. ¹H NMR [(CD₃)₂SO, ppm]: δ = 7.56–8.70 (m, 6H, bipyridine); 6.96–7.31 (m, 30H, Ph), 2.63 (s, 12H, Ph–CH₂), 4.54 (s, 2H, O–H), 3.31 (s, 6H, O–CH₃). ¹³C NMR[(CD₃)₂SO, ppm]: δ = 170.08 (COO); 120.09, 122.56, 139.39, 149.34, 155.67 [bipyridine(=CH)]; 130.43–137.43 (Ar–C); 26.63 (Ph–CH₂). ¹¹⁹Sn NMR [(CD₃)₂SO, ppm]: –152.7.

[(Me₃Sn)₂(dcbp)]_n 3. The procedure is similar to that of complex 1, 2,2'-bipyridine-4,4'-dicarboxylic acid (0.244 g, 1 mmol), sodium ethoxide (0.136 g, 2 mmol) and trimethyltin chloride (0.398 g, 2 mmol) were reacted for 12 h at 40°C. Recrystallized from ether, a transparent colorless crystal was formed. Yield: 81%; mp > 220°C. Anal. Calcd for C₁₈H₂₄N₂O₄Sn₂: C, 37.94; H, 4.25; N, 4.92%. Found: C, 37.61; H, 4.57; N, 4.70%. ν_{as}(COO), 1614; ν_s(COO), 1403; ν(Sn–C), 550; ν(Sn–O), 476. ¹H NMR [(CD₃)₂SO, ppm]: δ = 7.32–8.77 (m, 6H, bipyridine); 0.85–0.88 (s, 18H, CH₃). ¹³C NMR[(CD₃)₂SO, ppm]: δ = 169.38 (COO); 120.09, 122.56, 139.39, 149.34, 155.67 [bipyridine(=CH)]; 14.56 (CH₃). ¹¹⁹Sn NMR [(CD₃)₂SO, ppm]: –127.4.

[(Bu₃Sn)₂(dcbp)]_n 4. The procedure is similar to that of complex 1, 2,2'-bipyridine-4,4'-dicarboxylic acid (0.244 g, 1 mmol), sodium ethoxide (0.136 g, 2 mmol) and tri-*n*-butyltin chloride (0.651 g, 2 mmol) were reacted for 12 h at 40°C. Recrystallized from ether-petroleum, a transparent colorless crystal was formed. Yield: 88%; mp > 220°C. Anal. Calcd for C₇₂H₁₂₀N₄O₈Sn₄: C, 52.58, H, 7.35; N,

3.41%. Found: C, 52.42; H, 7.51; N, 3.24%. $\nu_{\text{as}}(\text{COO})$, 1613; $\nu_{\text{s}}(\text{COO})$, 1403; $\nu(\text{Sn}-\text{C})$, 524; $\nu(\text{Sn}-\text{O})$, 471. ^1H NMR $[(\text{CD}_3)_2\text{SO}]$, ppm]: δ = 7.27–8.81 (m, 12H, bipyridine); 1.34–1.73 (m, 72H, $\text{CH}_2\text{CH}_2\text{CH}_2$); 0.91–0.95 (t, 36H, CH_3). ^{13}C NMR $[(\text{CD}_3)_2\text{SO}]$, ppm]: δ 170.04 (COO); 121.59, 123.89, 141.09, 150.04, 156.97 [bipyridine(=CH)]; 13.83, 26.02, 27.25, 28.13 (*n*-Bu). ^{119}Sn NMR $[(\text{CD}_3)_2\text{SO}]$, ppm]: –105.9.

X-Ray Crystallographic Studies

Crystals were mounted in Lindemann capillaries under nitrogen. Diffraction data were collected on a Smart CCD area-detector with graphite monochromated $\text{MoK}\alpha$ radiation ($\lambda = 0.71073$ Å). A semiempirical absorption correction was applied to the data. The structure was solved by direct methods using SHELXS-97 and refined against F^2 by full matrix least-squares using SHELXS-97. Hydrogen atoms were placed in calculated positions. Crystal data and experimental details of the structure determinations are listed in Table 1.

RESULT AND DISCUSSION

Syntheses of the Complexes 1–4

The syntheses procedures are shown in Scheme 1.

IR Spectroscopic Studies of the Complexes 1–4

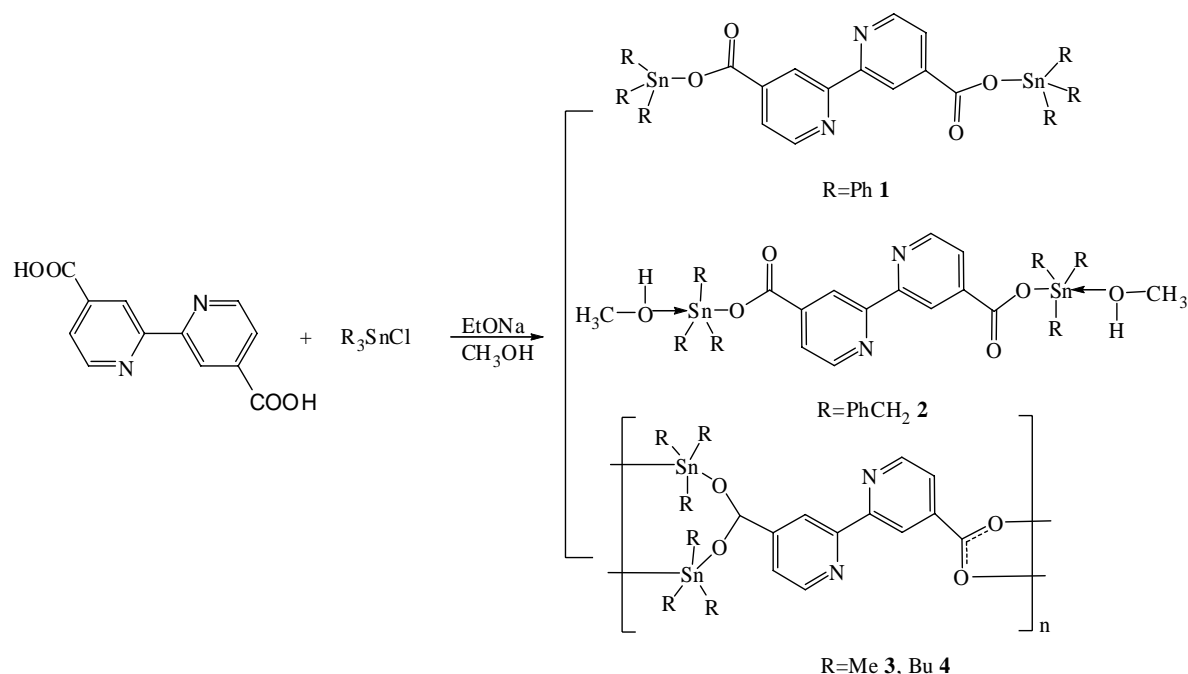
The stretching frequencies of interest are those associated with the $\text{C}(\text{O})\text{O}$, $\text{Sn}-\text{C}$, and $\text{Sn}-\text{O}$ groups. The strong absorption in the region $447\text{--}476\text{ cm}^{-1}$, which is absent in the spectrum of the free ligand, is assigned to the $\text{Sn}-\text{O}$ stretching mode. All these values are consistent with those detected in a number of organotin (IV)-oxygen derivatives [22,23]. Comparing the IR spectra of the free ligand with complexes **1**, **3**, and **4**, the explicit feature is the absence of a band in the region $3200\text{--}3500\text{ cm}^{-1}$, which appears in the free ligand as the $-\text{OH}$ stretching vibration, thus indicating metal-ligand bond formation through this site. The IR spectrum of **2** exhibits a broad band at 3207 cm^{-1} , attributed to $\nu(\text{MeO}-\text{H})$ stretching vibration.

^1H NMR, ^{13}C NMR, and ^{119}Sn NMR Data of Complexes 1–4

The ^1H NMR spectra show the expected integration and peak multiplicities. The single resonance of $-\text{OH}$ in the spectra of the free ligand is absent in the spectra of all the complexes **1–4** indicating the replacement of the carboxylic acid protons by a triorganotin moiety on complex formation.

TABLE 1 Crystal Data and Refinement Details for Complexes **1**, **2**, and **4**

Complex	1	2	4
Empirical formula	$\text{C}_{48}\text{H}_{36}\text{N}_2\text{O}_4\text{Sn}_2$	$\text{C}_{56}\text{H}_{56}\text{N}_2\text{O}_6\text{Sn}_2$	$\text{C}_{72}\text{H}_{120}\text{N}_4\text{O}_8\text{Sn}_4$
Formula weight	942.17	1,090.41	1,644.48
Wavelength (Å)	0.71073	0.71073	0.71073
Crystal system	Triclinic	Monoclinic	Triclinic
Space group	P-1	P2(1)/c	P-1
<i>a</i> (Å)	13.1560(13)	9.1017(10)	20.563(2)
<i>b</i> (Å)	14.9691(18)	12.7688(12)	20.569(2)
<i>c</i> (Å)	17.420(3)	22.927(3)	25.012(3)
α (°)	72.171(2)	90	110.077(2)
β (°)	81.329(3)	101.246(2)	93.9170(10)
γ (°)	69.270(2)	90	90.0460(10)
<i>V</i> (Å ³)	3,051.0(6)	2,613.4(5)	9,910.0(19)
<i>Z</i>	3	2	4
<i>D</i> _{calc}	1.538	1.386	1.102
<i>F</i> (000)	1,410	1,108	3,376
μ (mm ^{−1})	1.275	1.005	1.037
Crystal size	0.24 × 0.18 × 0.13	0.50 × 0.49 × 0.27	0.50 × 0.40 × 0.20
θ Range (°)	1.23–25.01	1.81–25.00	1.2–25.01
Reflection collected	15,652	12,518	50,572
Independent reflections	10,539	4,473	33,969
Data/restraints/parameters	10,539/0/757	4,473/486/ 99	33,969/3,635/1,607
Goodness-of-fit on	1.068	1.005	1.030
Final <i>R</i> indices [<i>I</i> > 2 sigma (<i>I</i>)]	<i>R</i> ₁ = 0.0520 <i>wR</i> ₂ = 0.1050	<i>R</i> ₁ = 0.0556 <i>wR</i> ₂ = 0.1173	<i>R</i> ₁ = 0.0762 <i>wR</i> ₂ = 0.1552
<i>R</i> indices (all data)	<i>R</i> ₁ = 0.1202 <i>wR</i> ₂ = 0.1371	<i>R</i> ₁ = 0.0694 <i>wR</i> ₂ = 0.1270	<i>R</i> ₁ = 0.1992 <i>wR</i> ₂ = 0.1685



SCHEME 1

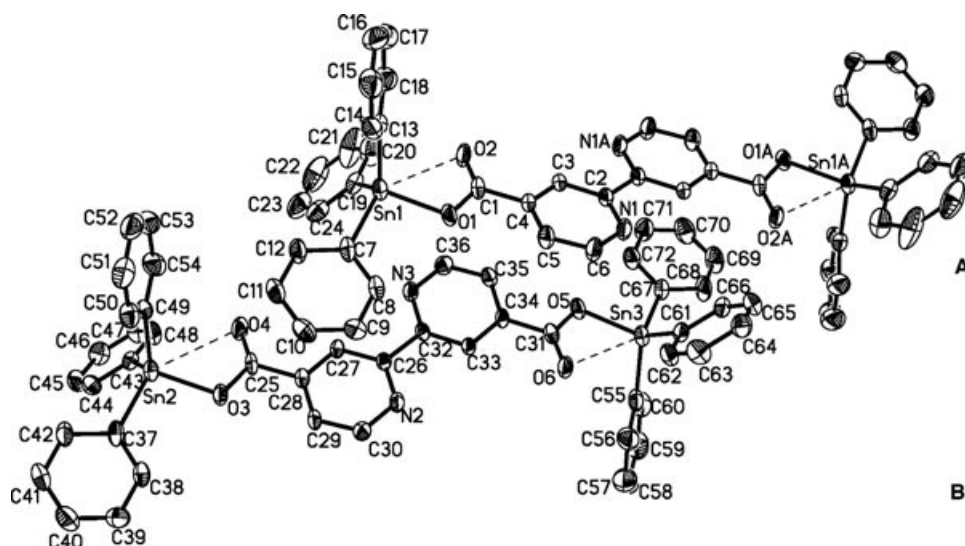
The ^{13}C NMR spectra of all complexes show a significant downfield shift of all carbon resonances compared with the free ligands; the shift is a consequence of an electron density transfer from the ligand to the metal atoms. The single resonances at 169.38–170.16 are attributed to the COO^- groups in the complexes **1–4**. These data are consistent with the structures of **1–4**.

The ^{119}Sn NMR spectra of complexes **1–4** show resonances between -44.8 and -152.7 ppm. As re-

ported in the literature [24], we can conclude that complex **1** ($\delta = -44.8$) is typical of four-coordinate and complexes **2–4** ($\delta = -152.7$, -127.4 , -105.9) are typical five-coordinate. This is confirmed by the X-ray crystal structures.

Crystal Structures of Complexes **1**, **2**, and **4**

*Structures of Complexes **1** and **2**.* The crystal structures of complexes **1** and **2** are shown in Figs. 1

FIGURE 1 The molecular structure of complex **1**.

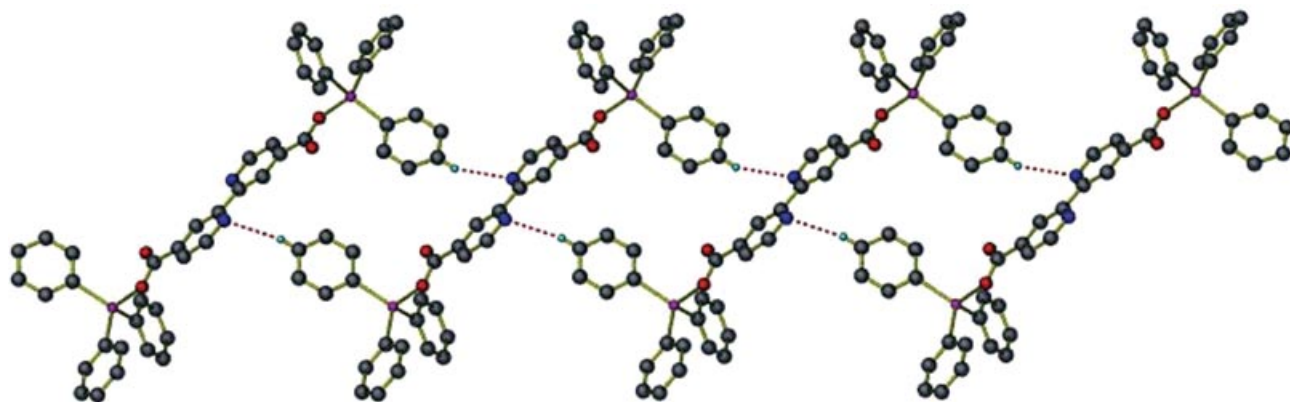


FIGURE 2 The 1D infinite chain structure of complex connected by intermolecular C—H...N hydrogen bonding.

and 2, and selected bond lengths and angles are given in Tables 2 and 3, respectively.

For complex **1**, the asymmetric unit contains two monomers A and B, which are crystallographically nonequivalent. The conformations of the two inde-

pendent molecules A and B are almost the same, with only small differences in bond lengths and bond angles. Each discrete molecule is a monomer with one ligand coordinated to two triorganotin moieties. As follows, the Sn(1)—O(1) [2.054(5) Å] bond length lies

TABLE 2 Selected Bond Lengths (Å) and Bond Angles (°) for **1**

Bond lengths			
Sn(1)—O(1)	2.054(5)	Sn(2)—C(43)	2.128(8)
Sn(1)—C(13)	2.112(9)	Sn(2)—C(37)	2.129(9)
Sn(1)—C(19)	2.115(9)	Sn(3)—O(5)	2.049(5)
Sn(1)—C(7)	2.128(8)	Sn(3)—C(67)	2.102(8)
Sn(2)—O(3)	2.050(5)	Sn(3)—C(55)	2.118(9)
Sn(2)—C(49)	2.122(8)	Sn(3)—C(61)	2.126(8)
Bond angles			
O(1)—Sn(1)—C(13)	104.7(3)	O(3)—Sn(2)—C(37)	95.7(3)
O(1)—Sn(1)—C(19)	115.2(3)	C(49)—Sn(2)—C(37)	111.1(3)
C(13)—Sn(1)—C(19)	116.3(4)	C(43)—Sn(2)—C(37)	111.2(3)
O(1)—Sn(1)—C(7)	94.6(3)	O(5)—Sn(3)—C(55)	108.8(3)
C(13)—Sn(1)—C(7)	111.8(3)	C(67)—Sn(3)—C(55)	110.1(4)
C(19)—Sn(1)—C(7)	112.0(3)	O(5)—Sn(3)—C(61)	111.9(3)
O(3)—Sn(2)—C(49)	105.8(3)	C(67)—Sn(3)—C(61)	113.6(3)
O(3)—Sn(2)—C(43)	114.1(3)	C(55)—Sn(3)—C(61)	116.2(3)
C(49)—Sn(2)—C(43)	116.9(3)		

TABLE 3 Selected Bond Lengths (Å) and Bond Angles (°) for **2**

Bond lengths			
Sn(1)—C(21)	2.124(6)	Sn(1)—C(14)	2.139(7)
Sn(1)—O(1)	2.123(4)	Sn(1)—O(3)	2.497(5)
Bond angles			
C(21)—Sn(1)—O(1)	93.7(2)	C(14)—Sn(1)—C(7)	120.5(3)
C(21)—Sn(1)—C(14)	117.2(3)	C(21)—Sn(1)—O(3)	77.4(2)
O(1)—Sn(1)—C(14)	100.5(2)	O(1)—Sn(1)—O(3)	170.25(17)
C(21)—Sn(1)—C(7)	118.4(3)	C(14)—Sn(1)—O(3)	87.2(2)
O(1)—Sn(1)—C(7)	95.6(3)	C(7)—Sn(1)—O(3)	85.3(3)
C(1)—O(1)—Sn(1)	123.7(4)		

Symmetry code: #1 $-x+1, -y, -z+1$.

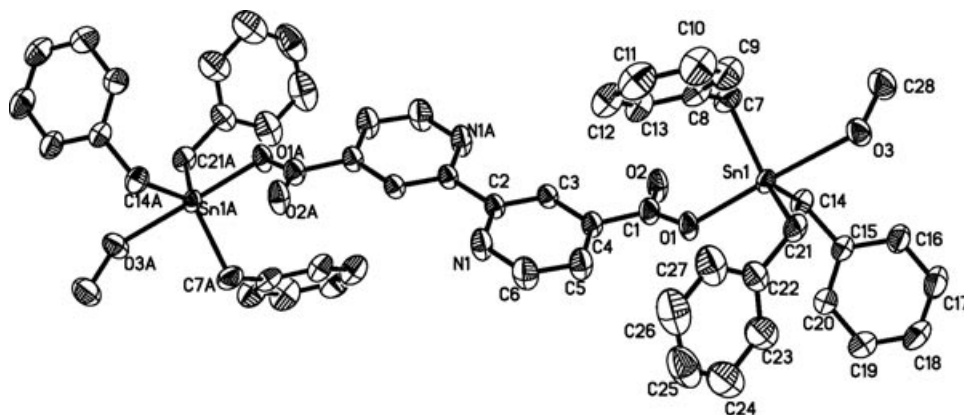


FIGURE 3 The molecular structure of complex 2.

in the range that has been reported as the Sn–O covalent bond length [2.054(3)–2.083 Å] [25]; the Sn(2)–O(3) [2.050(5) Å] and the Sn(3)–O(5) [2.049(5) Å] are little shorter than the reported. All the Sn–O bond lengths are shorter than the sum of the covalent radii of Sn and O (2.13 Å) [26] so they all prove that the oxygen atoms are coordinated to the tin atoms by a strong chemical bond.

Furthermore, it is noteworthy that a weak intramolecular Sn...O interaction is recognized between the Sn(1) and O(2), Sn(2) and O(4), and Sn(3) and O(6). Although the distances of Sn(1)...O(2)

[2.815 Å], Sn(2)...O(4) [2.878 Å], and Sn(3)...O(6) [2.853 Å] are all considerably longer than the normal Sn–O covalent bond length, they lie in the range of Sn...O distances of (2.61–3.02 Å), which have been confidently reported for intramolecular bonds [27,28]. As the oxygen atom is involved in a weak coordinative interaction with tin along one of the tetrahedral faces, the structure distortion for the tin atom in complex 1 is best described as a capped tetrahedral.

Moreover, intermolecular C–H...N hydrogen bonds are recognized in complex 1, which linked

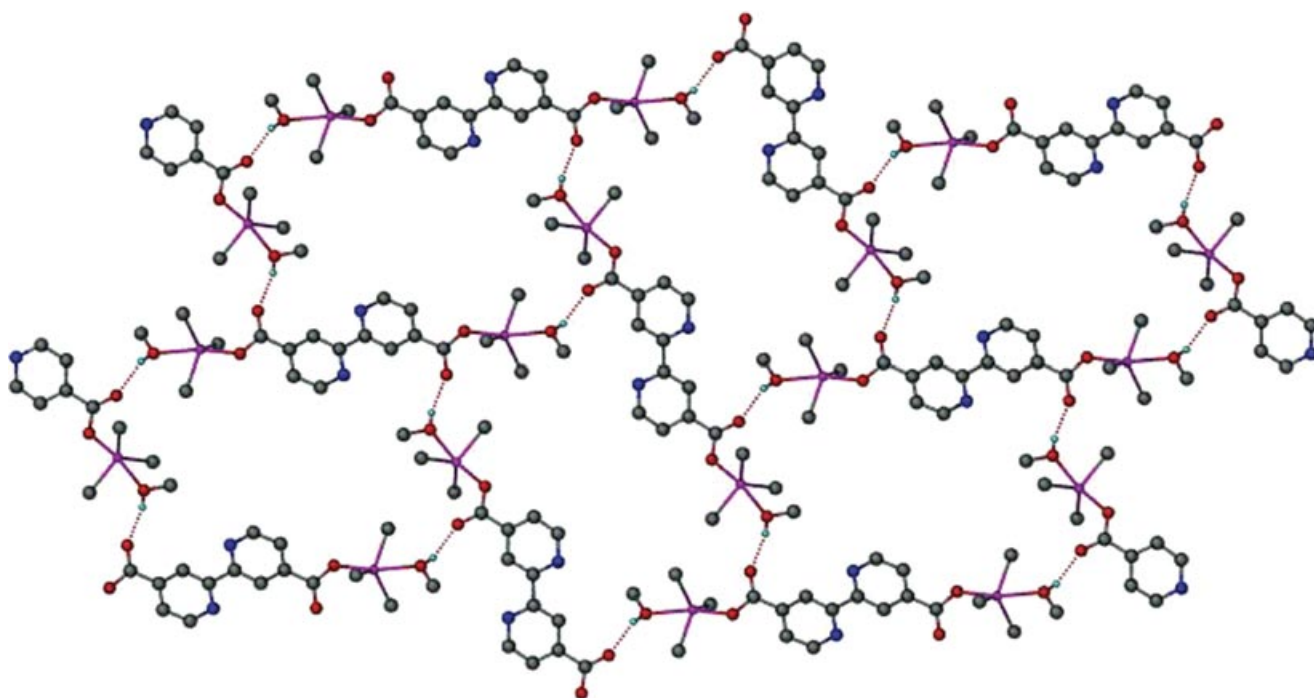


FIGURE 4 The 2D network structure of complex 2 connected by intermolecular O—H...O hydrogen bonding.

TABLE 4 Selected Bond Lengths (Å) and Bond Angles (°) for **4**

Bond lengths			
Sn(1)–C(33)	2.120(14)	Sn(5)–C(101)	2.154(13)
Sn(1)–C(29)	2.136(12)	Sn(5)–C(105)	2.181(12)
Sn(1)–C(25)	2.136(13)	Sn(5)–O(9)	2.168(8)
Sn(1)–O(1)	2.161(7)	Sn(5)–O(16)	2.591(11)
Sn(1)–O(8)	2.575(11)	Sn(6)–C(117)	2.101(11)
Sn(2)–C(45)	2.102(14)	Sn(6)–C(113)	2.140(12)
Sn(2)–C(37)	2.116(13)	Sn(6)–C(109)	2.162(12)
Sn(2)–C(41)	2.150(12)	Sn(6)–O(11)	2.168(8)
Sn(2)–O(3)	2.149(8)	Sn(6)–O(14)	2.594(11)
Sn(3)–C(57)	2.107(13)	Sn(7)–C(125)	2.106(13)
Sn(3)–C(53)	2.145(13)	Sn(7)–C(121)	2.127(14)
Sn(3)–C(49)	2.170(13)	Sn(7)–O(13)	2.149(8)
Sn(3)–O(5)	2.163(8)	Sn(7)–C(129)	2.156(13)
Sn(3)–O(2)	2.594(11)	Sn(7)–O(10)	2.577(11)
Sn(4)–C(65)	2.157(8)	Sn(8)–C(133)	2.103(14)
Sn(4)–C(69)	2.161(12)	Sn(8)–C(141)	2.095(13)
Sn(4)–O(7)	2.157(8)	Sn(8)–C(137)	2.139(13)
Sn(4)–C(61)	2.174(14)	Sn(8)–O(15)	2.152(7)
Sn(5)–C(97)	2.119(12)		
Bond angles			
C(33)–Sn(1)–C(29)	120.4(5)	C(101)–Sn(5)–C(105)	124.5(5)
C(33)–Sn(1)–C(25)	123.7(6)	C(97)–Sn(5)–O(9)	92.1(4)
C(29)–Sn(1)–C(25)	112.8(6)	C(101)–Sn(5)–O(9)	99.1(4)
C(33)–Sn(1)–O(1)	98.6(4)	C(105)–Sn(5)–O(9)	96.4(4)
C(29)–Sn(1)–O(1)	91.4(4)	C(97)–Sn(5)–O(16)	81.8(4)
C(25)–Sn(1)–O(1)	97.0(4)	C(101)–Sn(5)–O(16)	80.7(4)
C(33)–Sn(1)–O(8)	80.8(4)	C(105)–Sn(5)–O(16)	89.6(4)
C(29)–Sn(1)–O(8)	81.6(4)	O(9)–Sn(5)–O(16)	172.7(3)
C(25)–Sn(1)–O(8)	90.4(4)	C(117)–Sn(6)–C(113)	121.5(5)
O(1)–Sn(1)–O(8)	171.3(3)	C(117)–Sn(6)–C(109)	113.7(5)
C(45)–Sn(2)–C(37)	124.8(6)	C(113)–Sn(6)–C(109)	121.5(5)
C(45)–Sn(2)–C(41)	119.0(6)	C(117)–Sn(6)–O(11)	95.0(4)
C(37)–Sn(2)–C(41)	113.3(6)	C(113)–Sn(6)–O(11)	100.9(4)
C(45)–Sn(2)–O(3)	98.3(4)	C(109)–Sn(6)–O(11)	92.1(4)
C(37)–Sn(2)–O(3)	96.4(4)	C(117)–Sn(6)–O(14)	91.5(4)
C(41)–Sn(2)–O(3)	91.7(4)	C(113)–Sn(6)–O(14)	79.2(4)
C(57)–Sn(3)–C(53)	114.0(6)	C(109)–Sn(6)–O(14)	81.4(4)
C(57)–Sn(3)–C(49)	123.7(5)	O(11)–Sn(6)–O(14)	172.3(3)
C(53)–Sn(3)–C(49)	119.9(6)	C(125)–Sn(7)–C(121)	121.2(5)
C(57)–Sn(3)–O(5)	95.3(5)	C(125)–Sn(7)–O(13)	91.4(4)
C(53)–Sn(3)–O(5)	91.0(4)	C(121)–Sn(7)–O(13)	98.6(4)
C(49)–Sn(3)–O(5)	98.4(4)	C(125)–Sn(7)–C(129)	112.5(6)
C(57)–Sn(3)–O(2)	90.7(4)	C(121)–Sn(7)–C(129)	123.3(5)
C(53)–Sn(3)–O(2)	82.1(4)	O(13)–Sn(7)–C(129)	96.8(4)
C(49)–Sn(3)–O(2)	82.2(4)	C(125)–Sn(7)–O(10)	81.4(4)
O(5)–Sn(3)–O(2)	172.3(3)	C(121)–Sn(7)–O(10)	81.1(4)
C(65)–Sn(4)–C(69)	113.0(6)	O(13)–Sn(7)–O(10)	171.2(3)
C(65)–Sn(4)–O(7)	90.8(5)	C(129)–Sn(7)–O(10)	90.7(4)
C(69)–Sn(4)–O(7)	96.5(4)	C(133)–Sn(8)–C(141)	118.9(5)
C(65)–Sn(4)–C(61)	120.2(6)	C(133)–Sn(8)–C(137)	124.2(5)
C(69)–Sn(4)–C(61)	124.2(5)	C(141)–Sn(8)–C(137)	114.1(6)
O(7)–Sn(4)–C(61)	98.5(4)	C(133)–Sn(8)–O(15)	96.8(4)
C(97)–Sn(5)–C(101)	120.2(6)	C(141)–Sn(8)–O(15)	92.7(4)
C(97)–Sn(5)–C(105)	112.5(5)	C(137)–Sn(8)–O(15)	96.8(4)

the molecular into a 1D linear chain. The distances [C–H...N (2.612 Å), C...N (3.476 Å)], and the angle [C–H...N (154.82 Å)] are all close to be reported in Co(dpa)₂[29]. The view of the 1D linear chain is shown in Fig. 2.

For complex **2**, As can be seen from Fig. 3, complex **2** is also a monomer with one ligand coordinated to two triorganotin moieties, but different from complex **1**, all the Sn atoms are five-coordinate with a trigonal bipyramidal structure by

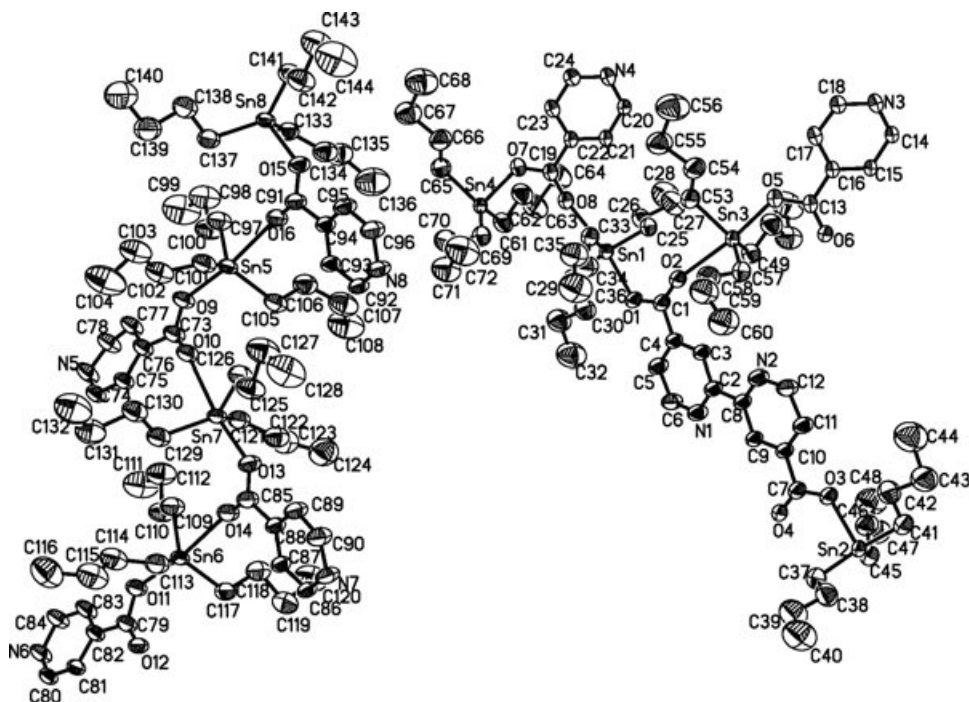


FIGURE 5 The molecular structure of complex **4**.

coordinating an additional methanol group. The Sn(1)–O(1) distance [2.123(4) Å] approaches the sum of the covalent radii of Sn and O (2.13 Å). The axial angle [O(1)–Sn(1)–O(3) = 170.25(17)°] suggests that the structure is near to a normal trigonal bipyramid.

As shown in Fig. 4, owing to the coordinated methanol molecules, a pair of intermolecular O–H...O hydrogen bonds is recognized. Intermolecular hydrogen bond interactions between the methanol and the oxygen atom of an adjacent molecule result in the formation of a 2D network. This is similar to that found in 1,3,5-benzenetricarboxylic acid with trimethyltin chloride [30]. The O...O distance, H...O distance, and the O–H...O angle are 2.709, 1.969 and 149.61 Å, respectively.

Structures of Complex 4. The molecular structures and 2D polymeric structures of complexes **4** are illustrated in Figs. 5 and 6, and selected bond lengths and bond angles are given in Table 4, respectively.

As can be seen from Fig. 5, complex **4** consists of two discrete units, conformations of the two independent units are almost the same, with only little differences in bond lengths and angles (see Table 4). We take molecule A for example, the tri-*n*-butyltin (IV) groups are linked by a carboxylate of

each ligand in turn, employing its two bipyridine carboxylic groups to coordinate to four metal centers. Thus, four ligands are linked by four metal centers into a 30-membered macrocycle, which is further linked to eight nearest-neighbor tin centers by a lattice 2D network (see Fig. 6) with a cavity that can be evaluated by the transannular Sn...Sn distances, which are 9.374–16.246 Å. Similar cavities have been found within the polymeric crystal structures of microporous metal–organic frameworks formed between 1,3,5-benzenetricarboxylic acid and Sn [30] and Co [31] centers. All the tin atoms possess the same coordination environment. The coordination about the tin atom is only slightly distorted from the regular trigonal bipyramidal geometry. The Sn–O distances [Sn(1)–O(1) 2.161(7), Sn(2)–O(3) 2.149(8), Sn(3)–O(5) 2.163(8), and Sn(4)–O(7) 2.157(8) Å], together with the other Sn–O distance [Sn(1)–O(8) 2.575(11), Sn(2)–O(6) (symmetry code: 1-*x*, 2-*y*, -*z*) 2.566, Sn(3)–O(2) 2.594(11), and Sn(4)–O(4) (symmetry code: 1-*x*, 1-*y*, -*z*) 2.600 Å] are all lie between the covalent bond length and the van der Waals radii. The O–Sn–O angles [O(1)–Sn(1)–O(8) 171.3(3), O(3)–Sn(2)–O(6) 171.20, O(5)–Sn(3)–O(2) 172.3(3), and O(4)–Sn(4)–O(7) 171.93°] are close to linear arrangement. The sum of the angles subtended at the tin atoms in the equatorial plane is 356.8° for Sn(1), 357.1° for Sn(2), 357.6° for Sn(3), and 361° for Sn(4) so that the atoms [Sn(1), C(25),

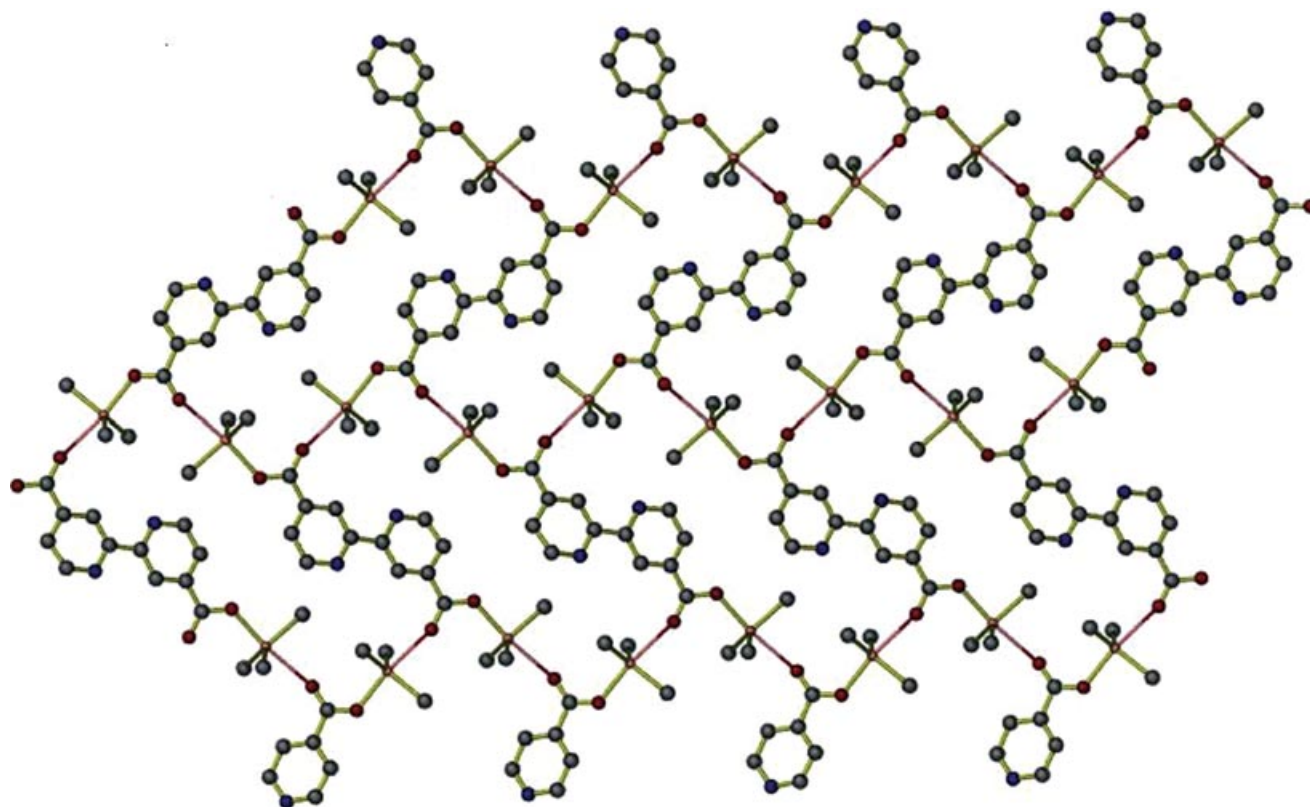


FIGURE 6 The 2D network structure of complex **4** (the β , γ , and δ carbon atoms of the Sn-butyl groups are omitted for clarity).

C(29), C(33)], [Sn(2), C(31), C(47), C(45)], [Sn(3), C(49), C(53), C(57)], and [Sn(4), C(61), C(65), C(69)] are all almost in the same plane.

CONCLUSIONS

In summary, a series of triorganotin (IV) complexes based on 2,2'-bipyridine-4,4'-dicarboxylic acid have been synthesized and characterized. In the crystals, complexes **1** and **2** are monomers, in contrast to complexes **3** and **4** forming 2D polymeric networks, which maybe caused by steric hindrance due to the presence of phenyl and benzyl groups. In addition, weak but significant intermolecular interactions (C—H \cdots N and O—H \cdots O) are observed. Therefore, multidimension self-assembly supramolecular structure is apt to form. At last, the nitrogen atoms in the bipyridine ring of ligand have no obvious influence on the coordination to the central tin atom.

SUPPLEMENTARY MATERIAL

Crystallographic data for the structure analysis of the compounds have been deposited with the Cambridge Crystallographic Data Center, CCDC No.

683177 **1**, 683178 **2**, 699165 **4**. Copies of these information may be obtained free of charge from The Director, CCDC, 12 Union Road, Cambridge, CB2 1EZ, UK (<http://www.ccdc.cam.ac.uk>; Fax: +44-1223-336033).

REFERENCES

- [1] Holmes, R. R. *Acc Chem Res* 1989, 22, 190.
- [2] Tiekink, E. R. T. *Appl Organomet Chem* 1991, 5, 1.
- [3] Tiekink, E. R. T. *Trends Organomet Chem* 1994, 1, 171.
- [4] Chandrasekhar, V.; Nagendran, S.; Baskar, V. *Coord Chem Rev* 2002, 235, 1.
- [5] Holmes, R. R.; Schmid, C. G.; Chandrasekhar, V.; Day, R. O.; Holmes, J. M. *J Am Chem Soc* 1987, 109, 1408.
- [6] Dokorou, V.; Ciunik, Z.; Russo, U.; Kovala-Demertzi, D. *J Organomet Chem* 2001, 630, 205.
- [7] Chandrasekhar, V.; Thirumoorathi, R.; Azhakar, R. *Organometallics* 2007, 26, 26.
- [8] García-Zarracino, R.; Höpfl, H. *J Am Chem Soc* 2005, 127, 3120.
- [9] Wang, L.B., *Acta Cryst* 2007, E63, m1883.
- [10] Ma, C. L.; Han, Y. F.; Zhang, R. F. *Dalton Trans* 2004, 12, 1832.
- [11] Ma, C. L.; Li, J. K.; Zhang, R. F. *J Organomet Chem* 2006, 691, 1713.

- [12] Tynan, E.; Jensen, P.; Kruger, P. E.; Lees, A. C.; Nieuwenhuyzen, M. *Dalton Trans* 2003, 7, 1223.
- [13] Tynan, E.; Jensen, P.; Kelly, N. R.; Kruger, P. E.; Lees, A. C.; Moubaraki, B.; Murray, K. S. *Dalton Trans* 2004, 21, 3440.
- [14] Tynan, E.; Jensen, P.; Lees, A. C.; Moubaraki, B.; Murray, K. S.; Kruger, P. E. *Cryst Eng Comm* 2005, 7, 90.
- [15] Tynan, E.; Jensen, P.; Kelly, N. R.; Kruger, P. E.; Lees, A. C.; Moubaraki, B.; Murray, K. S. *Dalton Trans* 2004, 3440.
- [16] Caspar, R.; Musatkina, L.; Tatosyan, A.; Amouri, H.; Gruselle, M.; Guyard-Duhayon, C.; Duval, R.; Cordier, C. *Inorg Chem* 2004, 43, 7986.
- [17] Caspar, R.; Amouri, H.; Gruselle, M.; Cordier, C.; Malezieux, B.; Duval, R.; Levwque, H. *Eur J Inorg Chem* 2003, 499.
- [18] Coronado, E.; Galan-Mascaros, J. R.; Marti-Gastaldo, C.; Palomares, E.; Durrant, J.R.; Vilar, R.; Gratzel, M.; Nazeeruddin, M. K. *J Am Chem Soc* 2005, 127, 12351.
- [19] Wu, J. Y.; Yeh, T. T.; Wen, Y. S.; Twu, J.; Lu, K. L. *Cryst Growth Des* 2006, 6, 467.
- [20] Stocco, G.; Guli, G.; Girasolo, M. A.; Bruno, G.; Nicolò, F.; Scopelliti, R. *Acta Cryst* 1996, C52, 829–832.
- [21] Sisido, K.; Takeda, Y.; Kinugawa, Z. *J Am Chem Soc* 1961, 83, 538.
- [22] Holmes, R. R.; Schmid, C. G.; Chandrasekhar, V.; Day, R. O.; Homels, J. M. *J Am Chem Soc* 2000, 122, 5158.
- [23] Sandhu, G. K.; Hundal, R. *J Organomet Chem* 1991, 412, 31.
- [24] Holecek, J.; Nadvornik, M.; Handlir, K.; Lycka, A. *J organomet Chem* 1986, 315, 299.
- [25] Vollano, J. F.; Day, R. O.; Rau, D. N.; Chandrasekhar, V.; Holmes, R. R. *Inorg Chem* 1984, 23, 3153.
- [26] Bondi, A. *J Phys Chem* 1964, 68, 441.
- [27] Molloy, K. C.; Purcell, T. G.; Quill, K.; Nowell, I. W. *J Organomet Chem* 1984, 267, 237.
- [28] Forrester, A. R.; Garden, S. J.; Howie, R. A.; Wardell, J. L. *J Chem Soc Dalton Trans* 1992, 2165.
- [29] Cotton, F. A.; Daniels, L. M.; Jordan IV, G. T.; Murillo, C. A. *Chem Commun* 1997, 1673.
- [30] Ma, C. L.; Han, Y. H.; Zhang, R. F.; Wang, D. Q. *Eur J Inorg Chem* 2005, 3024.
- [31] Yaghi, O. M.; Li, G.; Li, H. *Nature* 1995, 378, 703.

Reactions of 9,9'-Bibenzonorbornenylidene Sulfoxides with TMSOTf: Anomalous Pinacol-Type Rearrangement of Thiirane 1-Oxides

Yoshiaki Sugihara, Shuich Yamanaka, and Juzo Nakayama

Department of Chemistry, Graduate School of Science and Engineering, Saitama University, Sakura-ku, Saitama 338-8570, Japan

Received 10 October 2008; revised 13 November 2008

ABSTRACT: *syn*-9,9'-Bibenzonorbornenylidene sulfoxide **8b** underwent pinacol-type rearrangement to form **9**, together with a mixture of thiiranes **4a** and **4b** by reaction with TMSOTf in CH₂Cl₂ at room temperature. The rearrangement of anti-sulfoxide **8a** proceeded more slowly giving a mixture of **9**, **4a**, and **4b**. © 2009 Wiley Periodicals, Inc. *Heteroatom Chem* 20:29–34, 2009; Published online in Wiley InterScience (www.interscience.wiley.com). DOI 10.1002/hc.20507

INTRODUCTION

Quite recently, we succeeded in isolating thiirane 1-imides **1a** and **1b** for the first time and found that both undergo stereospecific ring enlargement, giving the corresponding 1,2-thiazetidines **2a** and **2b**, respectively, when keeping their solutions even at room temperature (Scheme 1) [1]. Ring enlargement of S-aminothiiranium salt **3b** proceeded to stereoselectively form 1,2-thiazetidin-2-ium salt **6b**, whereas reaction of **3a** under similar conditions gave the corresponding thiirane **4a** and alkene **5a** [2]. On the other hand, the related S-methylthiiranium salts, **7a**

and **7b**, isomerized each other in solution [3]. The products of their thermal decomposition in solution seemed to vary with the kind of atom connecting with the sulfur atom in their thiirane ring. In general, heating a solution of thiirane 1-oxide results in the formation of the corresponding alkene with the extrusion of sulfur monoxide [4], which can be trapped with diene [5–7]. The C–S bond dissociation of the thiirane 1-oxides seemed to proceed homolytically in the initial stage of thermal decomposition. If the C–S bond is cleaved heterolytically with the assistance of acid, other reaction pathways would occur. We found that 9,9'-bibenzonorbornenylidene sulfoxides **8a** and **8b** undergo pinacol-type rearrangement to form ketone **9** by action with TMSOTf. Acid-catalyzed rearrangement of thiiranes and their derivatives to form thioketones or ketones has not been reported [8], whereas that of oxiranes is well-known [9], and we reported only one example of aza-pinacol rearrangement of aziridines [10,11].

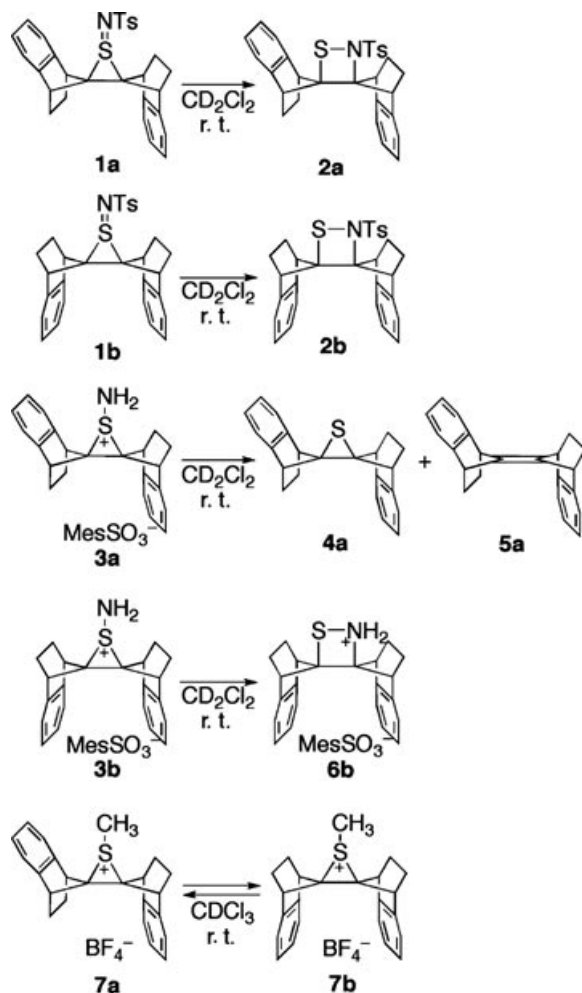
RESULTS AND DISCUSSION

Reaction of thiirane 1-oxide **8**, which was synthesized by reaction of the corresponding thiirane **4** with *m*-CPBA in a good yield, with an equimolar amount of TMSOTf, was examined (Scheme 2), and the results are summarized in Table 1. Thus, **8a** reacted with TMSOTf in CH₂Cl₂ at room temperature for 8 days to give **4a** (4%), **4b** (1%), and **9** (5%),

Correspondence to: Yoshiaki Sugihara and Juzo Nakayama; e-mail: ysugi@chem.saitama-u.ac.jp and nakayama@mail.saitama-u.ac.jp.

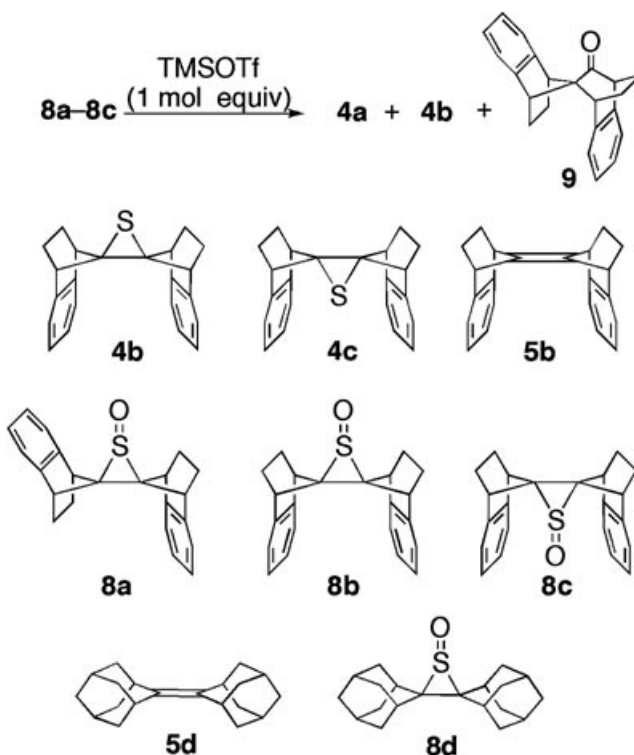
Contract grant sponsor: Japan Society for the Promotion of Science.

© 2009 Wiley Periodicals, Inc.



SCHEME 1

and the recovery of **8a** (90%) (entry 1). The stereochemistry of **9** was determined by COSY and NOESY experiments and ^1H and ^{13}C NMR experiments using $\text{Eu}(\text{fod})_3$ [12]. The reaction in refluxing CH_2Cl_2 for 2 days resulted in the consumption of **8a** and the formation of a mixture of **4a** (24%), **4b** (10%), and **9** (65%) (entry 2). When the reaction of **8b** was performed at room temperature, the same ketone **9** was obtained in 58% yield, together with a 3:1 mixture of **4a** and **4b** (entry 3). The pinacol-type rearrangement of **8a** and **8b** to **9** proceeded in a stereoselective but nonstereospecific manner. Surprisingly, the reaction of **8c** in toluene, even at reflux, resulted in a quantitative recovery of **8c** (entry 5). The stereochemistry of **8a–8c** seemed to exert a great influence on the progression of the rearrangement. On the other hand, 2,2'-biadamantylidene sulfoxide **8d** reacted with TMSOTf in refluxing toluene for 36 h to form 2,2'-biadamantylidene **5d** and the recovery of **8d** (entry 6). This reaction proceeded more



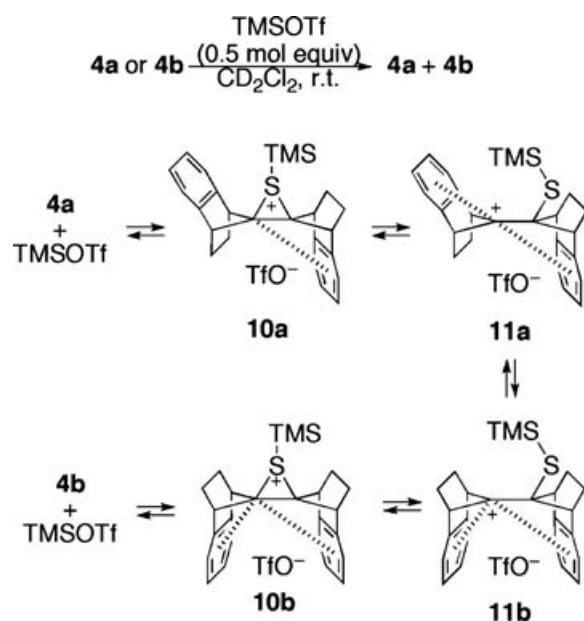
SCHEME 2

slowly than that without TMSOTf, giving **5d** as a sole product, reported by Harpp (entry 7) [6], indicating that TMSOTf seemed to prevent the extrusion of sulfur monoxide from **8**. Using other reagents, such as $\text{BF}_3\cdot\text{OEt}_2$, $\text{Cu}(\text{OTf})_2$, and PdCl_2 , in place of TMSOTf in the reactions of **8a** and **8b** did not produce a satisfactory rearrangement.

The formation of a 3:1 mixture of **4a–4b** in the reaction of each **8a** and **8b** suggests that isomerization between **4a** and **4b** probably proceeds under the reaction conditions. Therefore, reactions of **4a** and **4b** with TMSOTf (0.5 molar equivalent) in CD_2Cl_2 at room temperature were monitored by ^1H NMR (Scheme 3), and the results are summarized in Table 2. For the reaction of **4b**, signals of **4a** began to develop after mixing of **4b** and TMSOTf. The ratio of **4a–4b** decreased as time went by. For the reaction of **4a**, progression of the transformation of **4a–4b** slowed. The ratio was almost unchanged after 5 h. These observations indicate that **4a** and **4b** attained equilibrium under the applied conditions and the final equilibrium ratio of **4a–4b** was about 3:1. The isomerization must proceed through thiiranium salt **10** and carbenium salt **11**. Interestingly, **4a** and **4b** seemed to be more reactive against TMSOTf than **8a** and **8b**, but their pinacol-type rearrangement did not occur. These results are in harmony with

TABLE 1 Reactions of **8** with TMSOTf (1 Molar Equivalent)

Entry	Thiirane 1-Oxide	Conditions	Products (Yield/%)
1	8a	CH ₂ Cl ₂ , r. t., 8 d	4a (4), 4b (1), 9 (5), 8a (90)
2	8a	CH ₂ Cl ₂ , reflux, 2 d	4a (24), 4b (10), 9 (65)
3	8b	CH ₂ Cl ₂ , r. t., 8 d	4a (31), 4b (10), 9 (58)
4	8c	CH ₂ Cl ₂ , r. t., 8 d	8c (quant.)
5	8c	Toluene, reflux, 14 h	8c (quant.)
6	8d	Toluene, reflux, 36 h	5d (24), 8d (74)
7 ^a	8d	Toluene, reflux, 2.5 h	5d (97)

^aRef. 6. In the absence of TMSOTf.

SCHEME 3

isomerization of methylthiiranium salt **7**, where the final equilibrium ratio of **7a–7b** was about 4:1 [3].

On the basis of these findings, the following are proposed as the mechanisms of the reactions. Initially, **8a–8d** and TMSOTf react, giving thiiranium salt **12a–12d** (Fig. 1). The C–S bond of the thiirane ring in **12b** is cleaved, forming ring-opened

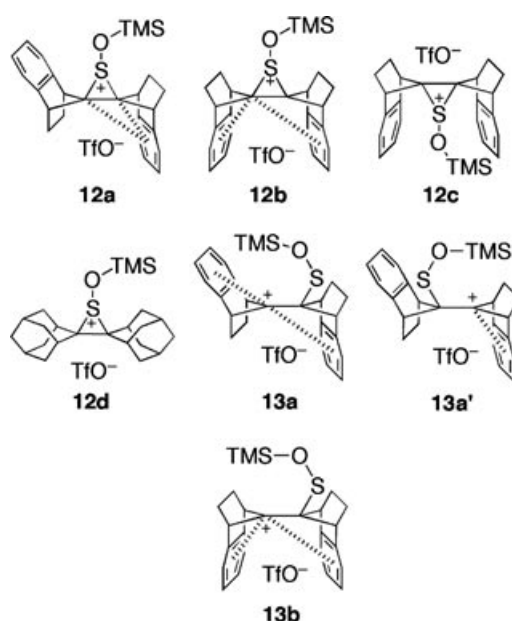


FIGURE 1

TABLE 2 Time-Course Study of Ratio of **4a–4b** in the Isomerization Between **4a** and **4b**^a

Time	4a : 4b	
	From 4a	From 4b
25 min	41:1	1:13
2 h	11:1	1.4:1
3 h	5.0:1	1.2:1
5 h	3.0:1	2.7:1
7.5 h	2.9:1	3.0:1

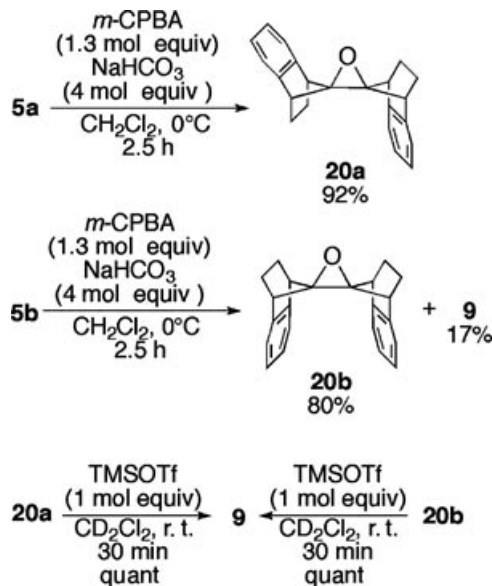
^aIn CD₂Cl₂ at r. t. Monitored by ¹H NMR.

carbenium salt **13b** with the assistance of neighboring group participation of the two benzene rings, which also stabilize **13b** by homoconjugation [13–15]. This participation must also affect the reactivity of **8**. Thus, in the case of **12a**, only one benzene ring, which exists on the back of the cleaved C–S bond, participates electronically in the thiirane-ring opening. As a result, the ring opening of **12a** proceeds more slowly than that of **12b** to form carbenium salt **13a** or **13a'**. Similar to **13b**, **13a** and **13a'** are stabilized by the participation of the two benzene rings and by the one benzene ring near its cation center, respectively. The process from **12a** to **13a'** is similar to that in the ring enlargement from **1a** to **2a** [1]. The reason **8c** and **8d** do not undergo the rearrangement is probably that no such participation acts on the C–S bond cleavage in **12c** and **12d**.

Three pathways from **13b** to **9** [paths (a)–(c)] would be possible (Scheme 4). Path (a) includes ring closure of **13b**, giving oxathietanium salt **14b**, which

then extrudes sulfur to form oxiranium salt **15b**. This is similar to the ring enlargement of **3b–6b**, followed by the decomposition of **6b** to aziridinium salt, where both proceeded with retention of the configuration of the original stereochemistry [2]. The salt **15b** undergoes pinacol-type rearrangement to form **9**. In the reaction of **8a**, oxiranium salt **15a**, which is formed either from **13a** through **14a** or from **13a'** through **14a'**, rearranges to form **9**. The stereoselectivity of the rearrangement can be interpreted by the neighboring group participation. Thus, this participation also acts as a leaving group in the rearrangement; hence, migration of the substituent occurs from the back of this participation [14]. In consequence, ketone **17**, which is a possible product, was not produced. The paths (b) and (c) contain direct pinacol-type rearrangement of **13**, giving oxathiirane **18** and sulfine **19**, which then transforms to **18** [16]. The oxathiirane **18** would be an unstable compound [17] and hence it extrudes sulfur to form **9**.

Oxiranes **20a** and **20b**, which are precursors of **15a** and **15b** [9], were synthesized by oxirane of **5a** and **5b** with *m*-CPBA in the presence of NaHCO₃ at 0°C (Scheme 5). Interestingly, **9** was obtained as a



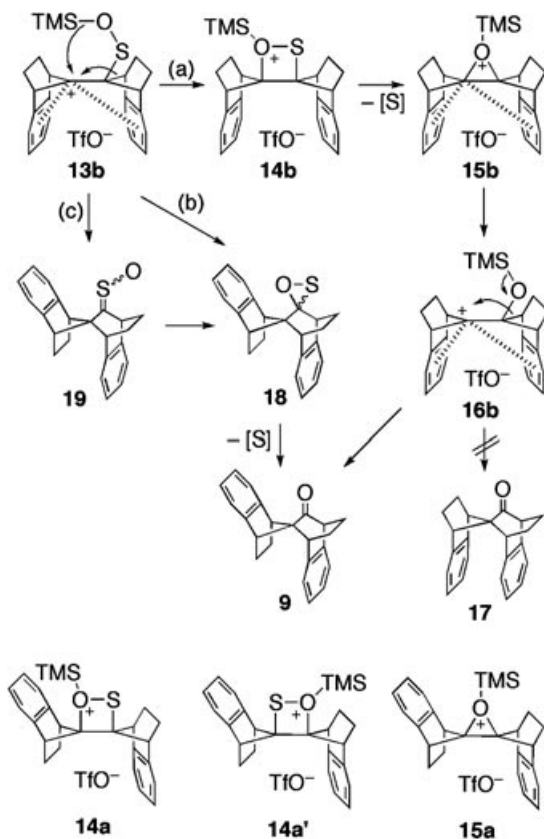
SCHEME 5

by-product in the oxirane of **5b** even under the basic conditions, whereas no formation of **9** was observed in the oxirane of **5a**. As expected, **20a** and **20b** underwent pinacol-type rearrangement to form the same **9** quantitatively, by action with TMSOTf. If **15** is an intermediate of the rearrangement of **8**, the transformation of **15** to **9** would proceed more rapidly than the ring opening of **12** forming **13**.

Formation of **4a** and **4b** from **8a** and **8b** under the reaction conditions seemed to proceed through a similar process to that of **4a** from **3a** [2]. Reactive species, such as sulfur, which is extruded from **14** or **18** as a by-product, may attack the oxygen atom next to the positively charged sulfur atom in **12a** and **12b** to form **4a** and **4b**, both of which isomerize each other under the reaction conditions, as mentioned above.

EXPERIMENTAL

Solvents were dried and purified in the usual manner. All the reactions were carried out under argon. Silica gel column chromatography was performed on silica gel 60N (Kanto, 63–210 μm, spherical, neutral). Melting points were determined on a Mel-Temp capillary tube apparatus and were uncorrected. ¹H and ¹³C NMR spectra were recorded on a Bruker DRX400, a Bruker ARX400, a Bruker AM 400 (400 MHz for ¹H and 101 MHz for ¹³C), a Bruker AC300P (300 MHz for ¹H), or a Bruker AC200 (200 MHz for ¹H and 50 MHz for ¹³C) spectrometer using CDCl₃ or CD₂Cl₂ as the solvent with TMS



SCHEME 4

for ^1H and with CDCl_3 or CD_2Cl_2 for ^{13}C as the internal standard. IR spectra were recorded on a Hitachi FT-IR 660+ spectrophotometer. Elemental analyses were performed by the Molecular Analysis and Life Science Center of Saitama University.

Synthesis of Thiirane 1-Oxide **8c**

To a solution of **4c** (100 mg, 0.32 mmol) in CH_2Cl_2 (10 mL) was added *m*-CPBA (65 mg, 0.38 mmol) at 0°C . After being stirred at the same temperature for 30 min, 5% aqueous NaHSO_3 solution was added to the reaction mixture. The organic layer was separated, washed with saturated aqueous NaHCO_3 solution and then with H_2O twice, dried over MgSO_4 , and evaporated. The residue was crystallized from CH_2Cl_2 and hexane to give 101 mg of **8c** (0.31 mmol, 96%). Thiirane 1-oxides **8a** and **8b** were synthesized by the same procedure [1]. **8c**: colorless crystals, mp $< 202^\circ\text{C}$ (dec) (CH_2Cl_2 /hexane). ^1H NMR (200 MHz): δ 1.59–1.72 (m, 4H), 2.17–2.35 (m, 4H), 3.07–3.11 (m, 2H), 3.88–3.93 (m, 1H), 7.12–7.20 (m, 6H), 7.28–7.32 (m, 2H). ^{13}C NMR (50 MHz): δ 26.8, 29.0, 44.7, 46.5, 84.9, 120.5, 121.1, 126.4, 126.8, 144.7, 146.0. IR: 3073, 3023, 2944, 2864, 1459, 1449, 1039, 760, 730 cm^{-1} . Anal. Calcd for $\text{C}_{22}\text{H}_{20}\text{OS}$: C, 79.48; H, 6.06. Found: C, 79.26; H, 6.02.

Reaction of **8b** with TMSOTf at Room Temperature

To a solution of **8b** (50.1 mg, 0.15 mmol) in CH_2Cl_2 (5.0 mL) was added TMSOTf (27.5 μL , 0.15 mmol) at 0°C . After being stirred at room temperature for 8 days, saturated aqueous NaHCO_3 solution and CH_2Cl_2 were added to the reaction mixture. The organic layer was separated, washed with H_2O twice, dried over MgSO_4 , and evaporated. The residue was placed on a column of silica gel and the column was eluted with CHCl_3 /hexane (1:4) to give 14.8 mg of **4a** (46 μmol , 31%) and 4.9 mg of **4b** (15 μmol , 10%) and with CHCl_3 to give 26.1 mg of **9** (87 μmol , 58%). **9**: colorless powder, mp $227\text{--}229^\circ\text{C}$ (Et_2O). ^1H NMR (400 MHz): δ 1.12–1.20 (m, 1H), 1.26–1.37 (m, 1H), 1.54–1.72 (m, 2H), 1.98–2.13 (m, 2H), 2.14–2.27 (m, 2H), 2.45–2.47 (m, 1H), 3.29–3.32 (m, 1H), 3.41–3.46 (m, 2H), 6.82–6.86 (m, 1H), 6.98–7.07 (m, 1H), 7.08–7.18 (m, 3H), 7.22–7.32 (m, 3H). ^{13}C NMR (101 MHz): δ 21.2, 24.9, 26.0, 26.3, 40.8, 49.0, 51.0, 53.9, 70.7, 120.0, 120.2, 124.3, 125.0, 125.6, 125.8, 126.9, 127.0, 137.0, 141.2, 145.3, 146.5, 211.8. IR: 3070, 3038, 3017, 2969, 2882, 1709, 1495, 1460, 761, 735 cm^{-1} . Anal. Calcd for $\text{C}_{22}\text{H}_{20}\text{O}$: C, 87.96; H, 6.71. Found: C, 87.59; H, 6.74.

Reaction of **8d** with TMSOTf in Refluxing Toluene

To a solution of **8d** (50.4 mg, 0.16 mmol) in toluene (5.0 mL) was added TMSOTf (29.0 μL , 0.16 mmol). After being heated at reflux for 36 h, the reaction mixture was evaporated and diluted with CH_2Cl_2 . The organic layer was washed with saturated aqueous NaHCO_3 solution and then with H_2O twice, dried over MgSO_4 , and evaporated. The residue was placed on a column of silica gel and the column was eluted with hexane to give 10.2 mg of **5d** (38 μmol , 24%) and with CHCl_3 / Et_2O (10:1) to give 37.3 mg of **8d** (118 μmol , 74%).

Reaction of **4** with TMSOTf

To a solution of **4a** or **4b** (10 mg, 32 μmol) and triptycene (3.0 mg, 12 μmol) as an internal standard in CD_2Cl_2 (0.45 mL) was added TMSOTf (3.0 μL , 17 μmol) at room temperature. The progression of the reactions was monitored by ^1H NMR. After 1.5 h, trace amounts of **5a** and **5b** were also detected by ^1H NMR.

Synthesis of Oxirane **20a**

To a suspension of **5a** (150 mg, 0.52 mmol) and NaHCO_3 (175 mg, 2.1 mmol) in CH_2Cl_2 (15 mL) was added *m*-CPBA (119 mg, 0.68 mmol) at 0°C . After being stirred at the same temperature for 2.5 h, 5% aqueous NaHSO_3 solution was added to the reaction mixture. The organic layer was separated, washed with saturated aqueous NaHCO_3 solution and then with H_2O twice, dried over MgSO_4 , and evaporated. The residue was crystallized from CH_2Cl_2 and hexane to give 142 mg of **20a** (0.47 mmol, 92%). **20a**: colorless crystals, mp $161\text{--}162^\circ\text{C}$ (CH_2Cl_2 /hexane). ^1H NMR (300 MHz): δ 0.95–1.05 (m, 2H), 1.26–1.40 (m, 4H), 2.18–2.28 (m, 2H), 2.98–3.06 (m, 4H), 7.08–7.28 (m, 8H). ^{13}C NMR (50 MHz): δ 24.9, 25.1, 44.1, 45.1, 83.8, 87.4, 120.8, 121.5, 126.2, 126.3, 144.3, 144.6. IR: 3051, 3027, 2983, 2950, 2879, 1464, 1374, 1210, 937, 760, 751, 547 cm^{-1} . Anal. Calcd for $\text{C}_{22}\text{H}_{20}\text{O}$: C, 87.96; H, 6.71. Found: C, 87.96; H, 6.73.

Synthesis of Oxirane **20b**

The residue containing **9** and **20b**, which were obtained using the same procedure for **5b** (150 mg, 0.52 mmol) as **5a**, was placed on a column of silica gel and the column was eluted with CHCl_3 /hexane (1:2) to give 123 mg of **20b** (0.41 mmol, 80%) and 26.6 mg of **9** (88 μmol , 17%). **20b**: colorless crystals, mp $172\text{--}173^\circ\text{C}$ (CH_2Cl_2 /hexane). ^1H NMR (300 MHz):

δ 0.86–0.94 (m, 4H), 1.95–2.10 (m, 4H), 2.36–2.46 (m, 4H), 6.88–6.96 (m, 4H), 7.09–7.17 (m, 4H). ^{13}C NMR (50 MHz): δ 25.9, 50.0, 94.6, 122.0, 125.8, 145.3. IR: 3045, 3024, 3962, 3945, 2867, 1463, 1258, 1028, 836, 741, 540 cm^{-1} . Anal. Calcd for $\text{C}_{22}\text{H}_{20}\text{O}$: C, 87.96; H, 6.71. Found: C, 87.82; H, 6.71.

Reaction of **20** with TMSOTf

To a solution of **20a** or **20b** (10 mg, 33 μmol) in CD_2Cl_2 (0.50 mL) was added TMSOTf (6.0 μL , 33 μmol) at room temperature. After keeping the solution at room temperature for 30 min, the quantitative formation of **9** was observed by ^1H NMR in each reaction.

ACKNOWLEDGMENT

This work was supported by Grants-in-Aid for Scientific Research from Japan Society for the Promotion of Science.

REFERENCES

- [1] Sugihara, Y.; Aoyama, Y.; Okada, H.; Nakayama, J. *Chem Lett* 2008, 37, 658–659.
- [2] Sugihara, Y.; Ohtsu, R.; Nakayama, J. *Heterocycles* 2008, 75, 2415–2420.
- [3] Sugihara, Y.; Aoyama, Y.; Nakayama, J. *Chem Lett* 2001, 30, 980–981.
- [4] Nakayama, J.; Tajima, Y.; Xue-hua, P.; Sugihara, Y. *J Am Chem Soc* 2007, 129, 7250–7251.
- [5] Abu-Yousef, I. A.; Harpp, D. N. *Tetrahedron Lett* 1995, 36, 201–204.
- [6] Abu-Yousef, I. A.; Harpp, D. N. *J Org Chem* 1997, 62, 8366–8371.
- [7] (a) Hartzell, G. E.; Page, J. N. *J Org Chem* 1967, 32, 459–460; (b) Lemal, D. M.; Chao, P. *J Am Chem Soc* 1973, 95, 922–924; (c) Aalbersberg, W. G. L.; Vollhardt, K. P. C. *J Am Chem Soc* 1977, 99, 2792–2794.
- [8] (a) Ando, W.; Choi, N.; Tokitoh, N. In *Comprehensive Heterocyclic Chemistry II*; Padwa A. (Ed.); Pergamon: Oxford, 1996; Vol. 1A, Ch. 1.05, pp. 173–240; (b) Harring, S. R.; Livinghouse, T. In *Comprehensive Heterocyclic Chemistry II*; Padwa A. (Ed.); Pergamon: Oxford, 1996; Vol. 1A, Ch. 1.06, pp. 241–258.
- [9] (a) Rickborn, B. In *Comprehensive Organic Synthesis*; Trost, B. M.; Fleming, I. (Eds.); Pergamon: Oxford, 1991; Vol. 3, Ch. 3.3, pp. 733–775; (b) Erden, I. In *Comprehensive Heterocyclic Chemistry II*; Padwa, A. (Ed.); Pergamon: Oxford, 1996; Vol. 1A, Ch. 1.03, pp. 98–144 and 1.04, pp. 145–171.
- [10] Sugihara, Y.; Iimura, S.; Nakayama, J. *Chem Commun* 2002, 134–135.
- [11] (a) Pearson, W. H.; Lian, B. W.; Bergmeier, S. C. In *Comprehensive Heterocyclic Chemistry II*; Padwa, A. (Ed.); Pergamon: Oxford, 1996; Vol. 1A, Ch. 1.01, pp. 1–60; (b) Rai, K. M. L.; Hassner, A. In *Comprehensive Heterocyclic Chemistry II*; Padwa, A. (Ed.); Pergamon: Oxford, 1996; Vol. 1A, Ch. 1.02, pp. 61–96.
- [12] (a) Gray, A. I.; Waigh, R. D.; Waterman, P. G. *J Chem Soc Chem Commun* 1974, 632–633; (b) Craig, R. E. R.; Craig, A. C.; Smith, G. D. *Tetrahedron Lett* 1975, 16, 1189–1192.
- [13] (a) Sugihara, Y.; Noda, K.; Nakayama, J. *Bull Chem Soc Jpn* 2000, 73, 2351–2356; (b) Sugihara, Y.; Noda, K.; Nakayama, J. *Tetrahedron Lett* 2000, 40, 8907–8911; (c) Sugihara, Y.; Noda, K.; Nakayama, J. *Tetrahedron Lett* 2000, 40, 8913–8916; (d) Noda, K.; Sugihara, Y.; Nakayama, J. *Heteroatom Chem* 2001, 12, 625–629.
- [14] (a) Okada, K.; Mukai, T. *J Am Chem Soc* 1978, 100, 6509–6510; (b) Paquette, L. A.; Hertel, L. W.; Gleiter, R.; Böhm, M. *J Am Chem Soc* 1978, 100, 6510–6512; (c) Paquette, L. A.; Hertel, L. W.; Gleiter, R.; Böhm, M. C.; Beno, M. A.; Christoph, G. G. *J Am Chem Soc* 1981, 103, 7106–7112.
- [15] (a) Winstein, S.; Shatavsky, M.; Norton, C.; Woodward, R. B. *J Am Chem Soc* 1955, 77, 4183–4184; (b) Winstein, S.; Stafford, E. T. *J Am Chem Soc* 1957, 79, 505–506; (c) Bartlett, P. D.; Giddings, W. P. *J Am Chem Soc* 1960, 82, 1240; (d) Tanida, H. *J Am Chem Soc* 1963, 85, 1703–1704; (e) Tanida, H.; Ishitobi, H. *J Am Chem Soc* 1966, 88, 3663–3664; (f) Tanida, H.; Hata, Y.; Ikegami, S.; Ishitobi, H. *J Am Chem Soc* 1967, 89, 2928–2932.
- [16] (a) Adam, W.; Deeg, O.; Weinkötz, S. *J Org Chem* 1997, 62, 7084–7085; (b) Chevie, D.; Metzner, P. *Tetrahedron Lett* 1998, 39, 8983–8986.
- [17] Murray, R. W.; Singh, M. In *Comprehensive Heterocyclic Chemistry II*; Padwa A. (Ed.); Pergamon: Oxford, 1996; Vol. 1A, Ch. 1.14, pp. 429–456.

Preparation and Crystal Structures of Two Salts with the 5-Nitrotetrazolate Anion

Thomas M. Klapötke, Carles Miró Sabaté, and Jan M. Welch

Department of Chemistry and Biochemistry, Energetic Materials Research, Ludwig-Maximilian University, Butenandtstr. 5-13 (D), 81377 Munich, Germany

Received 24 October 2008; revised 16 November 2008

ABSTRACT: Tetraphenylphosphonium 5-nitrotetrazolate (**2**) was prepared by metathesis of sodium 5-nitrotetrazolate dihydrate (**1**; NaNT) with tetraphenylphosphonium chloride in acetone. The new compound was fully characterized by vibrational (IR, Raman) and NMR (^1H , ^{13}C , and ^{14}N) spectroscopies, elemental analysis, and mass spectrometry. Attempted synthesis of 2-methyl-5-nitrotetrazole (2-MeNT) by methylation of **1** with dimethylsulfate at reflux from acetonitrile failed, and crystals of an explosive compound with the formula $(\text{NaNT})_2(\text{H}_2\text{O})_2\text{CH}_3\text{CN}$ (**3**), NT = 5-nitrotetrazolate, formed. X-ray diffraction techniques were used to determine the crystal structure of **2** and **3**. Compound **2** crystallizes in the orthorhombic space group $P2_12_12_1$ with four molecules in the unit cell and unit cell parameters $a = 7.7413(4) \text{ \AA}$, $b = 13.624(1) \text{ \AA}$, $c = 21.252(1) \text{ \AA}$, and $V = 2241.5(2) \text{ \AA}^3$, whereas **3** crystallizes in the orthorhombic space group $\text{Ama}2$ with four formula unit in the unit cell and unit cell parameters $a = 14.805(6)$

 \AA , $b = 9.908(4) \text{ \AA}$, $c = 8.940(3) \text{ \AA}$, and $V = 1311.4(1) \text{ \AA}^3$. © 2009 Wiley Periodicals, Inc. *Heteroatom Chem* 20:35–44, 2009; Published online in Wiley InterScience (www.interscience.wiley.com). DOI 10.1002/hc.20509

INTRODUCTION

The synthesis of nitrogen-rich compounds for use as highly energetic materials is the goal of our research group [1–4]. 5-Amino-1H-tetrazole (**A**) and 5-nitro-2H-tetrazole (**B**) are nitrogen-rich energetic compounds, which are readily deprotonated by bases [5,6]. Nitrogen-rich salts of **B** with easily protonated nitrogen bases [7] have shown interesting properties in terms of low sensitivities and high performances. We recently synthesized metal salts of **A**, which are prospective candidates for use in new environmentally friendly pyrotechnic compositions [5] and metal salts of **B**, which show an increased sensitivity to shock and friction [6]. The presence of crystal water in the solid-state structure of metal salts of **B** increases the distances between the metal center and the anion, and the sensitivity of the compounds toward classical stimuli is markedly reduced.

To investigate 5-nitrotetrazole moieties, which do not interact in the solid state we synthesized the tetraphenylphosphonium salt of **B** (**2**). In addition, synthesis of neutral 2-methyl-5-nitrotetrazole (2-MeNT) was attempted and bis-(sodium 5-nitrotetrazolate) dihydrate acetonitrile adduct (**3**) formed instead. Here, we would like to report on the synthesis and characterization of **2** and **3** as well as their crystal structures. To our knowledge, together

Correspondence to: Thomas M. Klapötke; e-mail: tmk@cup.uni-muenchen.de.

Contract grant sponsor: Ludwig-Maximilian University of Munich.

Contract grant sponsor: Fonds der Chemischen Industrie.

Contract grant sponsor: the European Research Office (ERO) of the U.S. Army Research Laboratory (ARL).

Contract grant sponsor: ARDEC (Armament Research, Development and Engineering Center).

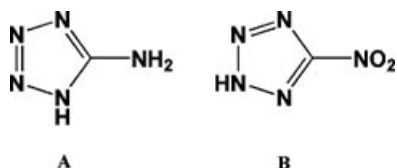
Contract grant numbers: N 62558-05-C-0027, R&D 1284-CH-01, R&D 1285-CH-01, 9939-AN-01, and W911NF-07-1-0569.

Contract grant sponsor: Bundeswehr Research Institute for Materials, Explosives, Fuels and Lubricants.

Contract grant numbers: E/E210/4D004/X5143 and E/E210/7D002/4F088.

© 2009 Wiley Periodicals, Inc.

with our reports [6,7] and that of the nickel salt [8], these are the only papers where the structure of the anion of **B** has been determined by X-ray analysis.



EXPERIMENTAL SECTION

Materials and Methods

CAUTION: Tetrazoles are energetic materials. Sodium 5-nitrotetrazolate dihydrate (**1**) has low sensitivity against friction and electrostatic discharge; however upon loss of water and/or rapid heating, it becomes highly sensitive and explosive. Safety equipment such as leather gloves, face shield, earplugs, and use of Teflon spatulas are recommended. It is not recommended the synthesis and manipulation of compound **1** on scales greater than 200 mg.

All chemicals and solvents were used as supplied by Sigma-Aldrich Fine Chemicals Inc. (Munich, Germany) without any further purification. Sodium 5-nitrotetrazolate dihydrate (**1**) was synthesized according to the literature [9,10]. ^1H , ^{13}C , ^{14}N , and ^{31}P NMR spectra were recorded on a JEOL Eclipse 400 instrument in $\text{DMSO-}d_6$ at room temperature. The infrared (IR) spectrum of **2** was recorded on a Perkin-Elmer spectrum one FT-IR instrument [11] (vs = very strong, s = strong, m = medium, w = weak, and vw = very weak). A Perkin-Elmer spectrum 2000R NIR FT-Raman instrument equipped with a Nd: YAG laser (1064 nm) was used for the recording of the Raman spectra (intensity percentages are given in brackets). A Netsch simultaneous thermal analyzer STA 429 was used to perform the elemental analyses. A differential scanning calorimetry (Linseis DSC PT-10 instrument [12], calibrated with standard pure indium and zinc) was used to determine the melting point and decomposition temperature of **2** (2°C min^{-1}). Closed aluminum sample pans with a 1- μm hole in the top for gas release under a nitrogen flow of 20 mL min^{-1} were used.

Tetraphenylphosphonium 5-Nitrotetrazolate (**2**)

Tetraphenylphosphonium chloride (0.314 g, 0.84 mmol) was dissolved in 15 mL dry acetone under an stream of nitrogen before a solution of sodium 5-nitrotetrazolate dihydrate (0.145 g, 0.84 mmol) in

5 mL dry acetone was added under a stream of nitrogen. Immediate precipitation of sodium chloride was observed, and the reaction mixture was stirred for further 20 min at room temperature. The insoluble solid was filtered and discarded, and the acetone solution was left to slowly evaporate yielding a slightly yellow residue of the product, which could be purified by dissolving it in minimal acetone and letting ether to diffuse into it overnight. The crystals formed were suitable for X-ray analysis (301 mg, 79%).

Analytical Data of 2. Raman $\tilde{\nu}/\text{cm}^{-1}$ (rel. int.): 3149(4), 3146(5), 3068(45), 2958(3), 1586(49), 1576(20), 1527(12), 1441(6), 1403(100), 1307(4), 1187(11), 1166(13), 1109(13), 1099(22), 1040(37), 1029(24), 1014(50), 1002(69), 834(7), 726(4), 679(14), 617(8), 531(5), 287(9), 254(21), 205(12), 143(6); IR $\tilde{\nu}/\text{cm}^{-1}$ (KBr, rel. int.): 3437(w), 3091(w), 3051(w), 3024(w), 2820(vw), 2691(vw), 2204(vw), 1991(vw), 1833(vw), 1700(vw), 1585(w), 1572(w), 1558(w), 1526(s), 1482(m), 1440(s), 1435(s), 1428(s), 1404(s), 1340(w), 1307(s), 1182(w), 1162(m), 1152(w), 1107(vs), 1038(w), 1020(w), 997(m), 853(vw), 835(s), 757(s), 723(s), 691(s), 678(m), 672(m), 614(w), 478(vs), 456(m); ^1H NMR ($\text{DMSO-}d_6$, 400.18 MHz, 25°C , TMS) δ/ppm : 7.98–7.94 (4H, m, *p*-H), 7.84–7.71 (16H, m, *o*-H/*m*-H); $^{13}\text{C}\{^1\text{H}\}$ NMR ($\text{DMSO-}d_6$, 100.6 MHz, 25°C , TMS) δ/ppm : 165.2 (1C, s, C1), 135.3 (4C, d, $^4J_{\text{C-P}} = 2.7\text{ Hz}$, *p*-C), 134.5 (8C, d, $^2J_{\text{C-P}} = 10.8\text{ Hz}$, *o*-C), 130.4 (8C, d, $^3J_{\text{C-P}} = 12.7\text{ Hz}$, *m*-C), 117.7 (4C, d, $^1J_{\text{C-P}} = 89.2\text{ Hz}$, *i*-C); ^{31}P NMR ($\text{DMSO-}d_6$, 162.00 MHz, 25°C , 35% H_3PO_4) δ/ppm : +23.0 (P); ^{14}N NMR ($\text{DMSO-}d_6$, 28.92 MHz, 25°C , CH_3NO_2) δ/ppm : +21 (2N, $\nu_{1/2} \sim 420\text{ Hz}$, N2/3), -21 (1N, $\nu_{1/2} \sim 80\text{ Hz}$, -NO₂), -58 (2N, $\nu_{1/2} \sim 400\text{ Hz}$, N1/4); $\text{C}_{25}\text{H}_{20}\text{N}_5\text{O}_2\text{P}$ (453.44 g mol^{-1} , calc/found): C 66.22/66.11, H 4.45/4.44, N 15.45/15.37; m/z (FAB^+ , xenon, 6 keV, *m*-NBA matrix): 339.34 [PPh_4] $^+$; (FAB^- , xenon, 6 keV, *m*-NBA matrix): 114.0 [NT] $^-$, 228.8 [$\text{H}(\text{NT})_2$] $^-$; DSC (2°C min^{-1}): 125.7°C (mp), $\sim 188^\circ\text{C}$ (dec); Sensitivity data: friction >360 N; shock >30 J; electrost disch insensitive.

Bis(sodium 5-nitrotetrazolate) Dihydrate Acetonitrile Adduct (**3**)

Sodium 5-nitrotetrazolate dihydrate (0.294 g, 1.70 mmol) was refluxed in 10 mL acetonitrile for 2 h after which time the heating was switched off, and the solvent was rotavaporated down at 60°C to $\sim 4\text{ mL}$. Immediate precipitation of the product was observed, and the yield was increased by putting the mother liquors in the fridge overnight. The solid was filtered and washed with ether, rendering 0.382 g of

a colorless solid. Some of the crystals precipitated in the fridge were measured by X-ray analysis, confirming the formation of **3**.

Analytical Data of 3. Raman $\tilde{\nu}/\text{cm}^{-1}$ (rel. int.): 3015(3), 2950(5), 1548(7), 1424(100), 1363(4), 1319(5), 1180(4), 1056(47), 1044(41), 921(2), 841(4), 774(2), 546(3), 459(2), 392(2), 248(2), 145(2); ^1H NMR ($\text{DMSO}-d_6$, 400.18 MHz, 25°C , TMS) δ/ppm : 4.57 (~4H, s, H_2O), 1.97 (3H, s, CH_3); $^{13}\text{C}\{^1\text{H}\}$ NMR ($\text{DMSO}-d_6$, 100.63 MHz, 25°C , TMS) δ/ppm : 165.2 (2C, C/C1), 118.2 (1C, CN), 1.4 (1C, CH_3); ^{14}N NMR ($\text{DMSO}-d_6$, 28.92 MHz, 25°C , CH_3NO_2) δ/ppm : +22 (2N, $\nu_{1/2} \sim 400$ Hz, N2/4), -19 (1N, $\nu_{1/2} \sim 70$ Hz, $-\text{NO}_2$), -60 (2N, $\nu_{1/2} \sim 370$ Hz, N1/3); m/z (FAB $^-$, xenon, 6 keV, m-NBA matrix): 114.0 $[\text{NT}]^-$, 228.8 $[\text{H}(\text{NT})_2]^-$; DSC (5°C min^{-1}): $\sim 200^\circ\text{C}$ (dec), Sensitivity data: friction > 360 N; shock > 30 J; electrost disch insensitive.

X-ray Structure Determinations of **2** and **3**

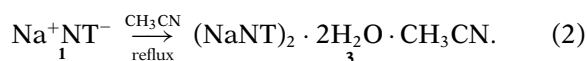
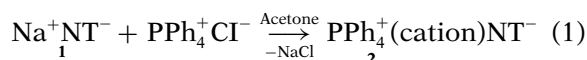
Compounds **2** and **3** were characterized by X-ray structure determination (Table 1). Crystals were grown as described in the Preparation Section. The X-ray crystallographic data were collected on an Oxford Diffraction Xcalibur 3 diffractometer equipped with a CCD detector at a temperature of 200 K (**2**) and 100 K (**3**) and using the CrysAlis CCD software [13]. All data were collected using graphite-monochromated Mo $K\alpha$ radiation. No absorption correction was applied to the data sets collected. The data reduction was performed with the CrysAlis RED software [14].

Structure Analysis and Refinement. The crystal structures of **2** and **3** were solved by direct methods using the corresponding programs available in the WinGX package [15–18], and the structures were finally checked using the program PLATON [19]. All non-hydrogen atoms were refined anisotropically, whereas the hydrogen atoms were located from difference Fourier electron density maps and refined isotropically. A SCALE3 ABSPACK multiscan method was used for the absorption correction [20].

Further information on the crystal-structure determinations (excluding structure factors) has been deposited at the Cambridge Crystallographic Data Centre (CCDC) under numbers CCDC 673959 (**2**) and CCDC 673958 (**3**) and is available free of charge by request from the CCDC. A copy of the cif file for compounds **2** and **3** can be obtained free of charge on application to The Director, CCDC, 12 Union Road, Cambridge CB2 1EZ, UK (Fax: int. code_(1223)336–033. E-mail for inquiry: fileserv@ccdc.cam.ac.uk. E-mail for deposition: deposit@ccdc.cam.ac.uk).

RESULTS AND DISCUSSION

Tetraphenylphosphonium 5-nitrotetrazolate (**2**) was prepared in high yield and purity by a metathesis reaction between sodium 5-nitrotetrazolate dihydrate (**1**) [9,10] and tetraphenylphosphonium chloride in acetone according to Eq. (1). After filtering the precipitated sodium chloride the solvent was stripped, and crystals were grown by storage of a saturated solution of the compound in acetonitrile in the refrigerator. Attempted synthesis of highly energetic neutral 2-methyl-5-nitrotetrazole (2-MeNT) by boiling **1** with an excess dimethylsulfate in acetonitrile failed, and an adduct with the formula $(\text{NaNT})_2(\text{H}_2\text{O})_2\text{CH}_3\text{CN}$ (**3**) was formed together with unreacted **1**. The result was reproducible when this reaction was repeated without the presence of dimethylsulfate (Eq. (2)).



Compounds **2** and **3** were characterized by vibrational spectroscopy. The shifts for the cation in **2** are well established, and thus a description is omitted. Much more interesting are the bands corresponding to the 5-nitrotetrazolate anion in **2** and **3** that could be assigned by comparison with the calculated shifts [7,21]: ~ 1530 [$\nu_{\text{asym}}(\text{NO}_2)$], ~ 1400 [$\nu_{\text{asym}}(\text{N}-\text{C}-\text{N})$], ~ 1380 [$\nu_{\text{sym}}(\text{NO}_2) + \nu_{\text{sym}}(\text{N}-\text{C}-\text{N})$, “in phase”], ~ 1300 [$\nu_{\text{sym}}(\text{NO}_2) + \nu_{\text{sym}}(\text{N}-\text{C}-\text{N})$, “out of phase”], ~ 1180 [$\nu_{\text{asym}}(\text{tetrazole})$], ~ 1160 [$\nu_{\text{sym}}(\text{tetrazole}) + \nu_{\text{sym}}(\text{NO}_2)$, “in phase”], ~ 1020 [$\delta(\text{N}-\text{C}-\text{N}) + \nu_{\text{sym}}(\text{NO}_2)$, “in phase”], ~ 1000 [$\nu(\text{N}-\text{N}) + \delta_{\text{sym}}(\text{tetrazole})$, “out of phase”], ~ 835 [$\delta(\text{NO}_2) + \delta(\text{N}-\text{C}-\text{N})$, “in of phase”], ~ 765 [$\gamma(\text{NO}_2) + \gamma(\text{N}-\text{C}-\text{N})$, “out of phase”], ~ 720 [$\gamma(\text{tetrazole})$ “in phase”], ~ 670 [$\gamma(\text{tetrazole})$ “out of phase”], 522 [$\omega(\text{NO}_2) + \omega(\text{tetrazole})$, “out of phase”], ~ 455 [$\nu(\text{C}-\text{N}) + \delta(\text{NO}_2)$], ~ 250 [$\omega(\text{NO}_2) + \omega(\text{tetrazole})$, “in phase”], and ~ 205 [$\gamma(\text{N}-\text{C}-\text{N})$] cm^{-1} . The most significant fact in the Raman spectrum of **2** is that the asymmetric nitro-group stretching is shifted and split in two signals at 1586 and 1576 cm^{-1} and the symmetric nitro-group stretching is strongly shifted (~ 15 cm^{-1}). This is indicative of little interaction between the nitro-group and the cation as confirmed by the crystal structure of the compound (see X-Ray Structure Discussion). On the other hand, for compound **3** the nitro-group stretches are observed much closer to the calculated values, indicative of strong interaction by the nitro-group oxygen atoms

TABLE 1 Crystal Data and Refinement for Compounds **2** and **3**

	2	3
Chemical formula	C ₂₅ H ₂₀ N ₅ O ₂ P	C ₄ H ₇ N ₁₁ O ₆ Na ₂
Molecular weight	453.43	351.19
Crystal size	0.3 × 0.15 × 0.1	0.15 × 0.15 × 0.05
Crystal system	Orthorhombic	Orthorhombic
Space group	<i>P</i> 2 ₁ 2 ₁ 2 ₁	<i>Ama</i> 2
<i>a</i> (Å)	7.7413(4)	14.805(6)
<i>b</i> (Å)	13.624(1)	9.908(4)
<i>c</i> (Å)	21.252(1)	8.940(3)
α (°)	90	90
β (°)	90	90
γ (°)	90	90
<i>V</i> (Å ³)	2241.5(2)	1311.4(1)
<i>Z</i>	4	4
$\rho_{\text{calc.}}$ (g/cm ³)	1.342	1.778
μ (mm ⁻¹)	0.156	0.211
<i>F</i> (000)	944	712
θ range (°)	3.84–28.99	4.11–29.97
Temperature (K)	200(2)	100(2)
Index range	–10 ≤ <i>h</i> ≤ 10 –18 ≤ <i>k</i> ≤ 18 –28 ≤ <i>l</i> ≤ 28	–20 ≤ <i>h</i> ≤ 20 –13 ≤ <i>k</i> ≤ 13 –12 ≤ <i>l</i> ≤ 12
Reflections collected	28111	8563
Reflections unique	5949	1045
Reflections observed (4 σ)	3421	787
<i>R</i> (int.)	0.0767	0.0597
Data/restraints/parameters	5949/0/298	1045/1/128
GOF	1.051	0.997
<i>R</i> ₁ , <i>wR</i> ₂ [<i>I</i> > 4 σ (<i>I</i>)]	0.0419, 0.0937	0.0345, 0.0801
<i>R</i> ₁ , <i>wR</i> ₂ (all data)	0.0726, 0.0988	0.0498, 0.0847

as seen in the coordination of the Na cations by the nitro-groups in the molecular structure.

The ¹H NMR spectrum of **2** (Fig. 1) shows two multiplets in the aromatic region corresponding to

the phenyl-group hydrogen atoms in the cation, whereas **3** shows a broad and a sharp resonances at 4.57 and 1.97 ppm corresponding to the coordination water and acetonitrile, respectively. The

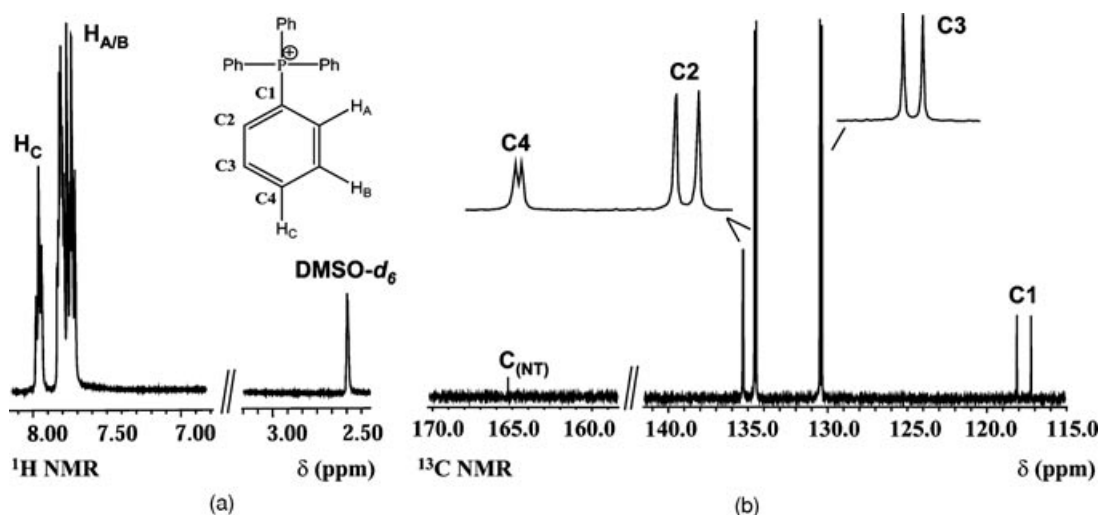


FIGURE 1 (a) ¹H NMR and (b) ¹³C NMR spectra of **2** in DMSO-*d*₆.

TABLE 2 Distances (Å) and Angles (°) for the 5-Nitrotetrazolate Anion in Compounds **2** and **3**

	2	3 (A)	3 (B)
N5–O1	1.205(3)	1.226(1)	1.227(1)
N5–O2	1.212(3)	1.226(1)	1.227(1)
N5–C1	1.436(3)	1.441(1)	1.441(1)
N1–N2	1.343(3)	1.354(1)	1.338(1)
N2–N3	1.299(3)	1.319(1)	1.342(1)
N3–N4	1.341(3)	1.354(1)	1.338(1)
C1–N1	1.298(3)	1.325(1)	1.328(1)
C1–N4	1.287(3)	1.325(1)	1.328(1)
	2	3 (A)	3 (B)
O1–N5–O2	123.0(3)	124.8(3)	125.0(2)
O1–N5–C1	118.2(2)	117.6(2)	117.5(2)
O2–N5–C1	118.8(2)	117.6(2)	117.5(2)
C1–N1–N2	103.7(2)	102.0(2)	103.2(2)
N1–N2–N3	108.6(2)	110.0(2)	109.5(2)
N2–N3–N4	109.6(2)	110.0(2)	109.5(2)
N3–N4–C1	103.4(2)	102.0(2)	103.2(2)
N4–C1–N1	114.7(2)	114.6(3)	115.9(2)
N4–C1–N5	122.8(2)	122.7(2)	122.0(2)
N1–C1–N5	122.5(2)	122.7(2)	122.0(2)

A and B denote two crystallographically independent anions in the crystal structure of **3**.

resonance of the anion carbon atom in the ^{13}C NMR of **2** and **3** has very low intensity and is found at 165.2 ppm in both cases. In addition, **3** shows the expected resonances for the coordinated acetonitrile (see Analytical Data of **3**) and **2** shows the resonances corresponding to the aromatic carbon atoms in the cation in the range between ~ 118 and ~ 135 ppm. In addition, Fig. 1 shows the ^{13}C NMR spectra of compound **2**. The coupling constants between the carbon and the phosphorous atoms have the following values: $^1J_{\text{C-P}} = 89.2$, $^2J_{\text{C-P}} = 10.8$, $^3J_{\text{C-P}} = 12.7$, and $^4J_{\text{C-P}} = 2.7$ Hz and are useful to assign the carbon atoms resonances by comparison with the literature [22]. Finally, the ^{14}N NMR shows two broad ($\Delta\nu_{1/2} \sim 400$ Hz) resonances at $\sim +20$ and ~ -60 ppm corresponding to the tetrazole-ring nitrogen atoms and the nitro-group resonance is much sharper ($\Delta\nu_{1/2} \sim 70$ Hz) and found at ~ -20 ppm.

The solid-state structures of **2** and **3** were determined experimentally by X-ray diffraction analysis. In Table 2, there are tabulated the distances and angles for the anion in both compounds. Whereas the crystal structure of **2** is composed of one only crystallographically independent anion, that of **3** is composed of two (A and B). The distances and angles in **3** are in agreement with previous reports [6–7], whereas **2** shows, in general, comparatively shorter bonds, indicating a better conjugation of the negative charge throughout the tetrazole ring as expected from the lack of interaction to the cation.

Figure 2 shows the asymmetric unit of **2** with the labeling scheme. As expected in the solid state,

there are no interactions between cations and anions due to the great bulk of the tetraphenylphosphonium cations and the lack of hydrogen atoms linked to an electronegative atom to form classical hydrogen bonds. The coordination around the phosphorus atoms is tetrahedral, and the phenyl groups arrange themselves in such a way as to diminish the clashes between the aromatic protons as seen in the structure of compounds, containing the same cation [23]. A further discussion of the bonds and angles in the cation (Table 3) of the cation is omitted here.

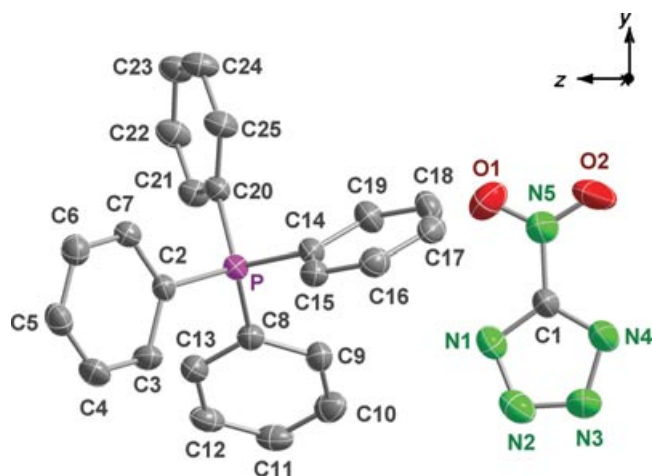


FIGURE 2 Asymmetric unit of **2**, showing the labeling scheme (diamond ellipsoids at the 50% probability). The hydrogen atoms have been omitted for the sake of simplicity.

TABLE 3 Distances (Å) and Angles (°) for the Tetraphenylphosphonium Cation in **2**

Distances (Å)			
P–C1	1.786(2)	C11–C12	1.392(3)
P–C7	1.793(2)	C12–C13	1.387(3)
P–C13	1.793(2)	C13–C14	1.388(3)
P–19	1.791(2)	C14–C15	1.382(3)
C1–C2	1.396(3)	C15–C16	1.376(3)
C3–C2	1.374(3)	C16–C17	1.382(3)
C4–C3	1.386(4)	C17–C18	1.387(3)
C4–C5	1.368(3)	C18–C13	1.394(3)
C6–C5	1.383(3)	C19–C20	1.393(3)
C6–C1	1.392(3)	C20–C21	1.374(3)
C7–C8	1.393(3)	C21–C22	1.387(3)
C8–C9	1.377(3)	C22–C23	1.373(3)
C9–C10	1.378(3)	C23–C24	1.373(3)
C10–C11	1.384(3)	C24–C19	1.393(3)
Angles (°)			
C1–P–C7	110.8(1)	C9–C8–C7	120.0(2)
C1–P–C13	109.9(1)	C16–C15–C14	120.3(2)
C1–P–C19	108.9(1)	C21–C20–C19	120.2(2)
C19–P–C13	109.9(1)	C15–C14–C13	120.1(2)
C19–P–C7	108.3(1)	C17–C18–C13	119.5(2)
C13–P–C7	108.7(1)	C7–C12–C11	119.8(2)
C24–C19–C20	119.3(2)	C16–C17–C18	120.4(2)
C24–C19–P	119.8(1)	C15–C16–C17	120.0(2)
C20–C19–P	120.7(1)	C5–C4–C3	120.8(2)
C10–C11–C12	119.8(2)	C23–C22–C21	120.3(2)
C5–C6–C1	120.1(2)	C4–C5–C6	120.0(2)
C12–C7–C8	119.8(2)	C8–C9–C10	120.2(2)
C12–C7–P	120.8(1)	C2–C3–C4	119.6(2)
C8–C7–P	119.3(2)	C20–C21–C22	119.9(2)
C6–C1–C2	119.1(2)	C9–C10–C11	120.4(2)
C6–C1–P	120.2(2)	C22–C23–C24	120.2(2)
C2–C1–P	120.4(2)	C18–C13–P	120.3(2)
C14–C13–C18	119.7(2)	C23–C24–C19	120.2(2)
C14–C13–P	119.9(2)		

Regardless of the bulk of the cations, there still exists a certain planarity among the 5-nitrotetrazolate anions, which sit on a layer with the nitro-groups pointing toward the opposite direction in respect to the nitro-groups of the anions on the next layer (Fig. 3). The distances between anions layers are approximately ~ 4 Å, which together with the big cations make for a very inefficient packing. This is reflected in the low-density value ($\rho_{\text{calc}} = 1.342 \text{ g/cm}^3$).

Figure 4 shows a view of the unit cell of **3** along the y axis. The two crystallographically independent 5-nitrotetrazolate anions can be distinguished easily: type A anions are found on the vertices of the unit cell, on two of the faces, on four edges and in the center, and they are roughly coplanar to one another and approximately perpendicular to the type B anions, which are found within the unit cell face-on to acetonitrile molecules. The water molecules, which are also found within the unit cell, are linked together through hydrogen bonds to the anions ($d_{\text{O-N}} = 2.899(1) \text{ Å}$) and the nitrogen corresponding to an acetonitrile molecule $d_{\text{O-N}} = 3.037(1) \text{ Å}$). In

Fig. 5, there is represented a view along the z axis of the unit cell of the compound. There exists lines of (type A) anions along the y axis that interact through π -stacking, and the acetonitrile molecules are coplanar to the plane formed by this type of anions as mentioned above. N3 and O2 (see Fig. 7 for labeling scheme) chelate the Na cations, and these are linked to other cations by coordination to water molecules forming the squares shown in Fig. 5, with lines of anions (type B) perpendicular to it with the axis created by C1 and N5 cutting through two Na atoms.

As shown in Fig. 6, every Na cation coordinates to seven electronegative atoms (four oxygen + three nitrogen atoms), forming a distorted pentagonal bipyramid where the axial positions are occupied by a water molecule and a 5-nitrotetrazolate anion ($\angle_{\text{O1-Na1-N1}} = 151.84(1)^\circ$). The rest of the coordination around the metal center is completed on the pentagonal base equatorial “plane” by a second water molecule, two single contacts to two nitrotetrazolates (one to the nitro-group oxygen and

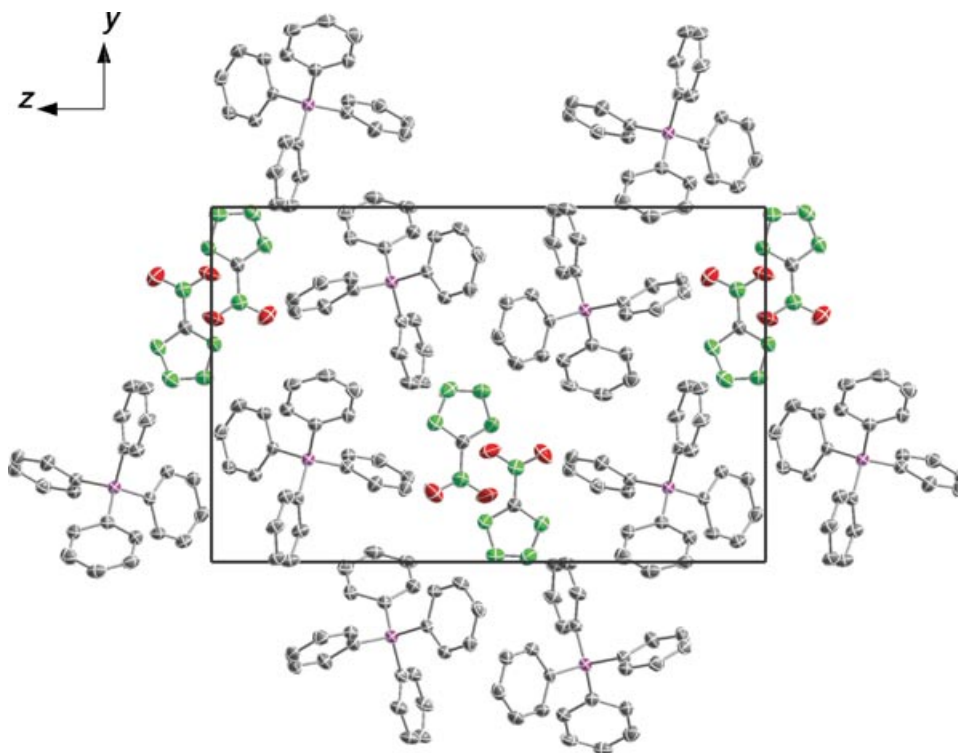


FIGURE 3 View of the unit cell of **2** along the *x* axis (diamond ellipsoids at the 50% probability). The hydrogen atoms have been omitted for the sake of simplicity.

one to a nitrogen atoms) and one nitrotetrazolate, which chelates the Na cation. On the pentagonal base the angles vary between $\angle_{\text{N2-Na1-N6}} = 91.60(1)^\circ$ and $\angle_{\text{O3-Na1-O5}} = 60.30(1)^\circ$ (Table 4).

The two types of crystallographically independent 5-nitrotetrazolate anions are represented in

Fig. 7. One of them chelates sodium through N3 and one of the nitro-group oxygen atoms with distances of 2.588(1) and 2.762(1) Å, respectively. A similar chelating effect is also observed for **1**, but is stronger ($d_{\text{N-Na}} = 2.467(2)$ Å, $d_{\text{O-Na}} = 2.641(2)$ Å) [6]. It can be argued that the insertion of acetonitrile molecules

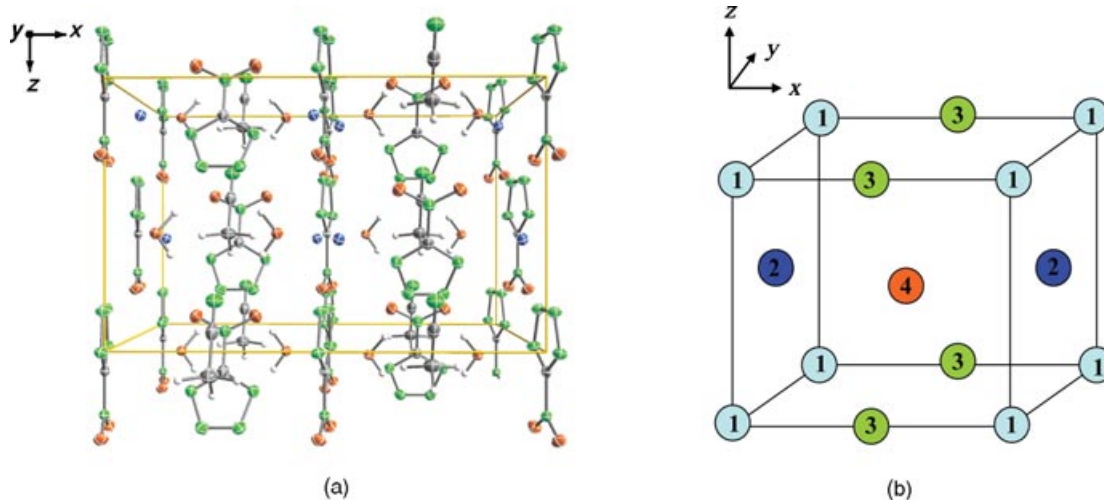


FIGURE 4 Diamond representation (ellipsoids at 50% probability) of a view of the unit cell along the *y* axis in **3** (a) and a schematic representation of the unit cell and (b) 1, 2, 3, and 4 represent 5-nitrotetrazolate anions placed at the edges, in the middle of a face, in the middle of a vertex or in the middle of the cell, respectively.

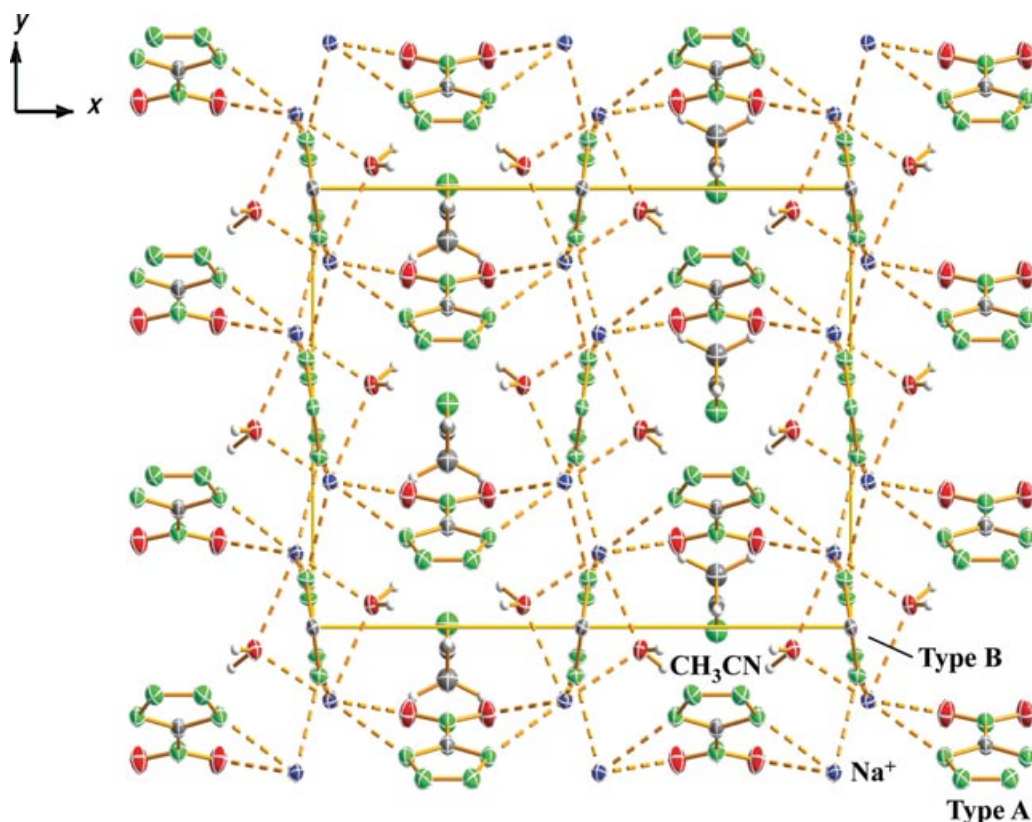


FIGURE 5 View of the unit cell of **3** along the *z* axis, showing the stacks of anions along the *y* axis (diamond ellipsoids at the 50% probability) and the coordination around the Na atoms (dotted lines).

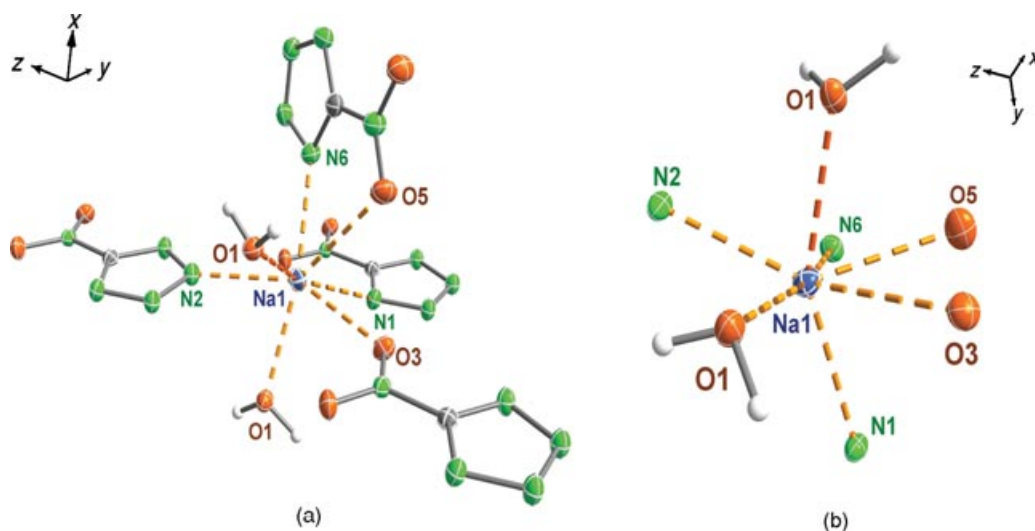


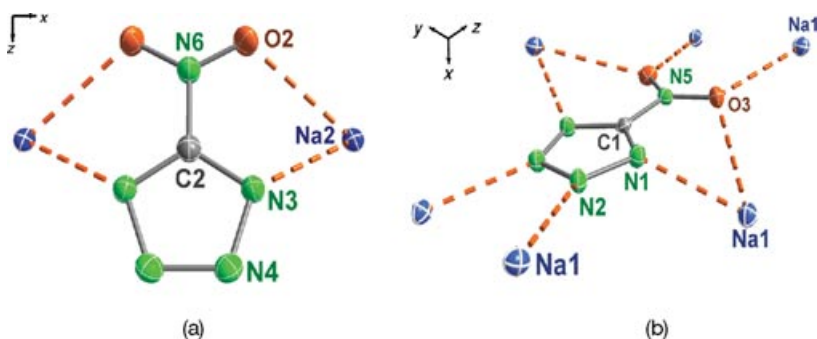
FIGURE 6 Coordination of the sodium atoms in **3** (a) and simplified coordination (b). Diamond ellipsoids at the 50% probability.

in the crystal structure of **2** forces the sodium atoms to place themselves more distant to the nitrotetrazolate anions than when there is no solvent molecules “disturbing” the packing; however, surprisingly, the presence of acetonitrile molecules in the structure of

2 ($\rho_{\text{calc.}} = 1.778 \text{ g/cm}^3$) seems to make for a more efficient overall packing than in the case of **1** where the density calculated from the crystal structure measurement is slightly lower ($\rho_{\text{calc.}} = 1.731 \text{ g/cm}^3$). The other type of anion is characterized by the

TABLE 4 Distances (Å) and Angles (°) for the Coordination Around the Metal Center in **3**

Distances (Å)			
Na–N2	2.527(1)	Na–N6	2.588(1)
Na–O1	2.391(1)	Na–O1	2.454(1)
Na–O3	2.734(1)	Na–N1	2.471(1)
Na–O5	2.763(1)		
Angles (°)			
N2–Na–N6	91.60(1)	O3–Na–O1	74.02(1)
N6–Na–O5	60.77(1)	O1–Na–N2	76.01(1)
O5–Na–O3	60.30(1)	O1–Na–N1	151.84(1)

FIGURE 7 Coordination of the 5-nitrotetrazolate anions to cations type A (a) and type B (b) in **3** with the labeling scheme.

coordination to one sodium cation of all electronegative atoms except for the nitro-group nitrogen atom (N5). The strongest coordination is observed, as expected, for the nitrogen atoms ($d_{\text{N1-Na}} = 2.471(1)$ Å, $d_{\text{N2-Na}} = 2.527(1)$ Å), whereas the oxygen atoms coordinate more loosely with $d_{\text{O-Na}} = 2.734(1)$ Å. In comparison to the other crystallographically independent nitrotetrazolate anions, this second type has a much closer bonding to the metal (type A: $d_{\text{N1-Na}} = 2.471(1)$ Å, $d_{\text{N2-Na}} = 2.527(1)$ Å; type B: $d_{\text{N-Na}} = 2.588(1)$ Å).

To assess the energetic properties of **2** and **3**, we measured its energetic properties, friction, and electrostatic discharge by standard BAM tests [24,25] and the thermal stabilities by differential scanning calorimetry (DSC) measurements [12]. Impact: Insensitive >40 J, less sensitive ≥ 35 J, sensitive ≥ 4 J, very sensitive ≤ 3 J; friction: Insensitive >360 N, less sensitive = 360 N, sensitive <360 N a. >80 N, very sensitive ≤ 80 N, extreme sensitive ≤ 10 N; According to the *UN Recommendations on the Transport of Dangerous Goods*, (+) indicates: not safe for transport.

At a heating rate of 2°C min^{-1} , **2** melts at $\sim 126^\circ\text{C}$ and decomposes at $\sim 188^\circ\text{C}$, whereas **3** decomposes at $\sim 200^\circ\text{C}$. Both compounds showed no sensitivity toward shock (>30 J) nor in the friction test (>360 N). Grinding the compounds in a mortar did not result in explosion either. Both compounds were

also insensitive to an electrostatic discharge of ~ 20 kV, ESD testing using a HF-vacuum-tester type VP 24. Rapid heating of **2** in the flame results in loud explosion, whereas compound **3** burns normally.

In conclusion, we synthesized a salt of 5-nitrotetrazole (**B**) with the bulky tetraphenylphosphonium cation (**2**) and fully characterized it by analytical and spectroscopic methods. The synthesis of highly energetic neutral 2-methyl-5-nitrotetrazole failed, and single crystals of explosive bis-(sodium 5-nitrotetrazolate) dihydrate acetonitrile adduct (**3**) were obtained. Both compounds showed decreased sensitivity to classical stimuli. Finally, the crystal structures of **2** and **3** were determined by X-ray diffraction techniques and are discussed in detail.

ACKNOWLEDGMENTS

The authors acknowledge collaborations Dr. M. Krupka (OZM Research, Czech Republic) in the development of new testing and evaluation methods for energetic materials and with Dr. M. Sucasca (Brodarski Institute, Croatia) in the development of new computational codes to predict the detonation parameters of high-nitrogen explosives. We are indebted to and thank Dr. Betsy M. Rice (ARL, Aberdeen, Proving Ground, MD) for many helpful and inspired discussions and support of our work.

REFERENCES

- [1] Hammerl, A.; Klapötke, T. M.; Nöth, H.; Warchhold, M.; Holl, G.; Kaiser, M. *Inorg Chem* 2001, 40, 3570–3575.
- [2] Hammerl, A.; Holl, G.; Kaiser, M.; Klapötke, T. M.; Piotrowski, H. *Z Anorg Allg Chem* 2003, 629, 2117–2121.
- [3] Hiskey, M. A.; Hammerl, A.; Holl, G.; Klapötke, T. M.; Polborn, K.; Stierstorfer, J.; Weigand, J. *J. Chem Mater* 2005, 17, 3784–3793.
- [4] Klapötke, T. M.; Miró Sabaté, C. *Z Anorg Allg Chem* 2007, 633, 2671–2677.
- [5] Ernst, V.; Klapötke, T. M.; Stierstorfer, J. *Z Anorg Allg Chem* 2007, 633, 879–887.
- [6] (a) Klapötke, T. M.; Miró, C. *Proceedings of the 10th Seminar on New Trends in Research of Energetic Materials*, April 25–27, 2007; Pardubice, Czech Republic. (b) Klapötke, T. M.; Miró Sabaté, C.; Welch, J. M. *Dalton Trans* 2008, 6372–6380.
- [7] Klapötke, T. M.; Mayer, P.; Miró Sabaté, C.; Welch, J. M.; Wiegand, N. *Inorg Chem* 2008, 47(13), 6014–6027.
- [8] Charalambous, J.; Georgiou, G. C.; Henrick, K.; Bates, L. R.; Healey, M. *Acta Crystallogr C* 1987, 43, 659–661.
- [9] Koldobskii, G. I.; Soldatenko, D. S.; Gerasimova, E. S.; Khokhryakova, N. R.; Shcherbinin, M. B.; Lebedev, V. P.; Obstrovskii, V. A. *Russ J Org Chem* 1997, 33(12), 1771–1783.
- [10] Kralj, J. G.; Murphy, E. R.; Jensen, K. F. *Joint Propulsion Conference and Exhibit*, July 10–13, 2005; Tucson, AZ.
- [11] <http://www.perkinelmer.com>.
- [12] http://www.linseis.net/html_en/thermal/dsc/dsc_pt10.php.
- [13] CrysAlis CCD, Version 1.171.27p5 beta. Oxford Diffraction Ltd., Oxford, UK, 2005.
- [14] CrysAlis RED, Version 1.171.27p5 beta. Oxford Diffraction Ltd., Oxford Diffraction Ltd., Oxford, UK, 2005.
- [15] Altomare, A.; Burla, M. C.; Camalli, M.; Casciarano, G. L.; Giacovazzo, C.; Guagliardi, A.; Moliterni, A. G. G.; Polidori, G.; Spagna, R. *J Appl Cryst* 1999, 32, 115–119.
- [16] SHELXS-97, Programs for Crystal Structure Solution. Sheldrick, G. M., Institut für Anorganische Chemie der Universität Göttingen, Germany, 1994.
- [17] SHELXS-97, Programs for Crystal Structure Solution. Sheldrick, G. M., Institut für Anorganische Chemie der Universität Göttingen, Germany, 1997.
- [18] Farrugia, L. J. *J Appl Crystallogr* 1999, 32, 837.
- [19] PLATON, A Multipurpose Crystallographic Tool. Spek, A. L., Utrecht, The Netherlands, 1999.
- [20] SCALE3 ABSPACK, An Oxford Diffraction program. Oxford Diffraction Ltd., Oxford, UK, 2005.
- [21] Colthup, N. B.; Daly, L. H.; Wiberley, S.E. *Introduction to Infrared and Raman Spectroscopy*; Academic Press: Boston, MA, 1990.
- [22] Kalinowski, H. O.; Berger, S.; Braun, S. *¹³C-NMR Spectroskopie*; Georg Thieme Verlag: Stuttgart, West Germany, 1984; p 532.
- [23] (a) Mtshali, T. N.; Purcell, W.; Visser, H. G. *Acta Crystallogr E* 2007, 63, m80–m82; (b) Neumüller, B.; Dehnicke, K.; *Z Anorg Allg Chem*, 2005, 631(13–14), 2535–2537.
- [24] <http://www.bam.de>.
- [25] Klapötke, T. M.; Rienäcker, C. M. *Propell Explos Pyrotech* 2001, 26, 43–47.

Hexacoordinated Spirocyclic Germanium(IV) Complex: Synthesis and Structural Characterization

Simplicio González-Montiel, Raymundo Cea-Olivares,
Vojtech Jancik, Leslie W. Pineda, and Rubén A. Toscano

*Instituto de Química, Universidad Nacional Autónoma de México, Circuito Exterior,
Ciudad Universitaria, México 04510, D.F., México*

Received 30 July 2008

ABSTRACT: *The spiro-dibenzogermocine [O(o-C₆H₄S)₂]₂Ge (**1**) was prepared in a reaction between O(o-C₆H₄SH)₂ and Ge(O^{*i*}Pr)₄, and its molecular structure was determined by X-ray diffraction studies. In the solid state, **1** shows the existence of two weak O → Ge transannular interactions, resulting in a hexacoordinated germanium atom that displays the geometry of a distorted bicapped tetrahedron. © 2009 Wiley Periodicals, Inc. Heteroatom Chem 20:45–49, 2009; Published online in Wiley InterScience (www.interscience.wiley.com). DOI 10.1002/hc.20510*

INTRODUCTION

Only three spiro-dibenzogermocine complexes of the type [D(o-C₆H₄E)₂]₂Ge (D = Se, S, P-Ph; E = O, S) [1–3] and two spiro-germocane complexes [D(CH₂CH₂S)₂]₂Ge (D = O, S) [4] (Fig. 1) in which the germanium atom is hexacoordinated have been structurally characterized. It was found that in the above-mentioned compounds, the secondary bonding [5] between the donor and the germanium atoms causes the hypercoordination phenomenon of these complexes, resulting in a hexacoordinated germa-

nium atom with a distorted octahedral geometry. To continue with our research about the influence of the combination of the donor atoms in the ligand and its rigidity on the strength of the transannular bond, we decided to use the O(o-C₆H₄SH)₂ ligand [6].

The ligands based on diphenylether should exhibit smaller flexibility than those derived from diphenylthioether due to the shorter C–O bonds, which should have together with the short C–O bond length and thus larger distance between the oxygen and germanium atoms a large effect on the transannular O → Ge distance in the spiro-dibenzogermocine compounds. Herein, we report the synthesis, characterization, and structural study of a spiro-dibenzogermocine [O(o-C₆H₄S)₂]₂Ge (**1**).

RESULTS AND DISCUSSION

Attempts to synthesize compound **1** by salt metathesis reaction between the lithium salt O(o-C₆H₄SLi)₂ and GeCl₄, or with the use of GeCl₄, the free ligand O(o-C₆H₄SH)₂ and an amine as an HCl acceptor (methods used in other cases) were unsuccessful [1–3]. Therefore, we decided to use Ge(O^{*i*}Pr)₄ as the source of germanium because its reactivity is lower than that of GeCl₄ and thus the reaction can be easily controlled. Furthermore, the only byproduct of the reaction of Ge(O^{*i*}Pr)₄ with the ligand O(o-C₆H₄SH)₂ would be isopropanol that is volatile and easy to remove, facilitating thus the isolation and

Correspondence to: Raymundo Cea-Olivares; e-mail: cea@servidor.unam.mx.

Contract grant sponsor: UNAM-DGAPA (PAPIIT).

Contract grant number: IN205208.

© 2009 Wiley Periodicals, Inc.

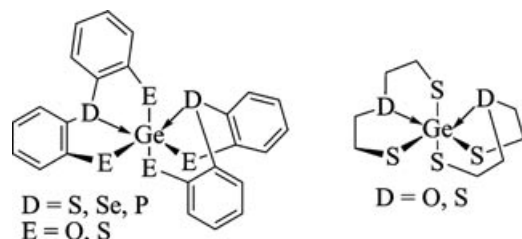


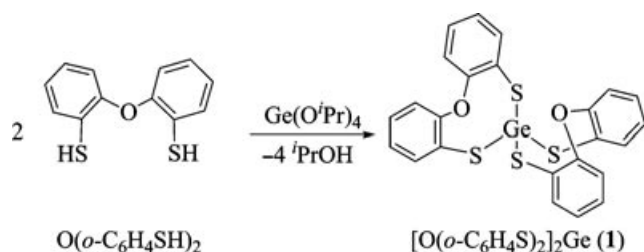
FIGURE 1 Spiro-dibenzogermocine and spiro-germocane complexes.

purification of the product. Therefore, the reaction between $\text{Ge}(\text{O}^i\text{Pr})_4$ and the free ligand $\text{O}(o\text{-C}_6\text{H}_4\text{SH})_2$ [6] in a molar ratio 1:2 in refluxing benzene leads to the formation of **1** in high yield (Scheme 1). Compound **1** is air-stable, soluble in benzene, toluene, dichloromethane, and chloroform but insoluble in pentane, hexane, and isopropanol.

There were no signals observed belonging to either the S–H protons or the protons from the $i\text{PrO}$ moieties in the ^1H NMR spectrum of **1** [6], confirming a complete substitution of the $i\text{PrO}$ groups on the Ge center by sulfur atoms. The four $\text{C}_6\text{H}_4\text{S}$ moieties are equivalent in solution showing an ABCD pattern for the aromatic protons. The ortho proton H-1 is shifted toward low frequencies when compared with complexes where the germanium atom is pentacoordinated [$\text{O}(o\text{-C}_6\text{H}_4\text{S})_2\text{GeEtCl}$ and $\text{O}(o\text{-C}_6\text{H}_4\text{S})_2\text{GePh}_2$] [7], but has a similar shift with respect to the free ligand [$\text{O}(o\text{-C}_6\text{H}_4\text{SH})_2$] [6].

The chemical shifts in the proton decoupled ^{13}C spectrum of **1** are similar as those reported for the dibenzogermocine [$\text{O}(o\text{-C}_6\text{H}_4\text{S})_2\text{GeEtCl}$ and $\text{O}(o\text{-C}_6\text{H}_4\text{S})_2\text{GePh}_2$] [7] complexes. The signal for the ipso carbon atom C-4a was found at 154.7 ppm, which is 2.6 ppm at higher frequency with respect to the free ligand [$\text{O}(o\text{-C}_6\text{H}_4\text{SH})_2$] [6]. Such trends have also been observed in other dibenzometalallocenes [6,8].

The study in solution by ^1H and ^{13}C NMR spectroscopy at ambient temperature suggests that either the system is highly symmetric or that the conformational interconversion is very fast on the



SCHEME 1

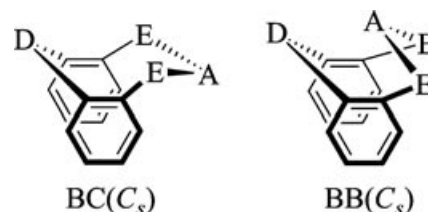


FIGURE 2 Conformational representations of eight-membered rings with C_s symmetry; boat-chair (BC) and boat-boat (BB) in dibenzometallocenes.

NMR time scale to be determined under these conditions. The chemical shifts also suggest that the $\text{O} \rightarrow \text{Ge}$ transannular interactions in complex **1** are very weak or completely lacking in solution; a similar phenomenon has been observed in the dibenzogermocine [$\text{O}(o\text{-C}_6\text{H}_4\text{S})_2\text{GeEtCl}$ and $\text{O}(o\text{-C}_6\text{H}_4\text{S})_2\text{GePh}_2$] [7] complexes under these conditions. Thus, the existence of the boat-chair conformer (BC) in solution can be suggested [2] (Fig. 2). This conformation is more stable than the boat-boat conformation required for the presence of the transannular bond.

The mass spectrum of **1** exhibits the molecular ion (M^+) for [$\text{O}(o\text{-C}_6\text{H}_4\text{S})_2$] $_2\text{Ge}$ with the appropriate isotopic pattern at m/z 538 albeit at low intensity, confirming the binding of germanium to sulfur atoms and the stability of the spiro-dibenzogermocine. The peak at m/z 506 corresponds to the fragment $M^+ - \text{S}$, the fragment at m/z 430 can be ascribed to $M^+ - \text{SPh}$ and the peaks at m/z 306 and 232 are assigned to the $\text{O}(\text{C}_6\text{H}_4\text{S})_2\text{Ge}$ and $\text{O}(\text{C}_6\text{H}_4\text{S})_2$ fragments, respectively. The base peak was assigned to the $\text{O}(\text{C}_6\text{H}_4)_2\text{S}$ moiety and appears at m/z 200.

X-ray Structure Description of Compound 1

The molecular structure of **1** has been determined by single-crystal X-ray diffraction analysis. Compound **1** crystallizes in the monoclinic space group $P2_1/c$ with one molecule of **1** and a solvating benzene molecule in the asymmetric unit. Selected crystallographic data are given in Table 1, and selected bond lengths, angles, and torsion angles are given in Table 2. The ORTEP drawing of **1** is depicted in Fig. 3.

The Ge–S(thiolate) bond lengths are in a good agreement with those reported for dibenzogermocine complexes [$\text{D}(o\text{-C}_6\text{H}_4\text{S})_2\text{GeL}^1\text{L}^2$] ($\text{D} = \text{S}, \text{O}$; $\text{L}^1 = \text{Ph}, \text{Cl}, \text{Br}$; $\text{L}^2 = \text{Et}, \text{Ph}$) (2.216(2)–2.255(1) Å) [7], the spiro-germocane [$\text{O}(\text{CH}_2\text{CH}_2\text{S})_2$] $_2\text{Ge}$ [2.210(3)–2.236(3) Å], and [$\text{S}(\text{CH}_2\text{CH}_2\text{S})_2$] $_2\text{Ge}$ [2.217(2)–2.222(1) Å] complex [4]. However, when compared

TABLE 1 Crystal Data and Summary of Data Collection and Refinement for **1**

Compound	1 · C ₆ H ₆
Formula	C ₃₀ H ₂₂ GeO ₂ S ₄
Formula weight	615.31
Temperature (K)	173(2)
Radiation (Å)	0.71073 (Mo K _α)
Crystal size (mm)	0.35 × 0.24 × 0.21
Crystal system, space group	Monoclinic, <i>P</i> 2 ₁ / <i>c</i>
<i>a</i> (Å)	9.008(2)
<i>b</i> (Å)	30.612(3)
<i>c</i> (Å)	9.873(2)
β (°)	101.60(2)
<i>V</i> (Å ³)	2667(1)
<i>Z</i>	4
<i>D</i> _{calc} (g cm ⁻³)	1.532
Absorption coefficient μ (mm ⁻¹)	1.490
<i>F</i> (000)	1256
θ Range for data collection (°)	2.21 to 25.38
Index ranges	−10 ≤ <i>h</i> ≤ 10 −36 ≤ <i>k</i> ≤ 36 −11 ≤ <i>l</i> ≤ 11
Collected reflections	15684
Independent reflections/ <i>R</i> _{int}	4868/0.0326
Data/restraints/parameters	4868/324/389
Goodness-of-fit on <i>F</i> ²	1.043
<i>R</i> ₁ , ^a <i>wR</i> ₂ ^b (<i>I</i> > 2.σ(<i>I</i>))	0.0379, 0.0918
<i>R</i> ₁ , ^a <i>wR</i> ₂ ^b (all data)	0.0468, 0.0965
Max./min. electron density (e Å ⁻³)	0.781/−0.235

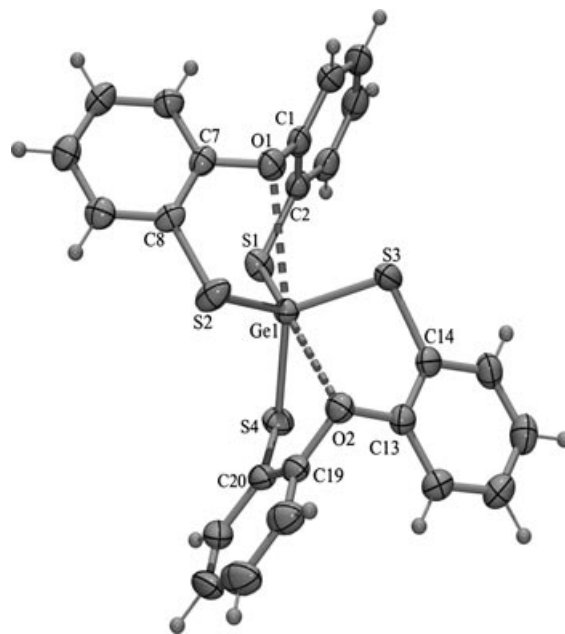
^a*R*₁ = $\sum ||F_o| - |F_c|| / \sum |F_o|$.^b*wR*₂ = $[\sum w(F_o^2 - F_c^2)^2 / \sum (F_o^2)^2]^{1/2}$.

to the Ge–S bond lengths in [PhP(*o*-C₆H₄S)₂]₂Ge [2.343(1)–2.400(1) Å] they are significantly shorter [3].

In addition to the four Ge–S bonds, two weak transannular O → Ge interactions are observed. The

TABLE 2 Selected Bond Lengths (Å), Angles, and Torsion Angles (°) for **1**

Bond Length			
O1 → Ge1	2.782(2)	Ge1–S2	2.219(1)
O2 → Ge1	2.827(2)	Ge1–S3	2.218(1)
Ge1–S1	2.232(1)	Ge1–S4	2.224(1)
Bond Angles			
S3–Ge1–S2	113.4(1)	S1–Ge1–S4	94.0(1)
S3–Ge1–S4	114.9(1)	O1–Ge1–S4	164.5(1)
S2–Ge1–S4	108.7(1)	O2–Ge1–S1	163.2(1)
S1–Ge1–S3	108.9(1)	O1–Ge1–O2	122.8(1)
S1–Ge1–S2	115.6(1)		
Torsion Angles			
C1–O1–C7–C8	142.2(1)	C13–O2–C19–C20	−81.3(1)
C7–O1–C1–C2	−79.5(1)	C19–O2–C13–C14	139.9(1)
S1–Ge1–S2–C8	−22.3(1)	S3–Ge1–S4–C20	91.9(1)
S2–Ge1–S1–C2	95.0(1)	S4–Ge1–S3–C14	−19.2(1)

**FIGURE 3** ORTEP diagram of [O(*o*-C₆H₄S)₂]₂Ge · C₆H₆ (**1**) (50% probability ellipsoids, benzene molecule is omitted).

O → Ge distances in **1** [2.782(2) and 2.827(2) Å] are in the middle of the range between the sum of the covalent radii of these elements [$\Sigma_{\text{rCov}}(\text{O,Ge}) = 1.88$ Å] [5] and the sum of their van der Waals radii [$\Sigma_{\text{rVdW}}(\text{O,Ge}) = 3.47$ Å] [9]. They are significantly longer than those in O(CH₂CH₂S)₂GeCl₂ [2.36(1) and 2.39(1) Å] [10], O(CH₂CH₂S)₂GeSO(C₂H₄) [2.492(3) Å] [11], O(CH₂CH₂S)₂GeS₂(C₂H₄) [2.616(1) Å] [10], and in O(C₆H₄S)₂GeEtCl [2.656(3) Å] [7], but shorter than those reported for [O(CH₂CH₂S)₂]₂Ge [2.915(3), 3.040(3), 2.955(3) and 2.946(3) Å] [4] and O(*o*-C₆H₄S)₂GePh₂ [2.872(3) Å] [7].

The geometry around the germanium atom in compound **1** can best be described as a distorted bi-capped tetrahedron [11,12], if the two weak transannular O → Ge interactions are taken into account. The tetrahedron is determined by the four covalent Ge–S bonds (S1–Ge1, S2–Ge1, S3–Ge1, and S4–Ge1), being distorted through the capping of the S1–S2–S3 and S2–S3–S4 faces by the O1 and O2 atoms, respectively, as shown in the Fig. 4. The relatively wide S3–Ge1–S2 [113.4(1)°] and rather acute S1–Ge1–S4 [94.0(1)° compared to the value for an ideal tetrahedral angle 109.5°] bond angles are attributed to the presence of the two transannular O → Ge interactions.

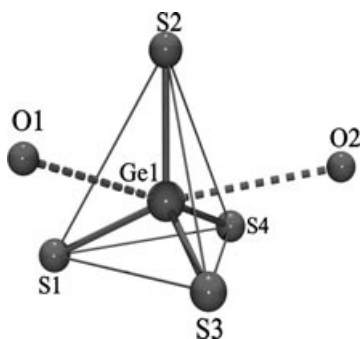
In the solid state, the eight-membered ring conformation in **1** can be described as a twisted boat (C₁ symmetry) according to the observed torsion angles [2].

TABLE 3 Comparison of D → Ge Geometrical Bond Parameters in Spirocyclic Germanium Compounds, Bond Lengths (Å), Bond Angles (°), and the Pauling Bond Order (BO)

Compound	D	E	D → Ge	D-Ge-D	Δd^a	BO ^b D → Ge	Reference
[D(CH ₂ CH ₂ E) ₂] ₂ Ge	O	S	2.914(3)	118.9	1.034	0.036	[4,11]
			3.040(3)	118.4	1.16	0.023	
			2.946(3)		1.07	0.030	
			2.955(3)		1.06	0.030	
[D(CH ₂ CH ₂ E) ₂] ₂ Ge	S	S	3.453(3)	111.0	0.977	0.042	[4,11]
			3.237(3)		1.193	0.020	
[D(o-C ₆ H ₄ E) ₂] ₂ Ge	O	S	2.782(2)	122.8(1)	0.902	0.053	This work
			2.827(2)		0.947	0.046	
[D(o-C ₆ H ₄ E) ₂] ₂ Ge	S	O	2.477(1)	97.19(6)	0.237	0.463	[3]
[D(o-C ₆ H ₄ E) ₂] ₂ Ge	Se	O	2.5959(6)	96.00(2)	0.2359	0.465	[1]
[PhD(o-C ₆ H ₄ E) ₂] ₂ Ge	P	S	2.4131(10)	100.34(3)	0.3331	0.339	[2]
			2.4173(12)		0.3373	0.335	

^aBond lengths, $\Delta d = (d_{\text{exp}} - \Sigma_{\text{rCov}})$, according to standard bond lengths Σ_{rCov} (O,Ge) = 1.88; Σ_{rCov} (S,Ge) = 2.24; Σ_{rCov} (Se,Ge) = 2.36, Σ_{rCov} (P,Ge) = 2.08 Å [5,8,15].

^bMode of calculation BO = $10^{-(1.41 \cdot \Delta d)}$ [13,14].

**FIGURE 4** View of the hexacoordinate geometry at germanium atom in 1.

To evaluate the magnitude of the transannular interactions (D → Ge) in the spiro-dibenzogermocines [D(o-C₆H₄E)₂]₂Ge (D = Se, S, P-Ph; E = O, S) and spiro-germocanes, the Pauling-type bond order (BO) was calculated [13,14]. These results are presented in Table 3.

It can be observed that the Pauling bond order of the transannular interactions D → Ge for spiro-dibenzogermocine D(o-C₆H₄E)₂]₂Ge (D = Se, S, P-Ph, O; E = O, S) compounds indicates that the interaction between the donor atom (D) and the germanium atom increases in the order O < P-Ph < S ≤ Se.

The comparison of the bond lengths and the Pauling bond orders at O → Ge in [O(o-C₆H₄S)₂]₂Ge shows that the transannular interactions O → Ge are stronger than those in a similar spiro-germocane [O(CH₂CH₂S)₂]₂Ge complex [3,11].

CONCLUSION

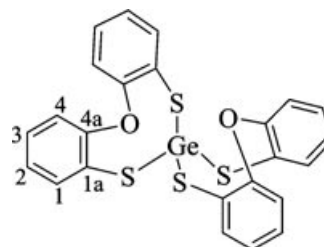
We have synthesized a novel homospiro-dibenzogermocine that exhibits two weak transan-

nular O → Ge interactions resulting in a hypercoordinated germanium atom. Ge(OⁱPr)₄ has proven to be an excellent starting material for the synthesis of spirocyclic germanium compounds.

EXPERIMENTAL SECTION

General Procedures

All manipulations were performed under a dry, oxygen-free atmosphere using standard Schlenk techniques. Solvents were dried by standard methods and distilled prior to use. The melting point was determined on a Mel-Temp II instrument. EI-MS (70 eV); spectrum was recorded with a JEOL JMS-AX505HA. NMR spectra were recorded at ambient temperature and measured on a Varian Inova 500 and a Bruker Avance 300 spectrometers using the solvent signals as internal reference (¹H and ¹³C{¹H}) (numbering scheme for the assignment of the NMR signals are shown in Scheme 2). The IR spectrum was recorded in the 4000–400 cm⁻¹ range on a Bruker tensor 27 spectrometer, as KBr pellet. O(o-C₆H₄SH)₂ was synthesized according to the

**SCHEME 2**

literature method [6]. $\text{Ge}(\text{O}^i\text{Pr})_4$ was purchased from Aldrich and used as supplied.

$[\text{O}(\text{o}-\text{C}_6\text{H}_4\text{S})_2]_2\text{Ge}$ (**1**): A solution of $\text{O}(\text{o}-\text{C}_6\text{H}_4\text{SH})_2$ (1.52 g, 6.40 mmol) in benzene (20 mL) was added via a syringe to $\text{Ge}(\text{O}^i\text{Pr})_4$ (1.0 mL, 3.20 mmol). The colorless reaction mixture was refluxed for 16 h, and then the resultant solution was cooled to room temperature. The solution was reduced to 5 mL of the volume, and the resulting colorless crystals of **1** were separated by suction filtration. Yield: 1.32 g (77%) mp = 142–146°C. MS-EI (70 eV): m/z (%) = 538 (8) (M^+), 506 (5) ($\text{M} - \text{S}^+$), 430 (7) ($\text{M} - \text{SPh}^+$), 306 (8) ($\text{M} - \text{S} - \text{SPhO}^+$), 232 (25) ($\text{M} - \text{S} - \text{SPhO} - \text{Ge}^+$), 200 (100) ($\text{M} - \text{S} - \text{SPhO} - \text{Ge} - \text{S}^+$). ^1H NMR (500 MHz, CDCl_3): δ = 7.35 (dd, 3J = 8.0, 4J = 2.0, H-1), 7.22 (ddd, 3J = 8.0, 4J = 2.0, H-3), 7.11 (dd, 3J = 8.0, 4J = 2.0, H-4), 7.05 (ddd, 3J = 8.0, 4J = 2.0, H-2) ppm. $^{13}\text{C}\{^1\text{H}\}$ NMR (300 MHz, CDCl_3): δ = 154.7 (C-4a), 133.2 (C-1), 128.8 (C-3), 126.1 (C-1a), 125.1 (C-2), 120.4 (C-4) ppm. IR (KBr pellet): 3062, 1569, 1463, 1438, 1258, 1219, 1120, 1060, 1032, 872, 799, 751, 733, 676 cm^{-1} .

X-Ray Crystallography

Suitable single crystals of complex **1** were grown by slow evaporation from a benzene solution. X-ray diffraction data on **1** were collected at 170 K on a Bruker-APEX three-circle diffractometer through the use of $\text{Mo } K_\alpha$ radiation (λ = 0.71073 Å, graphite monochromator). The structure was solved by direct methods (SHELXS-97) [16] and refined against all data by full-matrix least squares on F^2 [17]. CCDC-696800 contains the supplementary crystallographic data for this paper. These data can be obtained free of charge via <http://www.ccdc.cam.ac.uk/const/retrieving.html> (or from the Cambridge Crystallographic Data Centre, 12 Union Road, Cambridge CB21EZ, UK; fax: (+44)1223-336-033; or deposit@ccdc.cam.ac.uk).

ACKNOWLEDGMENTS

Simplicio González-Montiel and Leslie W. Pineda acknowledge the UNAM for their postdoctoral fellowships.

REFERENCES

- [1] Pastor, S. D.; Huang, V.; NabiRahni, D.; Koch, S. A.; Hua-Fen, H. *Inorg Chem* 1997, 36, 5966–5968.
- [2] Thompson, T. S.; Pastor, D.; Rihs, G. *Inorg Chem* 1999, 38, 4163–4167.
- [3] Chiang, M. Y.; Lin, J. W.; Zeng, W. F. *Acta Crystallogr C* 2005, 61, m84–m86.
- [4] Deng-Hai, C.; Hung-Cheh, C.; Chuen-Her, U. *Inorg Chim Acta* 1993, 208, 99–101.
- [5] Alcock, N. W. *Adv Inorg Chem Radiochem* 1972, 15, 1–58.
- [6] Alvarado-Rodríguez, J. G.; Andrade-López, N.; González-Montiel, S.; Merino, G.; Vela, A. *Eur J Inorg Chem* 2003, 3554–3561.
- [7] González-Montiel, S.; Andrade-López, N.; García-Montalvo, V.; Cogordan, J. A.; Alvarado-Rodríguez, J. G. *Eur J Inorg Chem* 2006, 4752–4760.
- [8] Alvarado-Rodríguez, J. G.; González-Montiel, S.; Andrade-López, N.; López-Feliciano, L. B. *Polyhedron* 2007, 26, 2929–2934.
- [9] Porterfield, W. W. *Inorganic Chemistry: A Unified Approach*, 2nd ed.; Academic Press: San Diego, CA, 1993; p. 214.
- [10] Draeger, M. Z. *Anorg Allg Chem* 1976, 423, 53–66.
- [11] Cea-Olivares, R.; García-Montalvo, V.; Moya-Cabrera, M. *Coord Chem Rev* 2005, 249, 859–872.
- [12] Cea-Olivares, R.; Lomeli, V.; Hernández-Ortega, S.; Haiduc, I. *Polyhedron* 1995, 14, 747–755.
- [13] Pauling, L. *The Nature of the Chemical Bond*, 3rd ed.; Cornell University Press: Ithaca, NY, 1960; p. 239.
- [14] Kolb, U.; Beuter, M.; Gerner, M.; Draeger, M. *Organometallics* 1994, 13, 4413–4425.
- [15] Huheey, J. E.; Keiter, E. A.; Keiter, R. L. *Inorganic Chemistry*, 4th ed.; Harper Collins: New York, 1993; p. 292.
- [16] Sheldrick, G. M. *Acta Crystallogr A* 1990, 46, 467–473.
- [17] Sheldrick, G. M. SHELXL-97; Program for Crystal Structure Refinement; Universität Göttingen; Göttingen, Germany, 1997.

Triorganotin(IV) Complexes Containing Multifunctional *meso*-Dimercaptosuccinic Acid Ligand: Syntheses, Characterizations, and Crystal Structures

Chunlin Ma,^{1,2} Qingfeng Wang,¹ and Rufen Zhang¹

¹Department of Chemistry, Liaocheng University, Liaocheng 252059, People's Republic of China

²Taishan University, Taian 271021, People's Republic of China

Received 22 June 2008; revised 5 October 2008

ABSTRACT: Four triorganotin complexes of the types $[(R_3Sn)_2(C_2H_2S_2)(COOH)_2] \cdot 2Et_2O$ ($R = Ph$, **1**) and $(R_3Sn)_2(C_2H_2S_2)(COOH)_2$ ($R = Me$ **2**, $R = n-Bu$ **3**, and $R = PhCH_2$ **4**) have been obtained by the reaction of *meso*-dimercaptosuccinic acid and sodium ethoxide with triorganotin(IV) chloride in 1:2:2 stoichiometry. All the complexes were characterized by elemental analyses, IR spectroscopy, and NMR spectroscopy. Furthermore, complexes **1** and **2** were characterized by X-ray diffraction analyses, which revealed that complexes **1** and **2** are mononuclear structures and further interlinked by intermolecular $C-H \cdots O$ and $O-H \cdots O$ hydrogen bonds, respectively. © 2009 Wiley Periodicals, Inc. *Heteroatom Chem* 20:50–55, 2009; Published online in Wiley InterScience (www.interscience.wiley.com). DOI 10.1002/hc.20511

INTRODUCTION

Organotin complexes have attracted more and more attention in recent years, partly owing to their determinately or potentially pharmaceutical value, which have been reported several times before

[1–9], as well as the versatile molecular structure and supramolecular architecture exhibited by these complexes [10–14]. It is well known that organotin carboxylates have versatile molecular structures both in solid and in solution, such as monomers, dimers, tetramers, oligomeric ladders, hexameric drums, etc [15]. It has also been demonstrated that other structural types are formed owing to the presence of additional heteroatom sites (S, N, or O) along with a carboxylate moiety [10–12,16]. In our previous work, we have reported several new molecular structures of triorganotin complexes by the reaction of *meso*-dimercaptosuccinic acid (H_4dmsa) and sodium ethoxide with triorganotin(IV) chloride in 1:4:4 stoichiometry [17]. Now, we synthesize other four triorganotin complexes by the reaction of H_4dmsa and sodium ethoxide with triorganotin(IV) chloride in 1:2:2 stoichiometry. In this paper, we report syntheses and characterization of these triorganotin(IV) complexes.

EXPERIMENTAL

Materials and Measurements

All reagents were commercially available, and they were used without further purification. The melting points were obtained with X-4 digital micro melting point apparatus and were uncorrected. Infrared spectra were recorded on a Nicolet-5700

Correspondence to: Chunlin Ma; e-mail: macl@lcu.edu.cn.
Contract grant sponsor: National Natural Foundation, People's Republic of China.
Contract grant number: 20741008.
© 2009 Wiley Periodicals, Inc.

spectrophotometer by using KBr discs and sodium chloride optics. ^1H and ^{119}Sn NMR spectra were recorded on a Varian Mercury Plus 400 spectrometer operating at 400 and 149.2 MHz, respectively. The spectra were obtained at 298 K. Chemical shift values were reported in ppm with respect to references and were expressed relative to external tetramethylsilane for ^1H NMR and neat tetramethyltin for ^{119}Sn NMR. Elemental analyses (C and H) were performed with a PE-2400II apparatus.

Syntheses of Complexes 1–4

$[(\text{Ph}_3\text{Sn})_2(\text{C}_2\text{H}_2\text{S}_2)(\text{COOH})_2] \cdot 2\text{Et}_2\text{O}$ **1**. The reaction was carried out under nitrogen atmosphere. H_4dmsa (0.182 g, 1 mmol), sodium ethoxide (0.136 g, 2 mmol), and Ph_3SnCl (0.770 g, 2 mmol) were added to ethanol (20 ml), continuing the reaction for 12 h at 40°C. The solid was recrystallized from ether, and colorless crystals were obtained. Yield: 79%. m.p. 160°C–162°C. Anal. found: C 56.77%, H 5.03%. Calc. for $\text{C}_{48}\text{H}_{54}\text{O}_6\text{S}_2\text{Sn}_2$: C 56.06%, H 5.29%. IR (KBr, cm^{-1}): $\nu(\text{COO}-\text{H})$ 3227, $\nu(\text{C}-\text{O}-\text{C})$ 944, $\nu(\text{Sn}-\text{C})$ 522, $\nu(\text{Sn}-\text{S})$ 331. ^1H NMR (CDCl_3 , ppm): δ 1.11 (t, 12H, CH_3), 3.53 (m, 8H, CH_2), 4.22 (s, 2H, CH), 7.35–7.72 (m, 30H, Ar–H), 12.63 (s, 2H, COOH). ^{13}C NMR (CDCl_3 , ppm): 174.2 (COOH), 136.5 (*i*-C, $^1J_{\text{SnC}} = 542$ Hz), 132.4 (*o*-C, $^2J_{\text{SnC}} = 40.4$ Hz), 129.2 (*m*-C, $^3J_{\text{SnC}} = 57.2$ Hz), 128.7 (*p*-C), 66.5 (O- CH_2), 52.4 (C–S), 15.3 (CH_3). ^{119}Sn NMR (CDCl_3 , ppm): 76.5.

$(\text{Me}_3\text{Sn})_2(\text{C}_2\text{H}_2\text{S}_2)(\text{COOH})_2$ **2**. The procedure is similar to that reported for complex **1**. H_4dmsa (0.182 g, 1 mmol), sodium ethoxide (0.136 g, 2 mmol), and Me_3SnCl (0.398 g, 2 mmol) were added to ethanol (20 ml), continuing the reaction for 12 h at 40°C. The solid was recrystallized from ether, and colorless crystals were formed. Yield: 73%. m.p. 153°C–155°C. Anal. found: C 23.85%, H 4.12%. Calc. for $\text{C}_{10}\text{H}_{22}\text{O}_4\text{S}_2\text{Sn}_2$: C 23.65%, H 4.37%. IR (KBr, cm^{-1}): $\nu(\text{COO}-\text{H})$ 3146, $\nu(\text{Sn}-\text{C})$ 503, $\nu(\text{Sn}-\text{S})$ 342. ^1H NMR [$(\text{CD}_3)_2\text{SO}$, ppm]: δ 0.85 (s, 18H, CH_3 , $^2J_{\text{SnH}} = 62.4$ Hz), 4.37 (s, 2H, CH), 12.59 (s, 2H, COOH). ^{13}C NMR (CDCl_3 , ppm): 172.8 (COOH), 54.1 (C–S), 13.8 (CH_3 , $^1J_{\text{SnC}} = 420$ Hz). ^{119}Sn NMR (CDCl_3 , ppm): 63.9.

$[(n\text{-Bu})_3\text{Sn}]_2(\text{C}_2\text{H}_2\text{S}_2)(\text{COOH})_2$ **3**. The procedure is similar to that reported for complex **1**. H_4dmsa (0.182 g, 1 mmol), sodium ethoxide (0.136 g, 2 mmol), and Me_3SnCl (0.650 g, 2 mmol) were added to ethanol (20 ml), continuing the reaction for 12 h at 40°C. The solvent is gradually removed by evaporation under vacuum until solid product is obtained. Yield: 76%. m.p. 131°C–134°C. Anal.

found: C 44.51%, H 7.87%. Calc. for $\text{C}_{28}\text{H}_{58}\text{O}_4\text{S}_2\text{Sn}_2$: C 44.24%, H 7.69%. IR (KBr, cm^{-1}): $\nu(\text{COO}-\text{H})$ 3197, $\nu(\text{Sn}-\text{C})$ 515, $\nu(\text{Sn}-\text{S})$ 328. ^1H NMR [$(\text{CD}_3)_2\text{SO}$, ppm]: δ 0.91 (s, 18H, CH_3), 1.29–1.58 (m, 36H, CH_2 - CH_2 - CH_2 , $^2J_{\text{SnH}} = 76.8$ Hz), 4.05 (s, 2H, CH), 12.61 (s, 2H, COOH). ^{13}C NMR (CDCl_3 , ppm): 169.4 (COOH), 53.3 (C–S), 28.7 (γCH_2 , $^3J_{\text{SnC}} = 68$ Hz), 26.4 (βCH_2 , $^2J_{\text{SnC}} = 22.4$ Hz), 25.6 (αCH_2 , $^1J_{\text{SnC}} = 364.8$ Hz), 14.6 (CH_3). ^{119}Sn NMR (CDCl_3 , ppm): 82.7.

$[(\text{PhCH}_2)_3\text{Sn}]_2(\text{C}_2\text{H}_2\text{S}_2)(\text{COOH})_2$ **4**. The procedure is similar to that reported for complex **1**. H_4dmsa (0.182 g, 1 mmol), sodium ethoxide (0.136 g, 2 mmol), and Me_3SnCl (0.650 g, 2 mmol) were added to ethanol (20 ml), continuing the reaction for 12 h at 40°C. The solvent is gradually removed by evaporation under vacuum until solid product is obtained. Yield: 84%. m.p. 182°C–185°C. Anal. found: C 57.01%, H 4.52%. Calc. for $\text{C}_{46}\text{H}_{46}\text{O}_4\text{S}_2\text{Sn}_2$: C 57.29%, H 4.81%. IR (KBr, cm^{-1}): $\nu(\text{COO}-\text{H})$ 3273, $\nu(\text{Sn}-\text{C})$ 526, $\nu(\text{Sn}-\text{S})$ 335. ^1H NMR [$(\text{CD}_3)_2\text{SO}$, ppm]: δ 2.72 (s, 12H, Ar- CH_2 , $^2J_{\text{SnH}} = 67.2$ Hz), 4.63 (s, 2H, CH), 7.15–7.69 (m, 30H, Ar–H), 12.68 (s, 2H, COOH). ^{13}C NMR (CDCl_3 , ppm): 170.5 (COOH), 137.3 (*i*-C, $^2J_{\text{SnC}} = 41.2$ Hz), 133.5 (*o*-C, $^3J_{\text{SnC}} = 19.2$ Hz), 130.8 (*m*-C), 128.9 (*p*-C), 51.7 (C–S), 24.3 (Ar- CH_2 , $^1J_{\text{SnC}} = 320.8$ Hz). ^{119}Sn NMR (CDCl_3 , ppm): 68.6.

X-ray Crystallography

Data were collected at 298 K on a Bruker SMART CCD 1000 diffractometer equipped with the Mo $\text{K}\alpha$ radiation. The structures were solved by direct methods and refined by a full-matrix least-squares procedure based on F^2 by using the SHELXL-97 program system. All nonhydrogen atoms were included in the model at their calculated positions. The positions of hydrogen atoms were calculated, and their contributions in structural factor calculations were included. Crystal data and experimental details of the structure determination are listed in Table 1.

RESULTS AND DISCUSSION

Syntheses of Complexes 1–4

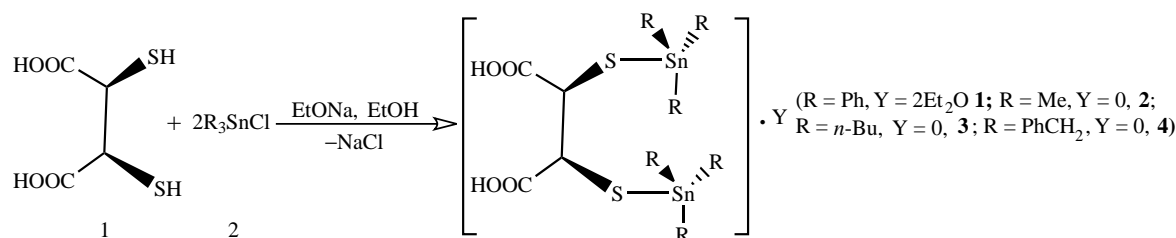
The synthetic procedure is shown in Scheme 1.

IR Spectroscopic Studies of Complexes 1–4

The explicit features in the infrared spectra of complexes **1–4**, that is, strong absorption appearing in the range from 328 to 342 cm^{-1} for the complexes, which are absent in the free ligand, are assigned to

TABLE 1 Crystal Data and Refinement Details for Complexes **1** and **2**

	Complex 1	Complex 2
Empirical formula	C ₄₈ H ₅₄ O ₆ S ₂ Sn ₂	C ₁₀ H ₂₂ O ₄ S ₂ Sn ₂
Formula weight	1028.41	507.78
Crystal system	Monoclinic	Monoclinic
Space group	<i>P</i> 2(1)/ <i>c</i>	<i>P</i> 2(1)/ <i>n</i>
Unit cell dimensions		
<i>a</i> (Å)	13.2002(12)	7.5434(12)
<i>b</i> (Å)	16.670(2)	14.390(2)
<i>c</i> (Å)	11.7247(10)	9.1840(16)
α (°)	90	90
β (°)	111.090(2)	110.822(2)
γ (°)	90	90
<i>V</i> (Å ³)	2407.1(4)	931.8(3)
<i>Z</i>	2	2
<i>D_c</i> (mg m ⁻³)	1.419	1.810
Absorption coefficient (mm ⁻¹)	1.169	2.907
<i>F</i> (0 0 0)	1044	492
Crystal size (mm)	0.40 × 0.36 × 0.34	0.49 × 0.45 × 0.44
θ range (°)	2.06–25.01	2.76–25.01
Reflections collected	11,861	4552
Independent reflections	4236	1635
Data/restraints/parameters	4236/0/284	1635/0/85
Goodness-of-fit on <i>F</i> ²	1.079	1.093
Final <i>R</i> indices [<i>I</i> > 2σ(<i>I</i>)]	<i>R</i> 1 = 0.0377, <i>wR</i> 2 = 0.0845	<i>R</i> 1 = 0.0347, <i>wR</i> 2 = 0.0709
<i>R</i> indices (all data)	<i>R</i> 1 = 0.0674, <i>wR</i> 2 = 0.1044	<i>R</i> 1 = 0.0477, <i>wR</i> 2 = 0.0752

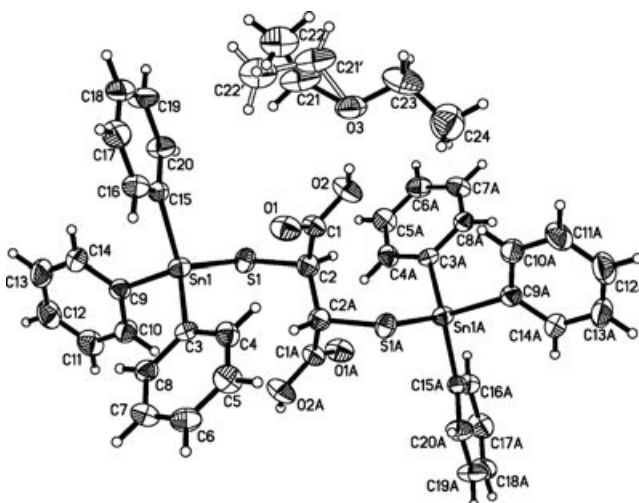


SCHEME 1

the Sn–S stretching mode [18]. While the broad absorption band at 3100–3300 cm⁻¹ is present in complexes **1–4**, which are assigned to the –COOH groups [19], indicating that the –COOH groups are not coordinate to the tin atoms. Moreover, a strong absorption band at about 944 cm⁻¹ in complex **1** is assigned to the C–O–C stretching mode, which indicates the presence of ether molecules in complex **1**.

NMR Data of Complexes **1–4**

¹H NMR data show that the signal of the –SH proton in the spectrum of the free ligand is absent in complexes **1–4**, indicating the removal of the –SH proton and the formation of Sn–S bonds. ¹³C NMR spectra show a downfield shift of all carbon resonances compared with the free ligand; the shift is a consequence of an electron density transfer from the ligand to the

FIGURE 1 Molecular structure of complex **1**.

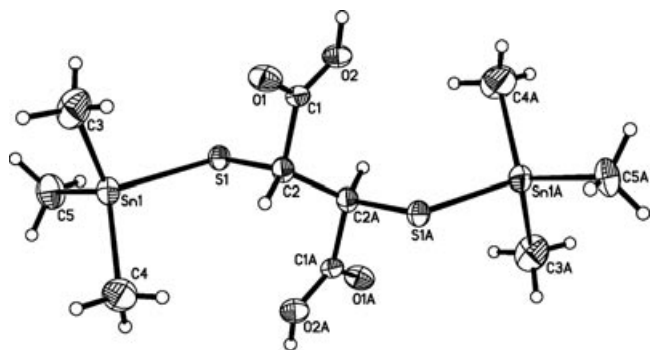


FIGURE 2 Molecular structure of complex **2**.

metal atoms. ^{119}Sn NMR spectra show resonances between 63 and 83 ppm. As reported in the literature [20], values of δ (^{119}Sn) in the ranges -210 to -400 , -90 to -190 , and 200 to -60 ppm have been associated with six-, five-, and four-coordinated tin centers, respectively. On the basis of these data, we can conclude that complexes **1–4** are typical of four-coordinated tin complexes, and these data are confirmed by the X-ray crystal structures of complexes **1** and **2**.

Crystal Structure of Complexes **1** and **2**

The molecular structures of complexes **1** and **2** are illustrated in Figs. 1 and 2, respectively; the two-dimensional and one-dimensional structures of complexes **1** and **2** are illustrated in Figs. 3 and 4, respectively; and selected bond lengths and bond angles are given in Tables 2 and 3, respectively. Both complexes **1** and **2** are dinuclear monomers, with one ligand coordinated to two triphenyltin moieties or trimethyl moieties. The ligand adopts its thiol sulfur atom to coordinate to the central tin atom. The central tin atom forms four primary bonds: three to the phenyl or methyl groups and one to the thiol sulfur atom. Thus, the geometry of the tin center displays a distorted tetrahedral coordinated sphere, with six angles ranging from $95.47(14)^\circ$ to $118.60(13)^\circ$ for **1** and $107.7(2)^\circ$ to $113.6(3)^\circ$ for **2**. The Sn–C bond lengths [2.129 – 2.147 Å for **1** and 2.121 – 2.135 Å for **2**, respectively] are consistent with those of our other reported organotin mercaptocarboxylate complexes [17,21]. The Sn–S bond lengths [$2.4258(14)$ Å for **1** and $2.4421(13)$ Å for **2**, respectively] are little longer than those found in other triorganotin complexes [22] and approach the sum of

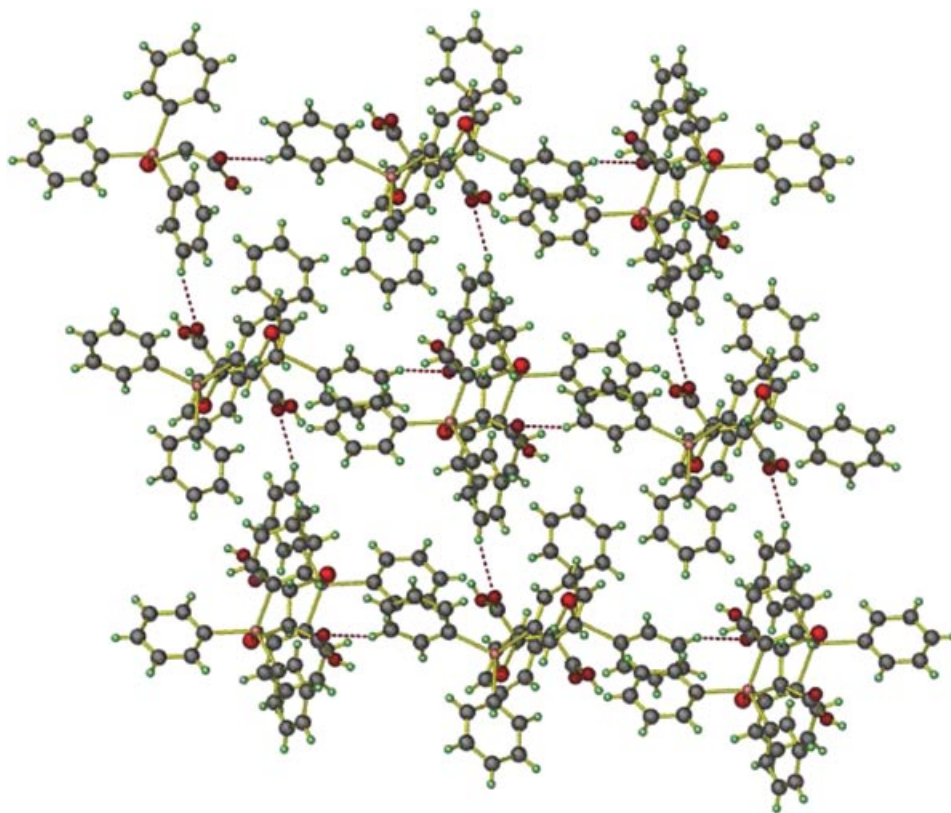


FIGURE 3 Two-dimensional network of complex **1** interlinked by intermolecular C—H...O hydrogen bonds (the disordered ether molecules are omitted for clarity).

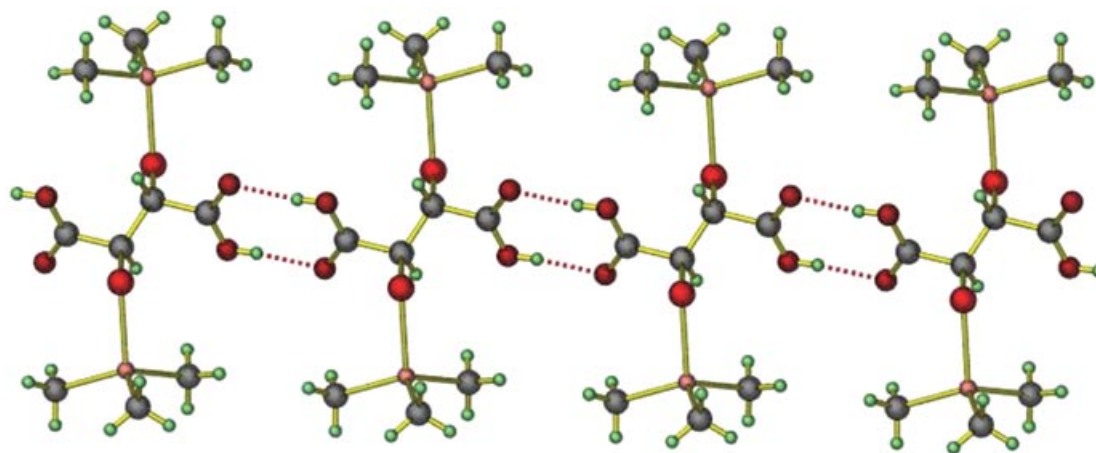


FIGURE 4 One-dimensional infinite chain of complex **2** interlinked by intermolecular O—H...O hydrogen bonds.

TABLE 2 Selected Bond Lengths (Å) and Bond Angles (°) for Complex **1**

Bond lengths			
Sn(1)—C(15)	2.129(4)	Sn(1)—C(3)	2.141(4)
Sn(1)—C(9)	2.147(5)	Sn(1)—S(1)	2.4258(14)
Bond angles			
C(15)—Sn(1)—C(3)	112.88(17)	C(15)—Sn(1)—C(9)	107.66(17)
C(3)—Sn(1)—C(9)	107.91(18)	C(15)—Sn(1)—S(1)	112.24(13)
C(3)—Sn(1)—S(1)	118.60(13)	C(9)—Sn(1)—S(1)	95.47(14)

TABLE 3 Selected Bond Lengths (Å) and Bond Angles (°) for Complex **2**

Bond lengths			
Sn(1)—C(4)	2.121(7)	Sn(1)—C(3)	2.135(7)
Sn(1)—C(5)	2.135(6)	Sn(1)—S(1)	2.4421(13)
Bond angles			
C(4)—Sn(1)—C(3)	113.6(3)	C(4)—Sn(1)—C(5)	113.0(3)
C(3)—Sn(1)—C(5)	113.4(3)	C(4)—Sn(1)—S(1)	107.27(19)
C(3)—Sn(1)—S(1)	107.7(2)	C(5)—Sn(1)—S(1)	100.7(2)

the covalent radii of tin and sulfur atoms (2.42 Å) [23], which proves that the sulfur atom is coordinated to the tin atom by a strong chemical bond.

Typical C—H...O hydrogen bonds are found between C(19)—H(19) and uncoordinated O(1) atom in complex **1**, which connect the adjacent molecules to give a two-dimensional network, the C(19)—H(19) and H(19)...O(1) distances are 0.930 Å and 2.670 Å, respectively, and the C—H...O angle is 158.40°. While typical O—H...O hydrogen bonds are found between O(2)—H(2) and uncoordinated O(1) atom in complex **2**, which connect the adjacent molecules to give rise to a one-dimensional linear chain, the O(2)—H(2) and H(2)...O(1) distances are 0.820 Å and 1.847 Å, respectively, and the O—H...O angle is 163.30°. These

weak but significant stacking interactions stabilize these crystal structures.

CONCLUSIONS

A series of triorganotin complexes derived from H₄dmsa have been synthesized and characterized. The results showed that when H₄dmsa and sodium ethoxide react with triorganotin(IV) chloride in 1:2:2 stoichiometry, the thiol protons are more easily deprotonated and coordinate to tin atoms. This results can enlighten us to design and synthesize some purposeful organotin complexes in different stoichiometry.

SUPPLEMENTARY DATA

Atomic coordinates, thermal parameters, and bond lengths and angles for complexes **1** and **2** have been deposited in the Cambridge Crystallographic Data Center, CCDC nos. CCDC 691662 and 691663. Copies of this information may be obtained free of charge from the Director, CCDC, 2 Union Road, Cambridge CB2 1EZ, UK, on request (fax: +44-1223-336-033, e-mail: deposit@ccdc.cam.ac.uk, or URL: <http://www.ccdc.cam.ac.uk>).

REFERENCES

- [1] Gielen, M.; Biesemans, M.; Willem, R. *Appl Organomet Chem* 2005, 19, 440.
- [2] Gielen, M. *Coord Chem Rev* 1996, 151, 41.
- [3] Gielen, M.; Tiekink, E. R. T. *J Braz Chem Soc* 2003, 14, 870.
- [4] Gielen, M.; *Appl Organomet Chem* 2002, 16, 481.
- [5] Nath, M.; Yadav, R.; Eng, R. G.; Nguyen, T. T.; Kumar, A. *J Organomet Chem* 1999, 577, 1.
- [6] Kemmer, M.; Dalil, H.; Biesemans, M.; Martins, J. C.; Mahieu, B.; Horn, E.; de Vos, D.; Tiekink, E. R. T.; Willem, R.; Gielen, M. *J Organomet Chem* 2000, 608, 63.
- [7] Gielen, M.; Khloufi, A.; Biesemans, M.; Willem, R.; Meunier-Piret, J. *Polyhedron* 1992, 11, 186.
- [8] Ma, C. L.; Jiang, Q.; Zhang, R. F. *Appl Organomet Chem* 2003, 17, 623.
- [9] Ma, C. L.; Zhang, J. H.; Zhang, R. F. *Heteroatom Chem* 2003, 14, 636.
- [10] Ma, C. L.; Jiang, Q.; Zhang, R. F.; Wang, D. Q. *Dalton Trans* 2003, 2975.
- [11] Ma, C. L.; Sun, J. F. *Dalton Trans* 2004, 1.
- [12] Ma, C. L.; Han, Y. F.; Zhang, R. F.; Wang, D. Q. *Dalton Trans* 2004, 1832.
- [13] Lockhart, T. P. *Organometallics* 1988, 7, 1438.
- [14] Meunier-Piret, J.; Bouâlam, M.; Willem, R.; Gielen, M. *Main Group Met Chem* 1993, 16, 329.
- [15] Ng, S. W.; Das, V. G. K. *J. Crystallogr Spectrosc Res* 1993, 23, 925.
- [16] Prabusankar, G.; Murugavel, R. *Organometallics* 2004, 23, 5644.
- [17] Ma, C. L.; Zhang, Q. F. *Eur J Inorg Chem* 2006, 3244.
- [18] May, J. R.; Mc Whinnie, W. R.; Pollerm, R. C. *Spectrochim Acta* 1971, 27A, 969.
- [19] Bellamy, L. J. In *The Infra-red Spectra of Complex Molecules*, 3rd ed.; New York: Wiley, 1975, 433.
- [20] Holecek, J.; Nadvornik, M.; Handlir, K.; Lycka, A. *J Organomet Chem* 1986, 315, 299.
- [21] Ma, C. L.; Zhang, Q. F.; Zhang, R. F.; Wang, D. Q. *Chem Eur J* 2006, 12, 420.
- [22] Ma, C. L.; Tian, G. R.; Zhang, R. F. *J Organomet Chem* 2006, 691, 2014.
- [23] Bondi, A. *J Phys Chem* 1964, 68, 441.

Synthesis, Structure, and Antifungal Activity of Dihydropyridones Containing Boronate Esters

Francis E. Appoh,¹ Susan L. Wheaton,¹ Christopher M. Vogels,¹
Felix J. Baerlocher,² Andreas Decken,³ and Stephen A. Westcott¹

¹Department of Chemistry, Mount Allison University, Sackville, NB E4L 1G8, Canada

²Department of Biology, Mount Allison University, Sackville, NB E4L 1G7, Canada

³Department of Chemistry, University of New Brunswick, Fredericton, NB E3B 5A3, Canada

Received 12 March 2008; revised 6 July 2008

ABSTRACT: We have prepared a series of novel 2,3-dihydro-4-pyridones containing boronate esters using the *aza* Diels–Alder reaction with Danishefsky's diene and imines derived from formylphenylboronic acids. This reaction can be carried out in moderate to high yields using $\text{Yb}(\text{OTf})_3$ as a Lewis acid catalyst. Two new boron compounds exhibited moderate antifungal activity (at $100 \mu\text{g disk}^{-1}$) using Amphotericin B as a control. © 2009 Wiley Periodicals, Inc. *Heteroatom Chem* 20:56–63, 2009; Published online in Wiley InterScience (www.interscience.wiley.com). DOI 10.1002/hc.20512

INTRODUCTION

Compounds containing boronic acids $[\text{RB}(\text{OH})_2]$ or boronate esters $[\text{RB}(\text{OR}')_2]$ are remarkably useful precursors for the Suzuki–Miyaura cross-coupling reactions [1] and as molecular recognition sensors [2]. Interest in these compounds also arises from their potent biological activities [3–10]. For instance, boron amino acid derivatives (Fig. 1a) are strong inhibitors of human arginase II, whose primary function appears to be in L-arginase homeostasis. Related α -aminoboronic acid derivatives are also well known for their ability to act as serine protease in-

hibitors [3]. Bortezomib (PS-341, Velcade; Fig. 1b) is a novel boronic acid dipeptide that potently, selectively, and reversibly inhibits 26S proteasome and was developed specifically for the therapy of human tumors [4]. Preclinical studies have shown that Bortezomib inhibited proliferation at a mean IC_{50} of 7 nM in 60 cell lines included in the National Cancer Institute's panel. Amino acid derivatives containing boron have also been investigated for their use in boron neutron capture therapy (BNCT) for the treatment of cancer [5]. BNCT is a bimodal form of therapy that depends on selectively depositing boron-10 atoms into the cancerous tumor before irradiation by slow neutrons. 4-Dihydroxyborylphenylalanine (Fig. 1c) has shown promise in the treatment of brain tumors. Also of importance is the recent observation that benzoxazole compounds (5-fluoro-3*H*-benzo[c] [1,2]oxaborol-1-ol, Fig. 1d) display considerable antifungal activity [6]. A remarkable property of boron, and in particular boronic acids, is their ability to selectively transport carbohydrates and other molecules across lipophilic membranes for potential applications in drug delivery [11]. A considerable amount of research has therefore focused on the synthesis of these potentially valuable compounds.

As part of our ongoing investigation into making novel boron compounds [12], and considering the wealth of bioactivities found in aminoboronic acid derivatives, we decided to examine the synthesis of boron-containing 2,3-dihydro-4-pyridones using the *aza* Diels–Alder reaction with Danishefsky's diene.

Correspondence to: Stephen A. Westcott; e-mail: swestcott@mta.ca.

Contract grant sponsor: Medical Research Fund of New Brunswick, Canada.

© 2009 Wiley Periodicals, Inc.

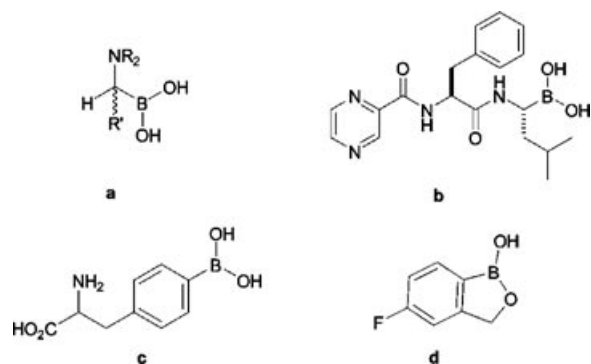


FIGURE 1 Bioactive boron compounds.

Previous studies have shown that compounds containing boronic acids can be extremely difficult to characterize in terms of elemental composition, owing to the ease with which they partially dehydrate to the corresponding trimeric and oligomeric anhydrides [13]. As such, we have decided to initially prepare the corresponding boronate ester derivatives; the results of which are presented herein.

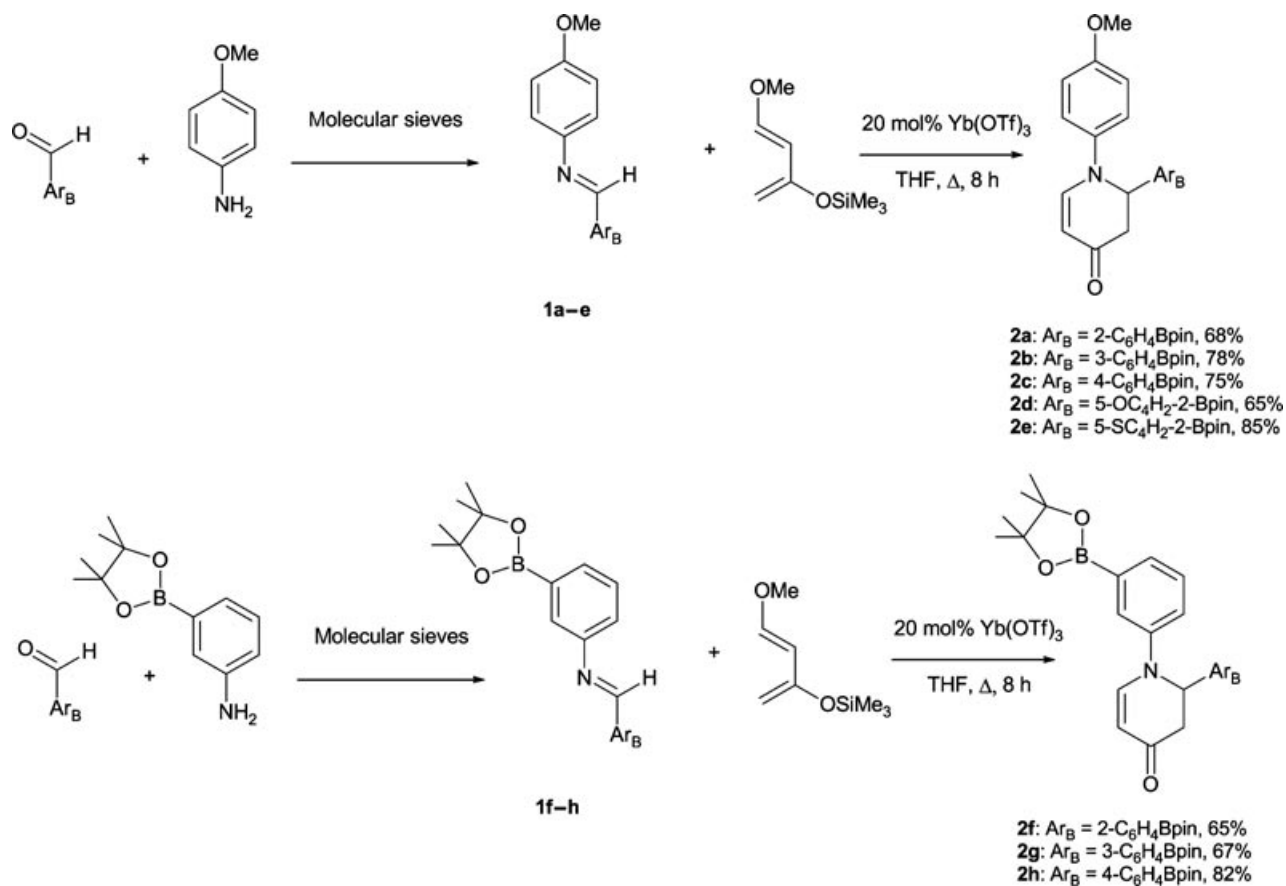
RESULTS AND DISCUSSION

Synthesis

The aza Diels–Alder reaction of Danishefsky's diene with imines is a powerful synthetic method for preparing 2-substituted 2,3-dihydro-4-pyridones that has received a considerable amount of attention. Dihydropyridone derivatives are highly versatile synthetic intermediates for the preparation of biologically important molecules [14]. As such, we have decided to prepare a series of boron-containing 2,3-dihydro-4-pyridones using Danishefsky's diene and preformed imines containing boronate esters. Imines incorporating boron groups have also received significant attention. For instance, Whiting and coworkers used imines containing boronate esters to make enantio-enriched γ -phenyl- γ -amino alcohols [15]. Incorporation of the boronate ester functionality in these cases was accomplished by deprotonation of acetophenone-derived imines followed by alkylation with ICH_2Bpin (pin = 1,2- $\text{O}_2\text{C}_2\text{Me}_4$) at low temperatures. Reduction of the imine was achieved using BH_3 reagents. In this study, we found that pinacol protected derivatives of formylphenylboronic acid [(4,4,5,5-tetramethyl-1,3,2-dioxaborolan-2-yl)benzaldehyde] add to anisidine or 3-(4,4,5,5-tetramethyl-1,3,2-dioxaborolan-2-yl)aniline (3-APBpin) in organic solvents to give

compounds having spectroscopic data consistent with the aldimines **1a–h** (Scheme 1). All imines have been characterized by multinuclear NMR spectroscopy and show a signal for the $\text{N}=\text{CH}$ methine proton between δ 8.43 and 9.18 ppm in the ^1H NMR spectra. A resonance at ca. 155 ppm in the ^{13}C NMR spectra corresponds to the sp^2 carbon of the $\text{N}=\text{CH}$ group. A broad peak at around 30 ppm in the ^{11}B NMR spectra suggests that the boron atom lies in a three-coordinate environment in solution [16]. The molecular structure of **1e** has also been confirmed by a single crystal X-ray diffraction study (Fig. 2). The imine $\text{C}(10)\text{--N}(9)$ bond distance of 1.277(3) Å is comparable to azomethine compounds derived from salicylaldehyde and phenylboronic acid [17]. The B--O bond distances (avg. = 1.361(3) Å) are also typical for three-coordinate boron [16,18–20] and significantly shorter than those observed in chelate complexes with diphenylborinic acid [21] or phenylboronic acid derivatives (ca. 1.5 Å [22], where the boron atom is four-coordinate).

Although a number of Lewis acids can be used to facilitate the aza Diels–Alder reaction, we have found that $\text{Yb}(\text{OTf})_3$ effectively catalyzes the addition of these boron-containing imines to Danishefsky's diene in moderate to high yields (Scheme 1) [23–27]. Attempts to improve yields using other Lewis acids or methodologies [27] proved unsuccessful. All new 2,3-dihydro-4-pyridones **2a–h** have been characterized by a number of physical methods including multinuclear NMR spectroscopy. The ^1H NMR for compounds **2a–h** shows a diagnostic pair of doublets for the alkene fragment of the pyridone ring in the aromatic region and a sharp singlet at ca. δ 1.35 ppm for the pinacol hydrogens. A broad peak at around 30 ppm is once again observed in the ^{11}B NMR spectra, where the boron atom remains three coordinate. This result is somewhat surprising in light of boron's propensity to form coordinate bonds with Lewis basic atoms [28]. The corresponding ^{13}C NMR data are also consistent with the formation of these novel pyridone, and the broad peak at ca. δ 140 ppm signifies the C--B bond for the Ar-Bpin groups. Compounds **2e** and **2f** have also been characterized by single crystal X-ray diffraction studies (Figs. 3 and 4), and the average B--O bond distances of 1.357(4) (**2e**) and 1.365(4) (**2f**) Å are consistent with three-coordinate boron compounds. Bond distances and angles within the pyridone ring are well within the range observed in related compounds [29]. No appreciable intra- or intermolecular interactions between the Lewis acidic boron atom and the nitrogen groups are observed in the solid state.



SCHEME 1

Antifungal Studies

Compounds **2f–h** are of special interest as they contain two boronate ester groups and are prepared from the [4+2] addition of Danishefsky's diene with

aldimines derived from 3-(4,4,5,5-tetramethyl-1,3,2-dioxaborolan-2-yl)benzenamine. Benzyamine compounds generated from this boron-containing aniline have shown moderate antifungal activities [30].

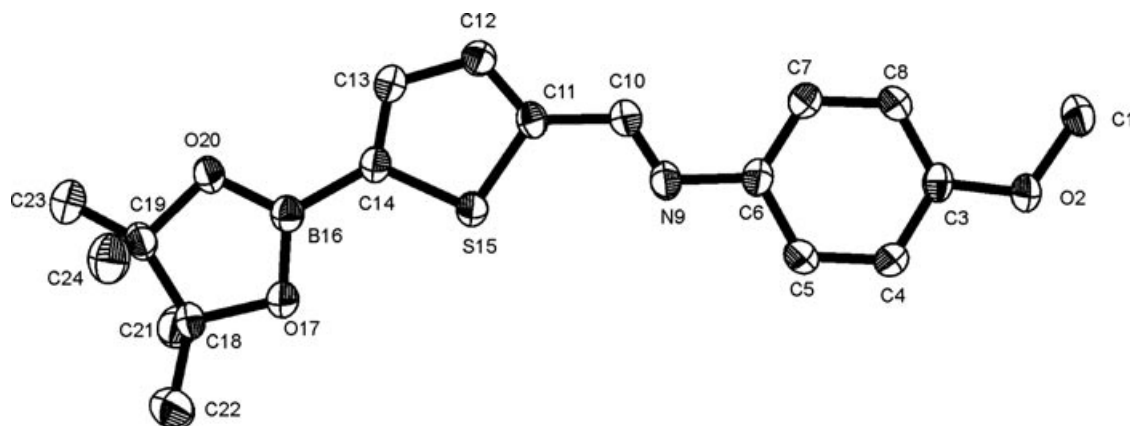


FIGURE 2 Perspective view of one of the independent molecules of **1e** with atom labeling scheme. Thermal ellipsoids are drawn at the 50% probability level, and hydrogen atoms are omitted for clarity. Selected bond lengths (Å) and angles (°): N(9)–C(10) 1.277(3), C(14)–B(16) 1.559(3), C(14)–S(15) 1.727(2), B(16)–O(20) 1.358(3), B(16)–O(17) 1.364(3), C(11)–S(15) 1.731(2); C(10)–N(9)–C(6) 120.4(2), O(20)–B(16)–O(17) 114.6(2), O(20)–B(16)–C(14) 122.5(2), O(17)–B(16)–C(14) 122.9(2).

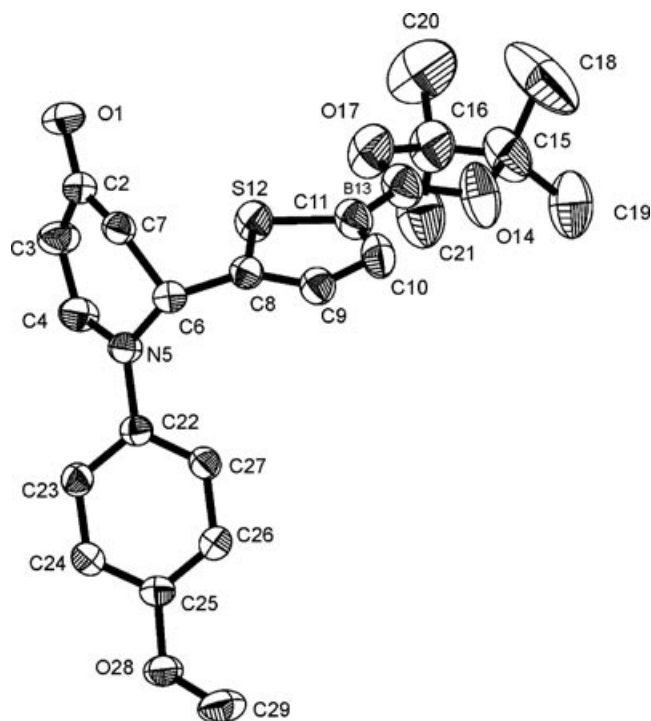


FIGURE 3 Perspective view of **2e** with atom labeling scheme. Thermal ellipsoids are drawn at the 50% probability level, and hydrogen atoms are omitted for clarity. Selected bond lengths (Å) and angles (°): O(1)–C(2) 1.234(3), C(3)–C(4) 1.364(3), C(11)–B(13) 1.559(4), B(13)–O(14) 1.355(4), B(13)–O(17) 1.358(4); O(1)–C(2)–C(3) 123.9(2), O(1)–C(2)–C(7) 121.4(2), O(14)–B(13)–O(17) 114.6(3), O(14)–B(13)–C(11) 121.6(3), O(17)–B(13)–C(11) 123.7 (3).

With this in mind, we have examined all new compounds for their ability to act as antifungal agents.

Given the wealth of bioactivities exhibited by 2,3-dihydro-4-pyridones [31] and 4-pyridone deriva-

tives [32], we have studied the potential antifungal activity of our new boron-containing compounds. Initial studies were carried out using four fungi, *Aspergillus niger*, *A. flavus*, *Candida albicans*, and *Saccharomyces cerevisiae*, employing Amphotericin B (AmB) as a control [12,33–35]. Although compounds **2a** and **2b** both showed appreciable activity (Table 1), the para derivative **2c** was inactive (not shown). Likewise, no activity was observed for **2f**, where the para methoxy substituent of the initial aniline derivative has been replaced with a meta-substituted boronate ester functionality. The non-boron control, prepared by the methodology developed by Feng et al. [25–27], showed no appreciable antifungal activity in this study. It is unclear at this time what role the boron groups have on the observed activities, and further work is therefore needed to fully understand the structure activity relationships in these compounds in an effort to design a more powerful antifungal agent.

CONCLUSION

In summary, we have prepared the first examples of boron-containing 2,3-dihydro-4-pyridones from the addition of imines, synthesized from commercially available aldehydes containing boronic acids, and Danishefsky's diene. Products have been characterized by a number of physical methods, including X-ray diffraction studies for **1e**, **2e**, and **2f**. Although most of these compounds showed no appreciable antifungal activity, the 2- and 3-boronated derivatives **2a** and **2b**, respectively, showed good activity against four fungi. We are in the process of preparing other

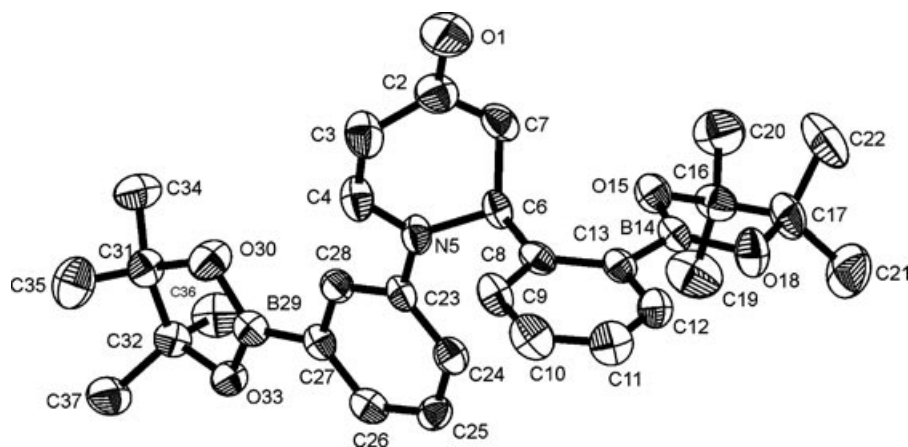


FIGURE 4 Perspective view of one of the independent molecules of **2f** with atom labeling scheme. Thermal ellipsoids are drawn at the 50% probability level, and hydrogen atoms are omitted for clarity. Selected bond lengths (Å) and angles (°): O(1)–C(2) 1.233(4), C(3)–C(4) 1.349(4), C(13)–B(14) 1.575(5), B(14)–O(15) 1.360(4), B(14)–O(18) 1.370(4), B(29)–O(33) 1.360(4), B(29)–O(30) 1.369(4); O(1)–C(2)–C(3) 123.7(4), O(1)–C(2)–C(7) 120.5(3), O(15)–B(14)–O(18) 112.9(3), O(15)–B(14)–C(13) 127.3(3), O(18)–B(14)–C(13) 119.7(3), O(33)–B(29)–O(30) 113.2(3), O(33)–B(29)–C(27) 124.7(3), O(30)–B(29)–C(27) 121.9(3).

TABLE 1 Antifungal Testing at a Dosage of 100 µg Disk⁻¹

Compound	Clear Zone (mm)			
	<i>A. niger</i>	<i>A. flavus</i>	<i>C. albicans</i>	<i>S. cerevisiae</i>
2a	7	0	7 halo	7 halo
2b	10	7	7 halo	9
2c	0	0	0	0
2d	0	0	0	0
2e	0	0	0	0
2f	0	0	0	0
2g	0	0	0	0
2h	0	0	0	0
AmB	11	11	9	9

2,3-dihydro-4-pyridones derived from formylphenylboronic acids and aniline derivatives and will report our findings in due course.

EXPERIMENTAL

General

Reagents and solvents used were purchased from Aldrich Chemicals. The synthesis of imines [36] and the transesterification of boronic acids with pinacol [37] were performed by established methods. NMR spectra were recorded on a JEOL JNM-GSX270 FT spectrometer. ¹H NMR chemical shifts are reported in ppm and referenced to residual solvent protons in deuterated solvent at 270 MHz. ¹¹B NMR chemical shifts are reported in ppm and are referenced to BF₃·OEt₂ as an external standard at 87 MHz. ¹³C NMR chemical shifts are referenced to solvent carbon resonances as internal standards at 68 MHz and are reported in ppm. Multiplicities are reported as singlet (s), doublet (d), broad (br), multiplet (m), and overlapping (ov). The infrared spectra were obtained using a Mattson Genesis II FTIR spectrometer and are reported in cm⁻¹. The melting points were determined using a Mel-Temp apparatus and are uncorrected. Microanalyses for C, H, and N were carried out at Guelph Chemical Laboratories (Guelph, ON, Canada). GCMS analyses were performed by DalChem MS Lab (Halifax, NS, Canada).

General Synthesis

To a stirring solution of the appropriate boronate ester in THF (20 mL), Danishefsky's diene (2 equivalents) and a catalytic amount of Yb(OTf)₃ (20 mol%) at RT were added. The reaction mixture was heated at reflux for 8–24 h, at which point the solvent was removed under vacuum. The resulting solid was dissolved in CHCl₃ (5 mL) and flashed through

a plug of silica gel. The CHCl₃ eluent was further purified by column chromatography, using CHCl₃/ethylacetate/hexanes (6:3:2) to afford the desired product.

2,3-Dihydro-1-(4-methoxyphenyl)-2-(2-(4,4,5,5-tetramethyl-1,3,2-dioxaborolan-2-yl)phenyl)pyridin-4(1H)-one (2a). Yield: 68%; mp = 72–74°C. ¹H NMR (CDCl₃) δ: 7.86 (d, *J* = 6.7 Hz, 1H), 7.70 (d, *J* = 6.4 Hz, 1H), 7.36–7.22 (ov m, 2H), 6.95 (d, *J* = 8.3 Hz, 2H), 6.77 (d, *J* = 8.3 Hz, 2H), 6.08 (dd, *J* = 7.8, 3.2 Hz, 1H), 5.27 (m, 2H), 3.72 (s, 3H), 3.30 (dd, *J* = 16.4, 7.8 Hz, 1H), 2.63 (dd, *J* = 16.4, 3.2 Hz, 1H), 1.35 (s, 12H); ¹³C{¹H} NMR (CDCl₃) δ: 191.7, 156.6, 150.1, 145.4, 141 (br, C-B), 138.6, 137.7, 131.5, 127.0, 125.5, 120.5, 114.6, 101.2, 84.0, 60.4, 55.5, 44.6, 25.0; ¹¹B (CDCl₃) δ: 30 (br). FTIR (Nujol): 2955 (s), 2935 (s), 2919 (s), 2853 (s), 1612 (w), 1601 (w), 1537 (w), 1508 (m), 1462 (m), 1345 (w), 1236 (m), 1166 (w), 1030 (m), 762 (w), 638 (w). Anal. Calcd for C₂₄H₂₈BNO₄ (405.29): C 71.11, H 6.98, N 3.46; Found: C 71.22, H 6.96, N 3.07. GCMS (CI+): required *m/z* = 405.2, found [M + H]⁺ = 406.2, [M + Na]⁺ = 428.3.

2,3-Dihydro-1-(4-methoxyphenyl)-2-(3-(4,4,5,5-tetramethyl-1,3,2-dioxaborolan-2-yl)phenyl)pyridin-4(1H)-one (2b). Yield: 78%; mp = 60–62°C. ¹H NMR (CDCl₃) δ: 7.84 (d, *J* = 6.4 Hz, 1H), 7.61 (d, *J* = 7.3 Hz, 1H), 7.34–7.17 (ov m, 2H), 6.90 (d, *J* = 7.5 Hz, 2H), 6.71 (d, *J* = 7.5 Hz, 2H), 6.04 (dd, *J* = 7.3, 3.2 Hz, 1H), 5.19 (m, 2H), 3.73 (s, 3H), 3.25 (dd, *J* = 15.4, 7.3 Hz, 1H), 2.60 (dd, *J* = 15.4, 3.2 Hz, 1H), 1.28 (s, 12H); ¹³C{¹H} (CDCl₃) δ: 190.8, 156.7, 153 (br, C-B), 150.0, 145.5, 138.6, 137.7, 131.5, 127.0, 125.5, 120.5, 114.6, 101.3, 84.0, 60.7, 55.6, 44.6, 25.0; ¹¹B (CDCl₃) δ: 31 (br). FTIR (Nujol): 2933 (s), 2912 (s), 2858 (s), 1645 (w), 1590 (w), 1510 (w), 1462 (m), 1377 (m), 1348 (w), 1227 (w), 1142 (w), 1033 (w), 964 (w), 723 (w). Anal. Calcd for C₂₄H₂₈BNO₄ (405.29): C 71.11, H 6.98, N 3.46; Found: C 71.09, H 7.06, N 3.14. GCMS (CI+): required *m/z* = 405.2, found [M + H]⁺ = 406.4, [M + Na]⁺ = 428.3.

2,3-Dihydro-1-(4-methoxyphenyl)-2-(4-(4,4,5,5-tetramethyl-1,3,2-dioxaborolan-2-yl)phenyl)pyridin-4(1H)-one (2c). Yield: 75%; mp = 82–84°C. ¹H NMR (CDCl₃) δ: 7.72 (d, *J* = 7.3 Hz, 2H), 7.50 (d, *J* = 7.9 Hz, 1H), 7.24 (d, *J* = 7.3 Hz, 2H), 6.90 (d, *J* = 8.8 Hz, 2H), 6.75 (d, *J* = 8.8 Hz, 2H), 5.20 (d, *J* = 7.9 Hz, 1H), 5.15 (m, 1H), 3.74 (s, 3H), 3.23 (dd, *J* = 15.7, 7.4 Hz, 1H), 2.75 (dd, *J* = 15.7, 4.1 Hz, 1H), 1.36 (s, 12H); ¹³C{¹H} (CDCl₃) δ: 189.9, 156.9, 149.9, 141.5, 138.2, 135.4, 129 (br, C-B),

125.8, 121.2, 114.7, 101.5, 83.9, 62.4, 55.5, 43.4, 24.9; ^{11}B (CDCl_3) δ : 30 (br). FTIR (Nujol): 2978 (s), 2927 (s), 2918 (s), 2854 (s), 1613 (w), 1547 (w), 1508 (w), 1462 (m), 1376 (m), 1326 (w), 1251 (w), 1222 (w), 1141 (w), 1088 (w), 1029 (w), 638 (w). Anal. Calcd for $\text{C}_{24}\text{H}_{28}\text{BNO}_4$ (405.29): C 71.11, H 6.98, N 3.46; Found: C 70.89, H 6.93, N 3.08. GCMS (CI^+): required m/z = 405.2, found $[\text{M} + \text{Na}]^+ = 428.3$.

2,3-Dihydro-1-(4-methoxyphenyl)-2-(5-(4,4,5,5-tetramethyl-1,3,2-dioxaborolan-2-yl)furan-2-yl)pyridin-4(1H)-one (2d). Yield: 65%; mp = 145–147°C. ^1H NMR (CDCl_3) δ : 7.30 (d, J = 7.6 Hz, 1H), 7.20 (d, J = 7.6 Hz, 1H), 7.02 (d, J = 8.8 Hz, 2H), 6.94 (d, J = 8.8 Hz, 2H), 6.86 (d, J = 3.2 Hz, 1H), 5.16–5.06 (ov m, 2H), 3.67 (s, 3H), 2.99–2.69 (ov m, 2H), 1.22 (s, 6H), 1.11 (s, 6H); $^{13}\text{C}\{^1\text{H}\}$ (CDCl_3) δ : 190.3, 157.2, 155.8, 148.8, 138.1, 130 (br, C-B), 124.3, 121.9, 114.7, 108.9, 101.5, 84.3, 57.2, 55.5, 40.2, 24.8; ^{11}B (CDCl_3) δ : 26 (br). FTIR (Nujol): 2952 (s), 2918 (s), 2856 (s), 1699 (w), 1577 (w), 1510 (w), 1462 (m), 1377 (m), 1350 (w), 1105 (w), 951 (w), 762 (w), 723 (w). Anal. Calcd for $\text{C}_{22}\text{H}_{26}\text{BNO}_5$ (395.26): C 66.84, H 6.64, N 3.54; Found: C 66.27, H 6.81, N 3.23. GCMS (CI^+): required m/z = 395.3, found $[\text{M} + \text{Na}]^+ = 418.3$.

2,3-Dihydro-1-(4-methoxyphenyl)-2-(5-(4,4,5,5-tetramethyl-1,3,2-dioxaborolan-2-yl)thiophen-2-yl)pyridin-4(1H)-one (2e). Yield: 85%; mp = 173–175°C. ^1H NMR (CDCl_3) δ : 7.40 (d, J = 7.3 Hz, 1H), 7.36 (d, J = 8.5 Hz, 2H), 7.03 (m, 1H), 6.82 (d, J = 8.5 Hz, 2H), 5.41 (dd, J = 7.5, 2.6 Hz, 1H), 5.21 (ov m, 2H), 3.78 (s, 3H), 3.28 (dd, J = 15.3, 7.5 Hz, 1H), 2.80 (dd, J = 15.3, 2.6 Hz, 1H), 1.31 (s, 12H); $^{13}\text{C}\{^1\text{H}\}$ (CDCl_3) δ : 189.8, 157.2, 149.0, 148.7, 137.8, 137.0, 129 (br, C-B), 127.2, 126.2, 114.5, 101.8, 84.2, 58.9, 55.5, 43.4, 24.8; ^{11}B (CDCl_3) δ : 28 (br). FTIR (Nujol): 2962 (s), 2945 (s), 2900 (s), 2870 (s), 1639 (w), 1576 (w), 1509 (w), 1462 (m), 1377 (m), 1346 (w), 1284 (w), 1242 (w), 1207 (w), 1142 (w), 1091 (w), 1025 (w), 955 (w), 829 (w), 665 (w). Anal. Calcd for $\text{C}_{22}\text{H}_{26}\text{BNO}_4\text{S}$ (411.32): C 64.23, H 6.38, N 3.41; Found: C 64.55, H 6.21, N 3.08. GCMS (CI^+): required m/z = 411.3, found $[\text{M} + \text{Na}]^+ = 434.3$.

2,3-Dihydro-2-(2-(4,4,5,5-tetramethyl-1,3,2-dioxaborolan-2-yl)phenyl)-1-(3-(4,4,5,5-tetramethyl-1,3,2-dioxaborolan-2-yl)phenyl)pyridin-4(1H)-one (2f). Yield: 65%; mp = 76–78°C. ^1H NMR (CDCl_3) δ : 7.91–7.82 (ov m, 2H), 7.58–7.47 (ov m, 2H), 7.35–7.22 (ov m, 3H), 6.98 (m, 1H), 6.17 (dd, J = 7.5, 2.5 Hz, 1H), 5.29–5.26 (ov m, 2H), 3.27 (dd, J = 15.6, 7.5 Hz, 1H), 2.64 (dd, J = 15.6, 2.5 Hz, 1H), 1.32 (s, 24H); $^{13}\text{C}\{^1\text{H}\}$ (CDCl_3) δ : 191.1, 149.4, 145.4, 144.3, 137.7,

131.5, 130.5, 129 (br, 2C, C-B), 128.9, 127.0, 125.3, 124.8, 121.2, 102.1, 84.2, 84.0, 59.8, 44.5, 24.9; ^{11}B (CDCl_3) δ : 31 (br). FTIR (Nujol): 2966 (s), 2935 (s), 2873 (s), 2846 (s), 1684 (w), 1645 (w), 1581 (w), 1570 (w), 1462 (m), 1377 (m), 1317 (w), 1267 (w), 1213 (w), 1144 (w), 1115 (w), 962 (w), 760 (w), 723 (w), 660 (w). Anal. Calcd. for $\text{C}_{29}\text{H}_{37}\text{B}_2\text{NO}_5$ (501.23): C 69.48, H 7.45, N, 2.79; Found: C 69.38, H 7.30, N 2.43. GCMS (CI^+): required m/z = 501.2, found $[\text{M} + \text{H}]^+ = 502.4$, $[\text{M} + \text{Na}]^+ = 524.4$.

2,3-Dihydro-1,2-bis(3-(4,4,5,5-tetramethyl-1,3,2-dioxaborolan-2-yl)phenyl)pyridin-4(1H)-one (2g). Yield: 67%; mp = 82–84°C. ^1H NMR (CDCl_3) δ : 7.76–7.67 (ov m, 3H), 7.56–7.46 (ov m, 2H), 7.32–7.21 (ov m, 3H), 6.95 (m, 1H), 5.30–5.24 (ov m, 2H), 3.25 (dd, J = 15.4, 6.4 Hz, 1H), 2.78 (dd, J = 15.4, 3.3 Hz, 1H), 1.36 (s, 24H); $^{13}\text{C}\{^1\text{H}\}$ (CDCl_3) δ : 190.4, 148.9, 144.2, 137.2, 134.3, 132.7, 131 (br, 2C, C-B), 130.9, 129.0, 128.8, 128.2, 125.1, 121.4, 102.8, 84.2, 84.0, 61.7, 43.6, 25.0, 24.9; ^{11}B (CDCl_3) δ : 30 (br). FTIR (Nujol): 2943 (s), 2902 (s), 2860 (s), 1649 (w), 1581 (w), 1570 (w), 1462 (m), 1377 (m), 1265 (w), 1213 (w), 1144 (w), 962 (w), 708 (w). Anal. Calcd for $\text{C}_{29}\text{H}_{37}\text{B}_2\text{NO}_5$ (501.23): C 69.48, H 7.45, N 2.79; Found: C 69.75, H 7.21, N 2.48. GCMS (CI^+): required m/z = 501.3, found $[\text{M} + \text{H}]^+ = 502.5$, $[\text{M} + \text{Na}]^+ = 524.4$.

2,3-Dihydro-1-(3-(4,4,5,5-tetramethyl-1,3,2-dioxaborolan-2-yl)phenyl)-2-(4-(4,4,5,5-tetramethyl-1,3,2-dioxaborolan-2-yl)phenyl)pyridin-4(1H)-one (2h). Yield: 82%; mp = 86–88°C. ^1H NMR (CDCl_3) δ : 7.75–7.69 (ov m, 3H), 7.55–7.50 (ov m, 2H), 7.26–7.18 (ov m, 3H), 6.95 (dd, J = 6.4, 3.3 Hz, 1H), 5.30–5.24 (ov m, 2H), 3.23 (dd, J = 15.4, 6.4 Hz, 1H), 2.78 (dd, J = 15.4, 3.3 Hz, 1H), 1.32 (s, 24H); $^{13}\text{C}\{^1\text{H}\}$ (CDCl_3) δ : 190.3, 149.0, 144.2, 141.2, 135.5, 130.9, 130 (br, 2C, C-B), 129.1, 125.7, 125.2, 121.6, 102.7, 84.2, 83.9, 61.8, 43.4, 25.9, 24.9; ^{11}B (CDCl_3) δ : 30 (br). FTIR (Nujol): 2943 (s), 2904 (s), 2858 (s), 1649 (w), 1581 (w), 1570 (w), 1462 (m), 1363 (w), 1327 (m), 1265 (w), 1219 (w), 1142 (w), 1088 (w), 1030 (w), 962 (w), 858 (w), 756 (w), 705 (w). Anal. Calcd for $\text{C}_{29}\text{H}_{37}\text{B}_2\text{NO}_5 \cdot 2\text{EtCO}_2\text{CH}_3$ (677.53): C 65.59, H 7.90, N 2.07; Found: C 65.19, H 7.34, N 2.28. GCMS (CI^+): required for $\text{C}_{29}\text{H}_{37}\text{B}_2\text{NO}_5$ m/z = 501.3, found $[\text{M} + \text{Na}]^+ = 524.4$.

Biological Testing

Compounds were tested for antifungal activity against pure cultures of *A. niger*, *A. flavus*, *C. albicans*, and *S. cerevisiae* supplied by Ward's Natural Science Ltd. (St. Catharines, Ontario, Canada). All cultures were maintained on Sabouraud dextrose

agar. Four agar plugs (10-mm diameter) of *A. niger* or *A. flavus* were cut from a 5–8 day-old colony and homogenized in distilled, sterilized water (2 mL). From this suspension, 0.5 mL was transferred aseptically to a Petri plate with Sabouraud dextrose agar (25 mL) and spread evenly over the entire surface. A 0.5-mL aliquot of a 1-month old liquid culture medium of *C. albicans* or *S. cerevisiae* was transferred and spread aseptically and allowed to dry. Each plate was provided with four evenly spaced paper disks (6-mm Fisherbrand P8 filter paper), containing the compound (0, 25, 50, and 100 μg , respectively). Each compound was applied to the disks as a solution (15 mg compound per 3 mL of acetone) where control disks were treated with neat acetone (20 μL). Amphotericin B in acetone acted as a standard (100 μg). Test plates with fungal homogenates were incubated at 20°C for 48 h. Four replicate plates were used for each test. Antifungal activity was taken by the diameter of the clear zone surrounding the disk; a halo indicates partial inhibition of growth.

X-Ray Diffraction Studies

Crystals of **1e**, **2e**, and **2f** were grown from saturated THF solutions at 20°C. Single crystals were coated with Paratone-N oil, mounted using a polyimide MicroMount and frozen in the cold nitrogen stream of the goniometer. A hemisphere of data was collected on a Bruker AXS P4/SMART 1000 diffractometer using ω and θ scans with a scan width of 0.3° and exposure time of 10 s (**1e** and **2e**) and 40 s (**2f**). The detector distance was 5 cm. The data were reduced and corrected for absorption [38–40]. The structures were solved by direct methods and refined by full-matrix least squares on F^2 . All non-hydrogen atoms were refined anisotropically. Hydrogen atoms were located in Fourier difference maps and refined isotropically (**1e**) or included in calculated positions and refined using a riding model (**2e** and **2f**). Crystallographic data for **1e**: $\text{C}_{18}\text{H}_{22}\text{BNO}_3\text{S}$, $M_w = 343.24$, orthorhombic, $P2(1)2(1)2(1)$, $a = 10.034(4)$ Å, $b = 12.880(5)$ Å, $c = 28.060(11)$ Å, $V = 3626(2)$ Å³, $Z = 8$, $D_{\text{calcd}} = 1.257$ g cm⁻³, $F(000) = 1456$, $\mu = 0.193$ mm⁻¹, $R1 = 0.0362$ ($I > 2\sigma(I)$), $wR2 = 0.0882$ (all data), $\text{GoF} = 1.118$. Crystallographic data for **2e**: $\text{C}_{22}\text{H}_{26}\text{BNO}_4\text{S}$, $M_w = 411.31$, monoclinic, $P2(1)/c$, $a = 16.475(4)$ Å, $b = 11.295(3)$ Å, $c = 12.109(3)$ Å, $\beta = 107.021(3)^\circ$, $V = 2154.6(8)$ Å³, $Z = 4$, $D_{\text{calcd}} = 1.268$ g cm⁻³, $F(000) = 872$, $\mu = 0.178$ mm⁻¹, $R1 = 0.0487$ ($I > 2\sigma(I)$), $wR2 = 0.1489$ (all data), $\text{GoF} = 1.038$. Crystallographic data for **2f**: $\text{C}_{29}\text{H}_{37}\text{B}_2\text{NO}_5$, $M_w = 501.22$, monoclinic, $P2(1)$, $a = 10.0450(19)$ Å, $b = 28.599(6)$ Å, $c = 10.900(2)$

Å, $\beta = 115.904(3)^\circ$, $V = 2816.8(9)$ Å³, $Z = 4$, $D_{\text{calcd}} = 1.182$ g cm⁻³, $F(000) = 1072$, $\mu = 0.078$ mm⁻¹, $R1 = 0.0518$ ($I > 2\sigma(I)$), $wR2 = 0.1203$ (all data), $\text{GoF} = 1.007$. Crystallographic information has also been deposited with the Cambridge Crystallographic Data Centre (CCDC 675383–675385).

ACKNOWLEDGEMENTS

The authors thank Mount Allison University, the Canada Research Chairs Program, the Canadian Foundation for Innovation/Atlantic Innovation Fund, Merck Frosst Canada and Co., and the Medical Research Fund of New Brunswick for financial support. The authors also thank Dan Durant (MtA) and Roger Smith (MtA) for expert technical assistance and anonymous reviewers for helpful comments.

REFERENCES

- [1] Alonso, F.; Beletskaya, I. P.; Yus, M. *Tetrahedron* 2008, 64, 3047.
- [2] Gamsey, S.; Miller, A.; Olmstead, M. M.; Beavers, C. M.; Hirayama, L. C.; Pradhan, S.; Wessling, R. A.; Singaram, B. *J Am Chem Soc* 2007, 129, 1278.
- [3] Yang, W.; Gao, X.; Wang, B. *Med Res Rev* 2003, 23, 346.
- [4] Adams, J. *Cancer Treat Rev* 2003, 29, 3.
- [5] Valliant, J. F.; Guenther, K. J.; King, A. S.; Morel, P.; Schaffer, P.; Sogbein, O. O.; Stephenson, K. A. *Coord Chem Rev* 2002, 232, 173.
- [6] Baker, S. J.; Zhang, Y.-K.; Akama, T.; Lau, A.; Zhou, H.; Hernandez, V.; Mao, W.; Alley, M. R. K.; Sanders, V.; Plattner, J. J. *J Med Chem* 2006, 49, 4447.
- [7] Amin, S. A.; Küpper, F. C.; Green, D. H.; Harris, W. R.; Carrano, C. J. *J Am Chem Soc* 2007, 129, 478.
- [8] Tran, T.; Quan, C.; Edosada, C. Y.; Mayeda, M.; Wiesmann, C.; Sutherland, D.; Wolf, B. B. *Bioorg Med Chem Lett* 2007, 17, 1438.
- [9] Reddy, V. J.; Chandra, J. S.; Reddy, M. V. R. *Org Biomol Chem* 2007, 5, 889.
- [10] Kumar, S. K.; Hager, E.; Pettit, C.; Gurulingappa, H.; Davidson, N. E.; Khan, S. R. *J Med Chem* 2003, 46, 2813.
- [11] Altamore, T. M.; Duggan, P. J.; Krippner, G. Y. *Bioorg Med Chem* 2006, 14, 1126.
- [12] Irving, A. M.; Vogels, C. M.; Nikolcheva, L. G.; Edwards, J. P.; He, X.-F.; Hamilton, M. G.; Baerlocher, M. O.; Baerlocher, F. J.; Decken, A.; Westcott, S. A. *New J Chem* 2003, 27, 1419.
- [13] Blatch, A. J.; Chetina, O. V.; Howard, J. A. K.; Patrick, L. G. F.; Smethurst, C. A.; Whiting, A. *Org Biomol Chem* 2006, 4, 3297.
- [14] Jørgensen, K. A. *Angew Chem, Int Ed Engl* 2000, 39, 3558.
- [15] Sailes, H. E.; Watts, J. P.; Whiting, A. *Tetrahedron Lett* 2000, 41, 2457.
- [16] Nöth, H.; Wrackmeyer, B. *Nuclear Magnetic Resonance Spectroscopy of Boron Compounds*; Springer-Verlag: Berlin, 1978.
- [17] Coapes, R. B.; Souza, F. E. S.; Fox, M. A.; Batsanov, A. S.; Goeta, A. E.; Yufit, D. S.; Leech, M. A.; Howard,

- J. A. K.; Scott, A. J.; Clegg, W.; Marder, T. B. *J Chem Soc, Dalton Trans* 2001, 1201.
- [18] Clegg, W.; Elsegood, M. R. J.; Lawlor, F. J.; Norman, N. C.; Pickett, N. L.; Robbins, E. G.; Scott, A. J.; Nguyen, P.; Taylor, N. J.; Marder, T. B. *Inorg Chem* 1998, 37, 5289.
- [19] Nguyen, P.; Coapes, R. B.; Woodward, A. D.; Taylor, N. J.; Burke, J. M.; Howard, J. A. K.; Marder, T. B. *J Organomet Chem* 2002, 652, 77.
- [20] Niu, W.; Smith, M. D.; Lavigne, J. J. *Cryst Growth Design* 2006, 6, 1274.
- [21] Grünefeld, J.; Kliegel, W.; Rettig, S. J.; Trotter, J. *Can J Chem* 1999, 77, 439.
- [22] Rodríguez, M.; Ochoa, M. E.; Santillan, R.; Farfán, N.; Barba, V. *J Organomet Chem* 2005, 690, 2975.
- [23] Bromidge, S.; Wilson, P. C.; Whiting, A. *Tetrahedron Lett* 1998, 39, 8905.
- [24] Qian, C.-T.; Wang, L.-C.; Chen, R.-F. *Chin J Chem* 2001, 19, 419.
- [25] Cheng, K.; Lin, L.; Chen, S.; Feng, X. *Tetrahedron* 2005, 61, 9594.
- [26] Cheng, K.; Zeng, B.; Yu, Z.; Gao, B.; Feng, X.; Synlett 2005, 1018.
- [27] Shang, D.; Xin, J.; Liu, Y.; Zhou, X.; Liu, X.; Feng, X. *J Org Chem* 2008, 73, 630.
- [28] Sánchez, M.; Sánchez, O.; Höpfl, H.; Ochoa, M.-E.; Castillo, D.; Farfán, N.; Rojas-Lima, S. *J Organomet Chem* 2004, 689, 811.
- [29] Mancheno, O. G.; Arraya, R. G.; Carretero, J. C. *J Am Chem Soc* 2004, 126, 456.
- [30] Vogels, C. M.; Nikolcheva, L. G.; Norman, D. W.; Spinney, H. A.; Decken, A.; Baerlocher, M. O.; Baerlocher, F. J.; Westcott, S. A. *Can J Chem* 2001, 79, 1115.
- [31] McCarthy, A. R.; Hartmann, R. W.; Abell, A. D. *Bioorg Med Chem Lett* 2007, 17, 3603.
- [32] Kitigawa, H.; Kumura, K.; Takahata, S.; Iida, M.; Atsumi, K. *Bioorg Med Chem* 2007, 15, 1106.
- [33] Baerlocher, F. J.; Baerlocher, M. O.; Chaulk, C. L.; Langer, R. F.; MacQuarrie, S. L. *Aust J Chem* 2000, 53, 399.
- [34] Anderson, J.; Langer, R. F.; Baerlocher, F. *Sydowia* 2002, 54, 121.
- [35] Babu, B. H.; Prasad, G. S.; Reddy, C. S.; Raju, C. N. *Heteroatom Chem* 2008, 19, 256.
- [36] Nikolcheva, L. G.; Vogels, C. M.; Stefan, R. A.; Darwish, H. A.; Duffy, S. J.; Ireland, R. J.; Decken, A.; Hudson, R. H. E.; Westcott, S. A. *Can J Chem* 2003, 81, 269.
- [37] Martichonok, V.; Jones, J. B. *J Am Chem Soc* 1996, 118, 950.
- [38] SAINT 6.02; Bruker AXS, Inc.: Madison, WI, 1997–1999.
- [39] Sheldrick, G. M. SADABS; Bruker AXS, Inc.: Madison, WI, 1999.
- [40] Sheldrick, G. M. SHELXTL 5.1; Bruker AXS, Inc.: Madison, WI, 1997.

Novel Synthesis of *N, N'*-Dialkyl Cyclic Ureas Using Sulfur-Assisted Carbonylation and Oxidation

Takumi Mizuno, Takeo Nakai, and Masatoshi Mihara

Osaka Municipal Technical Research Institute, 1-6-50, Morinomiya, Joto-ku,
Osaka 536-8553, Japan

Received 26 September 2008; revised 6 November 2008, 12 November 2008

ABSTRACT: *The first example of cyclic urea synthesis from secondary amines by the use of sulfur-assisted carbonylation and oxidation was established. By combined sulfur-assisted carbonylation of secondary α, ω -diamines under an ambient pressure of carbon monoxide at 20°C with oxidation by molecular oxygen (0.1 MPa, 20°C), a facile synthetic method for *N, N'*-dialkyl cyclic ureas including 1,3-dimethyl-2-imidazolidinone was developed.* © 2009 Wiley Periodicals, Inc. *Heteroatom Chem* 20:64–68, 2009; Published online in Wiley InterScience (www.interscience.wiley.com). DOI 10.1002/hc.20508

INTRODUCTION

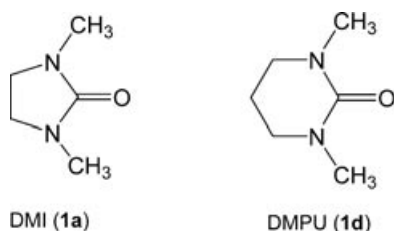
1,3-Dimethyl-2-imidazolidinone (DMI; **1a**) (Scheme 1) is a colorless, transparent, high polar solvent with high thermal and chemical stability and noncorrosiveness. It can be used in a variety of applications (detergents, dyestuffs, and electronic materials) and in the manufacture of polymers. Its versatility can be attributed to its chemical properties, which are its excellent solubility for inorganic and organic compounds, high dielectric constant, and solvation effect [1]. Also, 1,3-dimethyl-3,4,5,6-tetrahydro-2(1*H*)-pyrimidinone (**1d**) (Scheme 1) is used as a polar, aprotic organic solvent [2]. In particular, **1a** and **1d**

are suitable replacements for the carcinogenic solvent, hexamethylphosphoramide [3,4]. A variety of synthetic methods for *N, N'*-dialkyl cyclic ureas **1** containing **1a** and **1d** were developed, based on the carbonylation of secondary α, ω -diamines **2**. Among them, a general synthetic method for cyclic ureas **1** was based upon the carbonylation of **2** with phosgene as a carbonyl source [5,6]. However, use of this preparative method is considerably limited, because of high toxicity of phosgene. Urea and carbon dioxide in the presence of transition metal catalysts were recognized as a carbonyl source for the synthesis of **1** [7–11]. Also, cyclic ureas **1** were given by the displacement from corresponding cyclic thioureas [12,13]. Furthermore, carbon monoxide was a useful raw material for the preparation of **1**. *N, N'*-Dialkyl cyclic ureas **1** were afforded from secondary α, ω -diamines **2** and carbon monoxide in the presence of transition metal catalyst [14].

Recently, we found that sulfur-assisted carbonylation with carbon monoxide was strongly accelerated by *N, N*-dimethylformamide (DMF) or dimethyl sulfoxide (DMSO) [15] and developed a synthetic process of acyclic urea derivatives from primary amines, carbon monoxide, sulfur, and oxygen under mild conditions (0.1 MPa, 20°C) [16] or solvent-free conditions (0.1 MPa) [17]. However, this acyclic urea synthesis using sulfur-assisted carbonylation and oxidation has a serious limitation that is only applicable to the primary amines as reactants.

Therefore, our objective has been to develop a straightforward synthetic method for **1** by the

Correspondence to: Takumi Mizuno; e-mail: tmizuno@omtri.city.osaka.jp
© 2009 Wiley Periodicals, Inc.



SCHEME 1 1,3-Dimethyl-2-imidazolidinone (**1a**) and 1,3-dimethyl-3,4,5,6-tetrahydro-2(1*H*)-pyrimidinone (**1d**).

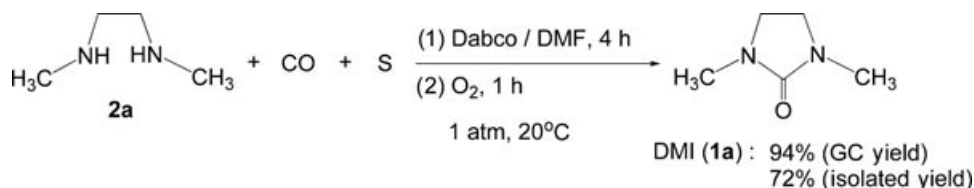
carbonylation of **2** with carbon monoxide and sulfur followed by oxidation with molecular oxygen under mild conditions (0.1 MPa, 20°C). To the best of our knowledge, this is the first example of cyclic urea synthesis from secondary amines by the sulfur-assisted carbonylation with carbon monoxide and oxidation using molecular oxygen.

RESULTS AND DISCUSSION

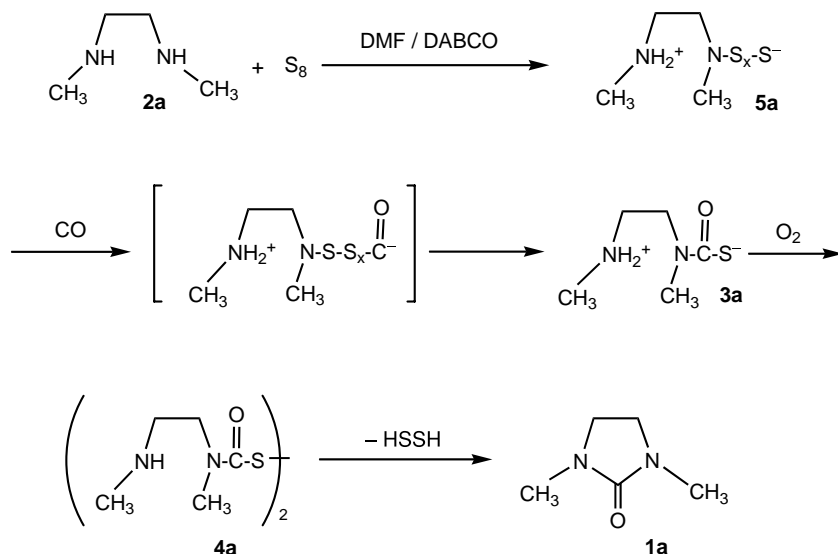
Our investigation into the sulfur-assisted carbonylation and oxidation of secondary α,ω -diamines **2** employing *N, N*-dimethylformamide as a sol-

vent led to the successful synthesis of *N, N'*-dialkyl cyclic ureas **1** (Schemes 2 and 3). *N, N'*-Dimethylethylenediamine (**2a**) readily reacted with carbon monoxide (0.1 MPa) and sulfur (1.5 equiv.) in the presence of 1,4-diazabicyclo[2.2.2]octane (Dabco®) (0.5 equiv.) at 20°C for 4 h in *N, N*-dimethylformamide solvent. Then, the generated thiocarbamate salt **3a** in the DMF solution was oxidized by molecular oxygen under an ambient pressure at 20°C for 1 h. Finally, 1,3-dimethyl-2-imidazolidinone (**1a**) was obtained in 94% yield (GC yield) based on **2a**.

First, the influence of base and solvent was examined on the synthesis of **1a** by the sulfur-assisted carbonylation and oxidation of **2a** (Table 1). In the absence of additional base, **1a** was obtained in good yield in *N, N*-dimethylformamide solvent (Entry 1). By addition of 0.5 equiv. of Dabco®, 1-methylpyrrolidine, or triethylamine in DMF, yields of **1a** were improved (Entries 2–4). 1,8-Diazabicyclo[5.4.0]undec-7-ene (DBU) did not have an additional effect for the preparation of **1a** (Entry 5), and potassium carbonate (K_2CO_3) lowered the yield of **1a**, because of low



SCHEME 2 Synthesis of 1,3-dimethyl-2-imidazolidinone (**1a**).



SCHEME 3 Proposed pathway for the synthesis of 1,3-dimethyl-2-imidazolidinone (**1a**).

TABLE 1 Effect of Base and Solvent on Synthesis of DMI (**1a**)

Entry	Base	Solvent	Yield (%) ^a
1	None	DMF	81
2	Dabco	DMF	94
3	1-Methylpyrrolidine	DMF	92
4	Triethylamine	DMF	87
5	DBU	DMF	81
6	K ₂ CO ₃	DMF	27
7	Dabco	DMAc	87
8	Dabco	DMSO	73
9	Dabco	THF	17
10	Dabco	MTBE	0
11	Dabco	Toluene	0

Reaction conditions: *N,N*-dimethylethylenediamine (**2a**) (1.07 mL, 10 mmol), sulfur (481 mg, 15 mmol), base (5 mmol), solvent (20 mL), CO (1 atm), 20°C, 4 h for carbonylation, and O₂ (1 atm), 20°C, 1 h for oxidation.

^aGC yields.

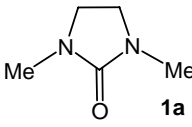
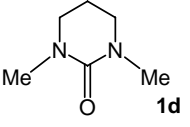
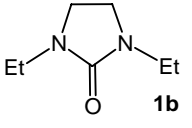
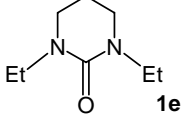
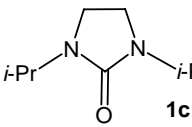
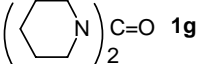
solubility of K₂CO₃ in DMF (Entry 6). Using *N,N*-dimethylacetamide (DMAc) or dimethyl sulfoxide as a solvent in the presence of Dabco®, **1a** was given in good yields (Entries 7,8). However, tetrahydrofuran (THF), *t*-butyl methyl ether (MTBE), and toluene were unsuitable for the preparation of 1,3-dimethyl-2-imidazolidinone (**1a**) (Entries 9–11).

Next, several *N,N*-dialkyl cyclic ureas (**1a–d**) including **1a** were synthesized by the sulfur-assisted carbonylation with carbon monoxide and oxidation with molecular oxygen under mild condition (0.1 MPa, 20°C) (Table 2). 1,3-Dimethyl-2-imidazolidinone (**1a**) and 1,3-diethyl-2-imidazolidinone (**1b**) were obtained in good to excellent yields. However, the yield of **1c** was lowered by bulkiness of *N*-isopropyl groups. Furthermore, the present method was ineffective in the formation of six-membered rings (**1d** and **1e**).

Under similar mild conditions, *S*-methyl *N,N*-dipropylthiocarbamate was obtained in excellent yield by esterification of *N,N*-dipropylthiocarbamate salt (**3f**) with methyl iodide [15]. However, secondary amines, dipropylamine (**2f**), and piperidine (**2g**) did not give acyclic ureas (**1f**, **g**) at all. In the case of **2f**, bis(*N,N*-dipropylcarbamoyl) disulfide (**4f**) was formed in place of tetrapropylurea (**1f**). Therefore, **4f** could not receive the nucleophilic substitution of **2f** by the bulkiness of **2f** and **4f**.

Scheme 3 shows possible pathways for the synthesis of **1a** by the carbonylation of **2a** followed by oxidation of the thiocarbamate **3a**. We have found that thiolate salts **5** readily react with carbon monoxide to give thiocarbamate salts **3** (Scheme 4) [18], and therefore we propose that a plausible pathway for this sulfur-assisted carbonylation of **2a** with carbon monoxide is via thiolate anion **5a**. At first, el-

TABLE 2 Synthesis of *N,N'*-Dialkyl Cyclic Ureas (**1a–e**) and Acyclic Ureas (**1f–g**)

Product	Yield (%) ^a	Product	Yield (%) ^a
 1a	94	 1d	17
 1b	72 ^b	 1e	Trace
 1c	70		
	41	(Pr ₂ N) ₂ C=O 1f	0 ^{b–d}
		 1g	0 ^c

Reaction conditions: Amine (10 mmol), sulfur (481 mg, 15 mmol), Dabco (561 mg, 5 mmol), DMF (20 mL), CO (1 atm), 20°C, 4 h for carbonylation, and O₂ (1 atm), 20°C, 1 h for oxidation.

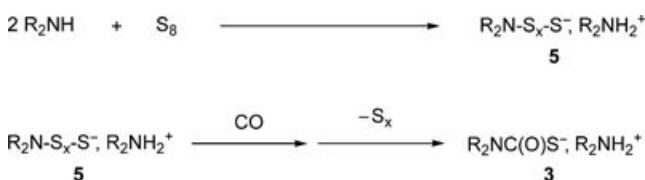
^aGC yields.

^bIsolated yields.

^cAmine (20 mmol) was used.

^dBis(*N,N*-dipropylcarbamoyl) disulfide (**4f**) was formed in 36% (1.81 mmol).

emental sulfur undergoes S–S bond fission by the reaction with **2a**, to form ammonium thiolate (**5a**). The reaction of **5a** with carbon monoxide gives the carbonylated species. Through an intramolecular rearrangement or elimination of carbonyl sulfide from the carbonylated species, thiocarbamate salt (**3a**) is generated. The thus formed thiocarbamate salt (**3a**) is oxidized by molecular oxygen, giving **1a** via dicarbamoyl disulfide (**4a**). Indeed, in the case of the reaction with **2f**, bis(*N,N*-dipropylcarbamoyl) disulfide (**4f**) was obtained in place of **1f**.

**SCHEME 4** The reaction of thiolate anions **5** with carbon monoxide.

In our previous reports [16,17] of urea synthesis from primary amines by sulfur-assisted carbonylation using carbon monoxide and oxidation with oxygen, isocyanate intermediates were suggested in this oxidation stage. Therefore, because of difficulty of aminolysis of bulky dicarbamoyl disulfides **4**, the formation of ureas **1** from the thiocarbamate salts **3** generated from primary amines is generally much easier, compared with from secondary amines.

CONCLUSION

In summary, a novel synthetic method for *N, N'*-dialkyl cyclic ureas **1**, especially 1,3-dimethyl-2-imidazolidinone (**1a**), has been developed under mild conditions (0.1 MPa, 20°C) in DMF, in which includes the sulfur-assisted carbonylation of secondary diamines **2** with carbon monoxide, and the oxidation of resulting thiocarbamate salts **3** with molecular oxygen. From the viewpoint of application to practical production of **1a**, the present method is very significant in terms of the use of easily available and cheap carbon monoxide, oxygen, sulfur, and DMF, and mild reaction conditions (0.1 MPa, 20°C).

EXPERIMENTAL

FT-IR spectra were recorded on a JASCO FT/IR-4100 instrument. ¹H and ¹³C NMR spectra were obtained on a JEOL JNM-AL300 (300, 75 MHz) instrument. Chemical shifts were reported in ppm relative to tetramethylsilane (δ -units). Mass and exact mass spectra were measured on a JEOL JMS-600 spectrometer. Amines **2a–g**, DMF, DMAc, DMSO, THF, MTBE, toluene, Dabco®, 1-methylpyrrolidine, triethylamine, DBU, K₂CO₃, sulfur (99.5%), carbon monoxide (99.9%), and oxygen (99.9%) were used as purchased.

Typical Procedure for the Synthesis of DMI **1a**

A dark red solution containing *N, N'*-dimethylethylenediamine (**2a**; 2.13 mL, 20 mmol), Dabco® (1.12 g, 10 mmol), and powdered sulfur (962 mg, 30 mmol) in DMF (20 mL) was vigorously stirred under CO (0.1 MPa) at 20°C for 4 h. Into the resulting brown emulsion of thiocarbamate salt (**3a**), O₂ (0.1 MPa) was charged at 20°C (exothermic reaction). The reaction mixture was stirred for an additional 1 h at 20°C. DMF was evaporated from the resulting brown emulsion, and 1,3-dimethyl-2-imidazolidinone (**1a**) was given by distillation.

1,3-Dimethyl-2-imidazolidinone (**1a**). Yield: 1.64 g (72%) yield; bp 107–109°C, 30 hPa (Lit. [1] 106–108°C, 23 hPa); ¹H NMR (CDCl₃): δ (ppm) 2.78 (s, 6H, CH₃), 3.27 (s, 4H, CH₂); ¹³C NMR (CDCl₃): δ (ppm) 31.3, 44.9, 161.9; MS *m/z* (%): 114 (M⁺, 100), 113 (54), 85 (11), 72 (10), 58 (14), 56 (21).

For the identification of **1a**, retention time of GC and NMR and MS spectra of **1a** was compared with those of commercially available DMI.

Procedure for the Formation of Bis(*N, N*-dipropylcarbamoyl) Disulfide **4f**

Dipropylamine (**2f**; 2.73 mL, 20 mmol), Dabco® (561 mg, 5 mmol), powdered sulfur (481 mg, 15 mmol), and DMF (10 mL) were placed in a 100-mL flask under an argon atmosphere. The flask was charged with an ambient pressure of CO, and vigorously stirred under CO from a balloon (0.1 MPa) at 20°C for 4 h. The color of the solution then changed from red to reddish black. The flask was purged of CO and charged with O₂ (0.1 MPa) at 20°C (slightly exothermic reaction). The reaction mixture was stirred under O₂ from a balloon (0.1 MPa) for another 1 h at 20°C. The resulting orange solution was then poured into 1 M HCl (100 mL) and extracted by *t*-butyl methyl ether (200 mL). Bis(*N, N*-dipropylcarbamoyl) disulfide (**4f**) was purified as an oil, by short-column chromatography (silica gel, EtOAc).

Bis(N, N-dipropylcarbamoyl) Disulfide (**4f**). Yield: 581 mg (36%, 1.81 mmol) yield; IR (neat, cm⁻¹): ν 2964, 2874, 1681(C=O), 1467, 1404, 1218, 1118; ¹H NMR (CDCl₃): δ (ppm) 0.82–1.03 (m, 12H, CH₃), 1.53–1.80 (m, 8H, CH₂), 3.36 (br s, 8H, CH₂); ¹³C NMR (CDCl₃): δ = 11.1, 20.9, 22.0, 50.3, 163.3; MS *m/z* (%): (ppm) 320 (M⁺, 15), 129 (13), 128 (100), 86 (41); Exact MS: calcd for C₁₄H₂₈O₂N₂S₂: 320.1592; found: 320.1611.

REFERENCES

- [1] O'Neil, M. J.; Heckelman, P. E.; Koch, C. B.; Roman, K. J. (Eds.). Merck Index, 14th ed.; Merck & Co., Inc.: Whitehouse Station, NJ, 2006; 3249.
- [2] Fieser, M. (Ed.). Fieser and Fieser's Reagents for Organic Synthesis; Wiley.: New York, 1984; Vol 11, p. 207.
- [3] Lo, C.-C.; Chao, P.-M. J Chem Ecol 1990, 16, 3245.
- [4] Mukhopadhyay, T.; Seebach, D. Helv Chim Acta 1982, 65, 385.
- [5] Boon, W. R. J Chem Soc 1947, 307.
- [6] Thomas, E. W.; Nishizawa, E. E.; Zimmermann, D. C.; Williams, D. J. J Med Chem 1989, 32, 228.

- [7] Butler, A. R.; Hussain, I. *J Chem Soc, Perkin Trans 2* 1981, 317.
- [8] Dehmlow, E. V.; Rao, Y. R. *Synth Commun* 1988, 18, 487.
- [9] Nomura, R.; Hasegawa, Y.; Ishimoto, M.; Toyosaki, T.; Matsuda, H. *J Org Chem* 1992, 57, 7339.
- [10] Nomura, R.; Hasegawa, Y.; Toyosaki, T.; Matsuda, H. *Chem Express* 1992, 7, 569.
- [11] Corriu, R. J. P.; Lanneau, G. F.; Mehta, V. D. *J Organomet Chem* 1991, 419, 9.
- [12] Malaschichin, S.; Fu, C.; Linden, A.; Heimgartner, H. *Helv Chim Acta* 2005, 88, 3253.
- [13] Bogatsky, A. V.; Lukyanenko, N. G.; Kirichenko, T. I. *Synthesis* 1982, 464.
- [14] McCusker, J. E.; Grasso, C. A.; Main, A. D.; McElwee-White, L. *Org Lett* 1999, 1, 961.
- [15] Mizuno, T.; Iwai, T.; Ishino, Y. *Tetrahedron* 2005, 61, 9157.
- [16] Mizuno, T.; Mihara, M.; Iwai, T.; Ito, T.; Ishino, Y. *Synthesis* 2006, 2825.
- [17] Mizuno, T.; Mihara, M.; Nakai, T.; Iwai, T.; Ito, T. *Synthesis* 2007, 3135.
- [18] Mizuno, T.; Daigaku, T.; Nishiguchi, I. *Tetrahedron Lett* 1995, 36, 1533.